Meteoritics & Planetary Science 38, Nr 5, 669–710 (2003)
Abstract available online at http://meteoritics.org

^{39}Ar-^{40}Ar ages of eucrites and thermal history of asteroid 4 Vesta

Donald D. BOGARD[1*] and Daniel H. GARRISON[1, 2]

[1]Astromaterials Research, SR, NASA Johnson Space Center, Houston, Texas 77058, USA
[2]Lockheed-Martin Corporation, Houston, Texas 77058, USA
[*]Corresponding author. E-mail: donald.d.bogard@nasa.gov

(Received 1 October 2002; revision accepted 31 January 2003)

Abstract–Eucrite meteorites are igneous rocks that derived from a large asteroid, probably 4 Vesta. Past studies have shown that after most eucrites formed, they underwent metamorphism in temperatures up to ≥800°C. Much later, many were brecciated and heated by large impacts into the parent body surface. The less common basaltic, unbrecciated eucrites also formed near the surface but, presumably, escaped later brecciation, while the cumulate eucrites formed at depths where metamorphism may have persisted for a considerable period.

To further understand the complex HED parent body thermal history, we determined new ^{39}Ar-^{40}Ar ages for 9 eucrites classified as basaltic but unbrecciated, 6 eucrites classified as cumulate, and several basaltic-brecciated eucrites. Precise Ar-Ar ages of 2 cumulate eucrites (Moama and EET 87520) and 4 unbrecciated eucrites give a tight cluster at 4.48 ± 0.02 Gyr (not including any uncertainties in the flux monitor age). Ar-Ar ages of 6 additional unbrecciated eucrites are consistent with this age within their relatively larger age uncertainties. By contrast, available literature data on Pb-Pb isochron ages of 4 cumulate eucrites and 1 unbrecciated eucrite vary over 4.4–4.515 Gyr, and ^{147}Sm-^{143}Nd isochron ages of 4 cumulate and 3 unbrecciated eucrites vary over 4.41–4.55 Gyr. Similar Ar-Ar ages for cumulate and unbrecciated eucrites imply that cumulate eucrites do not have a younger formation age than basaltic eucrites, as was previously proposed. We suggest that these cumulate and unbrecciated eucrites resided at a depth where parent body temperatures were sufficiently high to cause the K-Ar and some other chronometers to remain as open diffusion systems. From the strong clustering of Ar-Ar ages at ~4.48 Gyr, we propose that these meteorites were excavated from depth in a single large impact event ~4.48 Gyr ago, which quickly cooled the samples and started the K-Ar chronometer. A large (~460 km) crater postulated to exist on Vesta may be the source of these eucrites and of many smaller asteroids thought to be spectrally or physically associated with Vesta. Some Pb-Pb and Sm-Nd ages of cumulate and unbrecciated eucrites are consistent with the Ar-Ar age of 4.48 Gyr, and the few older Pb-Pb and Sm-Nd ages may reflect an isotopic closure before the large cratering event.

One cumulate eucrite gives an Ar-Ar age of 4.25 Gyr; 3 additional cumulate eucrites give Ar-Ar ages of 3.4–3.7 Gyr; and 2 unbrecciated eucrites give Ar-Ar ages of ~3.55 Gyr. We attribute these younger ages to a later impact heating. Furthermore, the Ar-Ar impact-reset ages of several brecciated eucrites and eucritic clasts in howardites fall within the range of 3.5–4.1 Gyr. Among these, Piplia Kalan, the first eucrite to show evidence for extinct ^{26}Al, was strongly impact heated ~3.5 Gyr ago. When these data are combined with eucrite Ar-Ar ages in the literature, they confirm that several large impact heating events occurred on Vesta between ~4.1–3.4 Gyr ago. The onset of major impact heating may have occurred at similar times for both Vesta and the moon, but impact heating appears to have persisted for a somewhat later time on Vesta.

INTRODUCTION

Eucrites are igneous meteorites produced by crystallization from a melt on a large asteroidal parent body, probably 4 Vesta (McCord et al. 1970; Binzel and Xu 1993; Keil 2002). Although eucrites rank among the oldest analyzed basalts in the solar system, they have experienced a complex thermal history that has affected a variety of characteristics ranging from mineral textures to isotopic chronologies. The thermal processing observed in eucrites has 2 sources: internal

© Meteoritical Society, 2003. Printed in USA.

parent body metamorphism, probably produced by decay of short-lived nuclides; and heating produced by impact cratering on the parent body. The extensive thermal history of eucrites is consistent with their derivation from an asteroid larger than that of most meteorite types, yet smaller than planetary bodies such as the moon and Mars, analyzed basalts of which were formed much later. Thus, eucrites present opportunities to study basalt generation on a body of significant size very early in solar system history and to assess the long-term thermal history of that parent body. Much of this kind of information is not available for the earth, moon, and Mars.

Most eucrites probably formed through surface basalt flows >4.555 Gyr ago, or shortly after accretion of the HED (howardite-eucrite-diogenite) parent body. A Pb-Pb model age of 4.560 ± 0.003 Gyr was reported for the Ibitira eucrite, and similarly old (but less precise) ^{147}Sm-^{143}Nd ages have been reported for a few eucrites (see Carlson and Lugmair [2000] and references therein). The existence of decay products of short-lived nuclides in some eucrites are also evidence of a requisite early formation. For example, evidence in several eucrites for live ^{53}Mn (half-life 3.8 Myr), ^{26}Al (half-life 0.7 Myr), and ^{60}Fe (half-life 0.1 Myr) have been reported (Carlson and Lugmair 2000; Srinivasan et al. 1999; Shukolyukov and Lugmair 1993; Nyquist et al. 2001; Srinivasan 2002). Based upon ^{53}Mn and Pb-Pb data, Lugmair and Shukolyukov (1998) suggested that the HED parent body formed 4564.8 ± 0.9 Myr ago. On the other hand, many radiometric ages (K-Ar, Pb-Pb, Rb-Sr, Sm-Nd) of eucrites are considerably younger than 4.56 Gyr and are variable (Bogard 1995; Carlson and Lugmair 2000). The reason for this variation in eucrite ages is the focus of this paper.

After their formation, most eucrites experienced metamorphism at ≥800°C, which was sufficient cause for Mg, Fe, and Ca in pyroxenes to undergo varying degrees of subsolidus diffusion and to produce more limited ranges of pyroxene compositions (Takeda and Graham 1991; Yamaguchi et al. 1997). Several models have been proposed to accomplish this metamorphism, including: 1) early differentiation of the parent body into layers (Takeda 1979; Takeda 1997); 2) heating during formation of large impact craters (Nyquist et al. 1986); and 3) heating at several kilometers depth after the rapid generation and burial of multiple layers of surface basalt (Yamaguchi et al. 1996; Yamaguchi et al. 1997). Although directly dating the time of this eucrite metamorphism is difficult, it most likely occurred very early in eucrite history. The 1st and 3rd models above imply that metamorphism occurred within a few million years after basalt formation.

Most eucrites (and all howardites) are breccias formed by impact events near the parent body surface. These impacts can not only disturb texture and mineralogy but can also reset isotopic ages (Bogard 1995; Kunz et al. 1995). Given the particular sensitivity of the K-Ar chronometer to moderate heating in crater ejecta, ^{39}Ar-^{40}Ar ages of almost all eucrites and howardites show disturbance and resetting. Further, Rb-Sr, Pb-Pb, and Sm-Nd ages of some eucrites are also disturbed or reset. Bogard (1995) summarized available impact-reset ages of eucrites and suggested that the HED parent body had experienced an analogous cataclysmic bombardment that reset the radiometric ages of many lunar highland rocks returned by the Apollo and Luna missions. The observation that such impact-reset ages are not commonly observed in most other meteorite types was attributed to the relatively large size of the HED parent body compared to parent bodies of most other meteorite types. Large size is a requirement for producing large crater deposits that remain hot for a significant time without disrupting the parent body.

Two uncommon types of eucrites, the unbrecciated, metamorphosed, basaltic eucrites and the cumulate eucrites, give neither very old (i.e., >4.55 Gyr) ages nor much younger impact-reset ages. Rather, their radiometric ages are intermediate. Four cumulate eucrites gave Pb-Pb and Sm-Nd isochron ages between 4.40 and 4.55 Gyr, and 3 unbrecciated eucrites gave Sm-Nd isochron ages of 4.46–4.54 Gyr (Tera et al. 1997; Yamaguchi et al. 2001; Carlson and Lugmair 2000). The ^{39}Ar-^{40}Ar ages for 2 of these unbrecciated eucrites are ~4.49 Gyr (Bogard and Garrison 1995; Yamaguchi et al. 2001). For the unbrecciated eucrite EET 90020, Yamaguchi et al. (2001) suggested that its Sm-Nd and Ar-Ar ages were reset during the formation of a very large crater on Vesta. Although the ages of cumulate eucrites are conceivably linked to this large Vesta crater, the possibility also exists that they were caused by sustained metamorphism deep within the parent body. From the published data, whether the various ages of cumulate and unbrecciated eucrites represent a single heating event or a broad spectrum of metamorphic and impact heating is not clear. Tera et al. (1997) suggested that the range of Pb-Pb and Sm-Nd ages of cumulate eucrites represented different times of formation or, at least, different times of isotopic closure.

In this paper, we present a large amount of new data on the ^{39}Ar-^{40}Ar ages of eucrites. Several of these newly analyzed meteorites are classified as unbrecciated, and others are classified as cumulate. Some of these give older ages, while others give younger ages that are consistent with later impact-resetting. We discuss and interpret these ages, along with literature data, in the context of the possible metamorphic and impact thermal history of the HED parent body, which we presume to be Vesta.

METHODS

The eucrite samples that we analyzed were whole rock chips, each weighing several tens of milligrams. Most samples were neutron irradiated at the University of Missouri reactor (MURR) in several batches at different times. However, Caldera was irradiated at the Brookhaven National Laboratory (BNL), and clasts from the EET howardites were

irradiated at Los Alamos. Each irradiation included several samples of the NL-25 hornblende, which serves as a flux and age monitor. The J value determined for each sample is given in the Appendix. The determined age of the NL-25 hornblende is 2.65 ± 0.01 Gyr (Bogard et al. 1995) and has been cross-calibrated against other dated Ar-Ar age monitors (Alexander and Davis 1974; Renne 2000). Argon was released from each eucrite sample by stepwise temperature extraction in a furnace equipped with a thermocouple, and the Ar isotopic composition was measured on a mass spectrometer. Most measurements were made using a Nuclide 6–60 spectrometer. This instrument produces a relatively large but constant ^{39}Ar signal in its source, which dominates the total ^{39}Ar blank correction. A few samples having very low potassium concentrations were measured on a VG-3600 instrument, which possesses a much lower Ar background. Isotopic data were corrected for system blanks, radioactive decay, and reactor-produced isotopic interferences. Furnace extraction blanks were generally constant up to temperatures of ~1100°C and increased moderately at higher temperatures. For the extraction of most samples, the ^{40}Ar and ^{39}Ar blank corrections were 1% and, in many cases, ≤1%. Smaller ^{40}Ar and ^{39}Ar signals for samples possessing low K concentrations generally were accommodated by the smaller blanks for measurements using the VG spectrometer. Based on long-term variability in blank measurements, we assume the uncertainties in blank corrections equaled 50% and 20% of the magnitudes of the ^{40}Ar and ^{39}Ar blanks, respectively. The ^{39}Ar/^{37}Ar reactor correction factor applied to each sample was determined from measurements of ^{39}Ar/^{37}Ar in irradiated samples of pure CaF_2 crystals. The ^{39}Ar/^{37}Ar correction factor applied to the samples irradiated at MURR (the majority of samples) was $7.6 \pm 0.2 \times 10^{-4}$ and was determined by irradiating 10 CaF_2 samples at several different times. The correction factor used for the BNL irradiation of Caldera was $6.4 \pm 0.3 \times 10^{-4}$, and the correction factor used for the Los Alamos irradiations was $6.5 \pm 0.2 \times 10^{-4}$. The reactor correction to ^{39}Ar typically amounted to a few percent for those extractions releasing Ar from feldspar but was considerably larger for high temperature extractions where the K/Ca ratio was lower.

Ar-Ar ages were calculated using the ^{40}K decay parameters recommended by Steiger and Jäger (1977). The uncertainties assigned to the calculated ages for individual temperature extractions shown in the Ar age spectra include uncertainties in ^{40}Ar/^{39}Ar ratio measurements and in all applied corrections but do not include the uncertainty in the irradiation constant (J) value. This permits direct comparisons among ages of individual extractions, which have the same uncertainty produced by the error in J. An event age, usually, is derived from the mean of the ages of several extractions (i.e., an age plateau). The given event age uncertainty is the one-sigma uncertainty in this mean age, statistically combined with the determined uncertainty in J for that sample (see Bogard et al. 2000). Similarly, where we refer to the specific age of an individual extraction in the context of an event age, its age uncertainty also contains the uncertainty in J. None of the Ar-Ar age uncertainties presented in the figures or data table consider uncertainties in the absolute age of the NL-25 hornblende nor in the ^{40}K decay constants. These do not affect the comparison of relative Ar-Ar ages obtained in the JSC laboratory. For comparison with ages obtained from other chronometers, the uncertainty in the age of the NL-25 hornblende is estimated at 0.5% (Bogard et al. 1995; Renne 2000).

In interpreting the Ar-Ar age spectra for these samples, we consider the behavior of all Ar isotopic ratios as a function of extraction temperature. For example, rapidly decreasing ^{36}Ar/^{37}Ar, ^{36}Ar/^{38}Ar, and K/Ca ratios in the first few extractions are interpreted to indicate the release of adsorbed atmospheric Ar and Ar from terrestrial weathering products. In contrast, constant ^{36}Ar/^{37}Ar and ^{36}Ar/^{38}Ar ratios at intermediate and higher temperatures are interpreted to indicate a lack of terrestrial Ar, the presence of cosmogenic Ar, and the presence of Ar produced in the reactor from Ca. Most K in eucrites resides in plagioclase, which has a higher K/Ca ratio compared to the other major mineral—pyroxene. Thus, a sudden decrease in the K/Ca ratio at a higher extraction temperature usually indicates that pyroxene has begun to degas the ^{37}Ar produced in the reactor from Ca. A decrease in the Ar age associated with this decrease in K/Ca can indicate recoiled ^{39}Ar, which was produced in the reactor from the reaction ^{39}K(n, p)^{39}Ar and which has recoiled from surfaces of K-rich feldspar grains into surfaces of K-poor pyroxene grains. Commonly, in such cases, an Ar age spectrum will decrease for a time when this recoiled ^{39}Ar is released from pyroxene grain surfaces and then increase again as the recoiled ^{39}Ar is quantitatively degassed. In some of the eucrites studied here, significant diffusive loss of ^{40}Ar by terrestrial weathering has occurred, and this loss can produce a sloped Ar age at low and intermediate extraction temperatures. If such samples also show a significant ^{39}Ar recoil effect, then the Ar age may show a sloped spectrum at low to intermediate temperatures, followed by an age decrease caused by recoiled ^{39}Ar degassing from pyroxene, followed by an older Ar age plateau at high extraction temperatures. In such cases, we usually interpret the older age as the event degassing age. Occasionally, distinct peaks in the rate of release of ^{39}Ar with temperature suggest that K occurs in phases with different Ar diffusion properties, such as zoned feldspar grains or grain populations having different sizes. Some of this type of detailed analysis of Ar-Ar isotopic data is discussed in Garrison et al. (2000). In assigning event degassing ages to these eucrites, we try to understand the entire age spectrum of each sample by applying these techniques in a consistent manner. To determine an Ar-Ar age, a well-developed age plateau is always preferred but is not always present. However, we feel reasonably confident in

assigning an Ar degassing event age based on a limited age plateau in those cases where the entire Ar age spectrum has a reasonable interpretation. For this reason, we discuss each Ar age spectrum in some detail.

We do not make extensive use of isochron plots of $^{40}Ar/^{36}Ar$ versus $^{39}Ar/^{36}Ar$, as is commonly done for terrestrial samples and occasionally for meteorite data. Isochrons for multi-mineralogic samples showing quite different K/Ca ratios during Ar release can be misleading and are, for these eucrite samples, less informative than the Ar-Ar age spectrum. The existence of mineral phases that have different ratios of radiogenic Ar to cosmogenic ^{36}Ar produces a linear isochron in eucrites. The cosmogenic ^{36}Ar is not generally well-correlated with any radiogenic component or with any trapped Ar, excess ^{40}Ar, or reactor-recoiled ^{39}Ar. The slope of an isochron plot for eucrites, from which the age is derived, is primarily determined by the larger $^{40}Ar/^{36}Ar$ and $^{39}Ar/^{36}Ar$ ratios arising from degassing of feldspar at intermediate temperatures. In contrast, the $^{40}Ar/^{36}Ar$ intercept value of the isochron is primarily determined by high temperature extractions degassing pyroxene, for which larger releases of cosmogenic ^{36}Ar produce lower $^{40}Ar/^{36}Ar$ and $^{39}Ar/^{36}Ar$ ratios. However, these extractions releasing ^{36}Ar from pyroxene are often the same ones that show lower Ar-Ar ages due to the gain of recoiled ^{39}Ar produced in the reactor. This situation means that, on the isochron plot, those extractions releasing more ^{36}Ar and plotting closer to the origin may also give slightly younger ages. As a consequence, in whole rock samples, the isochron can be rotated counter-clockwise, thereby giving an older apparent age and a lower $^{40}Ar/^{36}Ar$ intercept. In fact, meteorites showing lowered Ar-Ar ages at higher temperatures caused by a gain of recoiled ^{39}Ar commonly show negative $^{40}Ar/^{36}Ar$ intercepts on isochron plots. Such negative intercepts have no physical meaning in terms of a trapped component but can be an indicator of the redistribution of recoiled ^{39}Ar. Even in cases where there is no obvious effect of ^{39}Ar recoil on the age spectrum, situations can exist where the isochron gives a false age. For example, occasionally we observe that the ^{39}Ar is released in two distinct phases, and the higher temperature phase shows both a lower $^{39}Ar/^{36}Ar$ ratio and an older age. In this case, the isochron can be rotated clock-wise and yield an isochron age that is too young. We illustrate these subtle phenomena with isochrons in discussing a few of the individual eucrite data below.

SAMPLE DESCRIPTIONS AND ^{39}AR-^{40}AR AGE RESULTS

We recently analyzed several Antarctic eucrites that have been described as being either unbrecciated or cumulate. Now, in addition to some previously published data, we have have analyzed the 3 unbrecciated eucrites with reported Pb-Pb and/or Sm-Nd ages and 3 of the 4 cumulate eucrites with reported Pb-Pb and Sm-Nd isochron ages, as well as several additional eucrites. Argon isotopic data are given in the Appendix. Below, we discuss details of the Ar-Ar data and derive ages for individual samples.

Unbrecciated Basaltic Eucrites

Basaltic eucrites are pigeonite-plagioclase rocks having fine to medium grain sizes (Mittlefehldt et al. 1998a). They are thought to have formed as extrusive flows or shallow intrusions on the parent asteroid. Post-formational annealing has caused the original mineral pigeonite to undergo subsolidus exsolution of augite. The degree of post-formational thermal annealing varies among basaltic eucrites, and a metamorphism classification scheme was defined by Takeda and Graham (1991). The lowest metamorphic class (#1) shows narrow augite lamellae and preservation of the original igneous zoning texture. The highest metamorphic class (#6) shows much wider augite lamellae, and solid state diffusion of Mg and Fe has caused the pyroxene composition to become nearly homogeneous and, in some cases, has caused the pyroxene to partly invert to orthopyroxene. Plagioclase in basaltic eucrites can show a wide range in anorthite content and is probably the only significant K-bearing mineral. Most basaltic eucrites are breccias and consist of clasts of either similar basalt types (monomict) or different rock types (polymict), often set in a fine-grained, fragmental matrix. Eucritic clasts also occur in howardites, which are mixtures of eucritic and diogenitic material. The brecciated nature of most eucrites can make their determined isotopic chronologies difficult to decipher. However, a small fraction of eucrites appear unbrecciated, meaning that they do not give evidence of having been broken and mixed by impacts on their parent body surface. The Ar-Ar ages of several unbrecciated basaltic eucrites are presented in this section.

QUE 97053

This 75 g unbrecciated eucrite (weathering category A) is coarse grained and shows pervasive shock effects (Antarctic Meteorite Newsletter). The Ar-Ar age spectrum for QUE 97053 is shown in Fig. 1a. The $^{36}Ar/^{37}Ar/^{38}Ar$ ratios indicate that only the first temperature extraction released significant atmospheric Ar. Overall, the Ar-Ar age spectrum is relatively flat, and those few extractions releasing the first ~4% of the ^{39}Ar suggest modest diffusion loss of ^{40}Ar. A very small decline in age is suggested by extractions releasing ~12–60% of the ^{39}Ar. The 3 lowest ages at ~48–60% ^{39}Ar release occur at the point that the K/Ca ratio starts to decrease, and these may have been lowered by the release of recoil-implanted ^{39}Ar from pyroxene grain surfaces. The summed Ar-Ar age for all extractions above ~4% ^{39}Ar release is 4.468 ± 0.021 Gyr, and this would be a lower limit to the time of K-Ar closure. If we omit 4 low-age extractions

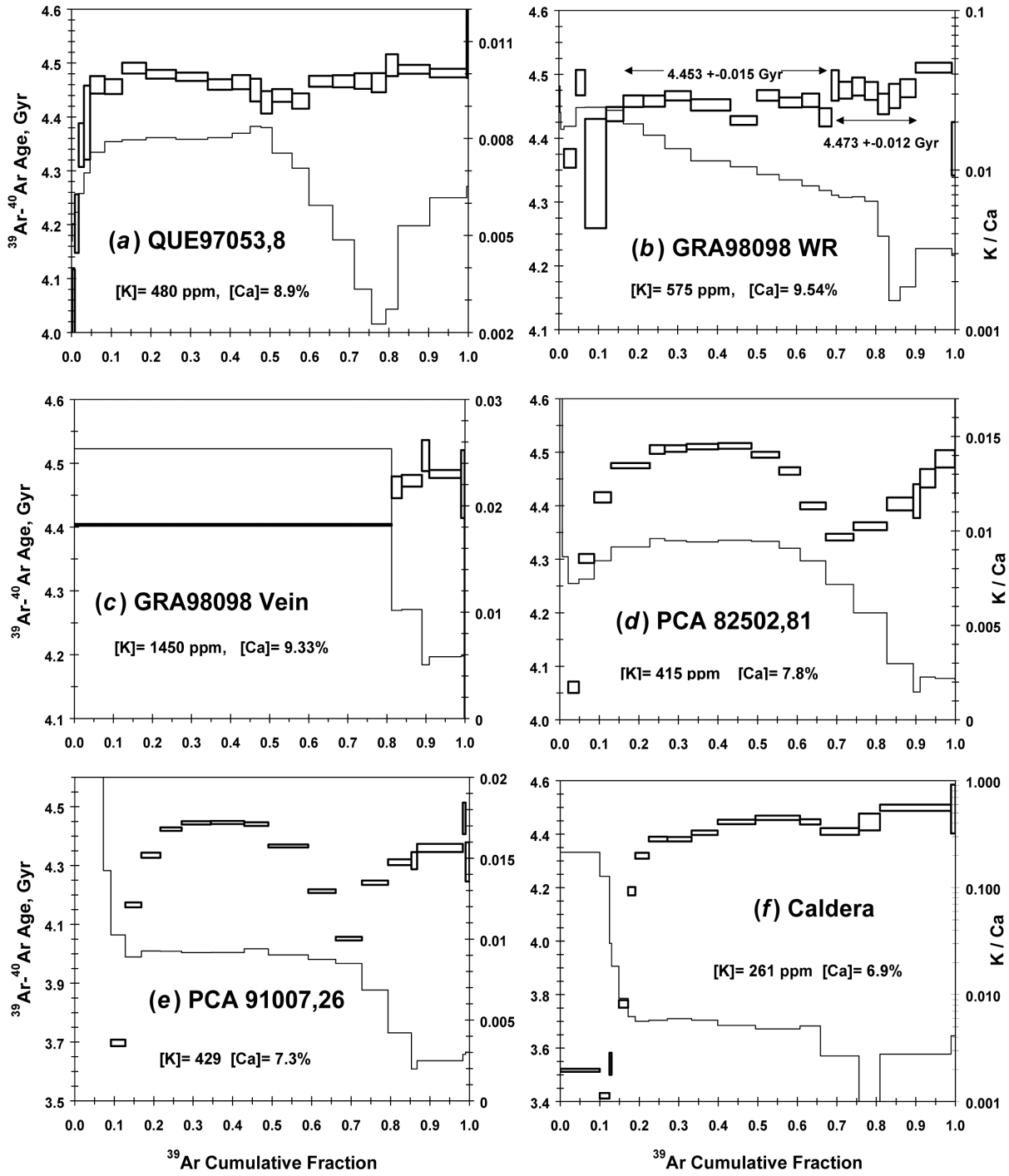

Fig. 1. ^{39}Ar-^{40}Ar ages (rectangles, left scale) and K/Ca ratios (stepped line, right scale) as a function of cumulative ^{39}Ar release for unbrecciated basaltic eucrites: a) QUE 97053; b) GRA 98098 host; c) GRA 98098 melt vein; d) PCA 82502; e) PCA 91007; and f) Caldera. The concentrations of K and Ca measured on these samples are also given.

(releasing 45–60% of the ^{39}Ar) and omit two extractions releasing ~4–13% ^{39}Ar (which may have recently lost ^{40}Ar by diffusion), then the 12 remaining extractions releasing 72% of the total ^{39}Ar give an average age of 4.476 ± 0.014 Gyr. However, slightly higher ages exist for the extractions releasing at >80% ^{39}Ar release. For example, 9 extractions releasing ~12–79% of the ^{39}Ar but omitting the 4 low ages at ~45–60% ^{39}Ar give an age of 4.471 ± 0.012 Gyr. Three extractions releasing ~80–100% of the ^{39}Ar give an age of 4.486 ± 0.007 Gyr. Giving slightly greater weight to the older age, we adopt an age of 4.480 ± 0.015 Gyr as the time of the last significant Ar degassing of QUE 97053.

GRA 98098

This 779 g unbrecciated eucrite (weathering category B) is a recrystallized, granular aggregate and possesses a texture and chemical composition atypical of other eucrites (Mittlefehldt and Lee 2001). The Ar-Ar age spectrum for a whole rock sample is shown in Fig. 1b. The $^{36}Ar/^{37}Ar/^{38}Ar$ ratios indicate that only the first 2 extractions released significant amounts of terrestrial atmospheric Ar. The K/Ca ratio decreases throughout most of the extraction and suggests that the degassing of multiple mineral phases significantly overlap. None of the extractions suggest significant ^{39}Ar recoil effects. However, the age does increase slightly with extraction temperature. Nine extractions releasing ~16–69% of the ^{39}Ar give an age of 4.453 ± 0.015 Gyr. Seven extractions releasing ~69–90% of the ^{39}Ar give an age of 4.473 ± 0.012 Gyr. The age of these combined 16 extractions, releasing 74% of the total ^{39}Ar, is 4.459 ± 0.012 Gyr. The 1425°C extraction releasing ~90–99% of the ^{39}Ar gives an even higher age of 4.511 ± 0.010 Gyr. This slope in the age spectrum has 2 possible explanations. First, the age slope could signify not quite complete degassing of ^{40}Ar by an impact event ~4.45 Gyr ago. Secondly, the age slope may represent closure of the K-Ar chronometer in different K lattice sites over an extended period of time during very slow cooling of the meteorite deep in the parent body. A similar explanation was argued for sloped Ar-Ar age spectra observed in several mesosiderites (Bogard and Garrison 1995). We will adopt an age of 4.45 ± 0.01 Gyr for the case of impact degassing and an age of 4.49 ± 0.02 Gyr for the case of the early stages of slow cooling.

The isochron plot of $^{40}Ar/^{36}Ar$ versus $^{39}Ar/^{36}Ar$ for 17 extractions of GRA 98098 (12–90% ^{39}Ar release) is highly linear ($R^2 = 0.9998$) and gives a younger age of 4.444 ± 0.006 Gyr and a $^{40}Ar/^{36}Ar$ intercept of 5 ± 3. All 17 extractions, except 2, give ages that are older than this isochron age by significant amounts. This is an example of a false, rotated isochron mentioned above for the case where the Ar age increases with extraction temperature and the higher temperature extractions have lower $^{39}Ar/^{36}Ar$ ratios.

The Ar-Ar age spectrum for a vein of impact melt in GRA 98098 is shown in Fig. 1c. Except for the last extraction, which released very little Ar, both the $^{36}Ar/^{37}Ar$ and the $^{36}Ar/^{38}Ar$ ratios are nearly constant. Unfortunately, the first extraction was greatly overheated (accidentally) and released 81% of the total ^{39}Ar. Its age of 4.40 Gyr probably reflects some diffusive loss of ^{40}Ar. For subsequent extractions, the Ar-Ar age varies between 4.46 and 4.48 Gyr. Thus, we conclude that this impact melt vein probably has a similar age to the whole rock sample.

PCA 82502

This 890 g unbrecciated eucrite is listed as weathering category A (Mason et al. 1989) but has not been studied in detail. Its Ar-Ar age spectrum and K/Ca ratios as a function of ^{39}Ar release are shown in Fig. 1d. Several extractions releasing the first ~20% of total ^{39}Ar suggest some diffusive loss of ^{40}Ar. The $^{36}Ar/^{37}Ar$ and $^{36}Ar/^{38}Ar$ ratios indicate that only the first extraction released significant amounts of adsorbed terrestrial Ar. The K/Ca ratios and relative rate of release of ^{39}Ar with extraction temperature suggest that a change in phases degassing Ar occurs at ~60% ^{39}Ar release, and a decrease in the Ar-Ar age also begins to occur there. The summed Ar-Ar age above ~12% ^{39}Ar release is 4.45 Gyr and is a lower limit to the last significant degassing event. Between ~22% and ~55% ^{39}Ar release, 5 extractions with identical ages, within mutual uncertainties, show constant K/Ca and give an average age of 4.506 ± 0.009 Gyr. At even higher extraction temperatures, a second phase of lower K/Ca begins degassing, and the age decreases and then increases again. This age decrease is likely caused by the degassing of ^{39}Ar recoiled into grain surfaces of pyroxene. The source of this recoiled ^{39}Ar (surfaces of feldspar grains) probably degasses at low temperatures and is masked by ^{40}Ar diffusive loss. After these pyroxene grain surfaces have released their recoiled ^{39}Ar, the Ar-Ar age from high temperature plagioclase sites returns almost to the age level shown before the start of Ar degassing from pyroxene. We have observed this type of recoil behavior in several other meteorites. Thus, we adopt the 4.506 Gyr plateau age as giving the time of the last significant thermal event experienced by the meteorite.

The isochron plot of $^{40}Ar/^{36}Ar$ versus $^{39}Ar/^{36}Ar$ ($R^2 = 0.9965$) for those 14 extractions releasing 12–100% of the ^{39}Ar yields an age of 4.512 ± 0.028 Gyr and a negative $^{40}Ar/^{36}Ar$ intercept of –40 ± 29. This isochron age is greater than the ages of all 14 extractions, except 1, for which it is the same. This false isochron has been rotated clockwise because those extractions that released recoiled ^{39}Ar also released more cosmogenic ^{36}Ar, as discussed in the section, Methods.

PCA 91007

This 223 g unbrecciated eucrite (weathering category A/B) contains vesicles and is only moderately metamorphosed, with the original igneous texture being largely preserved (Warren et al. 1996). These authors suggested that this meteorite might represent the best example among eucrites of a quenched melt. Its Ar-Ar age spectrum (Fig. 1e) resembles that of PCA 82502, but ^{40}Ar diffusive loss and ^{39}Ar recoil redistribution are even more pronounced. The first few extractions (~0–13% ^{39}Ar release) show higher K/Ca ratios and much lower ages and suggest weathering mobilization of K and its redistribution onto grain surfaces. The first extraction (0–7% ^{39}Ar release) also suggests significant amounts of adsorbed terrestrial Ar. Three extractions releasing ~27–49% of the ^{39}Ar show the same age within their uncertainties, as well as constant K/Ca ratios, and give an average age of 4.444 ± 0.008 Gyr. The age then decreases just before a decrease in K/Ca, then increases again at higher temperatures, although it does not return to its previous high value. We attribute this

behavior to ^{39}Ar recoil, as discussed above. Whether the 4.444 Gyr plateau age defined over 27–49% ^{39}Ar release is the actual K-Ar closure time or whether it has been lowered by ^{40}Ar diffusion loss is not clear. Thus we take 4.44 Gyr as a lower limit to the time of K-Ar closure.

Caldera

The Caldera, Chile find has a chemical composition similar to main group eucrites, and its pyroxene suggests prolonged annealing (Boctor et al. 1994). After Ibitira, Caldera was the second unbrecciated, non-cumulate eucrite recognized. Our sample (obtained from R. Haag) was friable and appeared extensively weathered. The Ar age spectrum (Fig. 1f) suggests Ar release in three stages. As with PCA 91007, the first few extractions (~0–15% ^{39}Ar release) show much higher K/Ca ratios and much lower ages and suggest weathering mobilization of K and its redistribution onto grain surfaces. These first few extractions also show significant amounts of adsorbed terrestrial Ar, and corrections for air-Ar on the first extraction lowers its age to nearly zero. Over ~20–65% ^{39}Ar release, the K/Ca ratio is constant and the Ar-Ar age slowly increases, as might be expected if this meteorite phase had experienced a small amount of recent diffusive loss of ^{40}Ar caused by terrestrial weathering. Above ~65% ^{39}Ar release, the K/Ca decreases slightly, and a small ^{39}Ar recoil effect appears. The single 1400°C extraction released 18% of the total ^{39}Ar and gave an age of 4.493 ± 0.012 Gyr. The average age of 4.45 Gyr for 7 extractions releasing 40–100% of the ^{39}Ar would be a lower limit to the K-Ar age. We adopt the age of the 1400°C extraction to be the probable K-Ar closure age of Caldera.

For Caldera, Carlson and Lugamir (2000) report a Pb-Pb age of 4.516 ± 0.003 Gyr and a Sm-Nd age of 4.544 ± 0.019 Gyr. Based on ^{146}Sm-^{142}Nd, ^{147}Sm-^{143}Nd, and ^{53}Mn-^{53}Cr data, Wadhwa and Lugmair (1996) give a formation age of 4.537 ± 0.012 Gyr. The Ar-Ar age is smaller than this Sm-Nd age by an amount that is slightly greater than the combined age uncertainties but is within uncertainties of the Pb-Pb age. But, as will be discussed later, this does not mean that the actual K-Ar closure time for Caldera was earlier than ~4.49 Gyr.

Asuka-881388

This is a fine-grained, crystalline eucrite with a granulitic texture that has been thermally annealed (Takeda et al. 1997). Its Ar-Ar age spectrum is given in Fig. 2a. Slightly higher K/Ca ratios and small amounts of ^{40}Ar loss in the first ~13% of

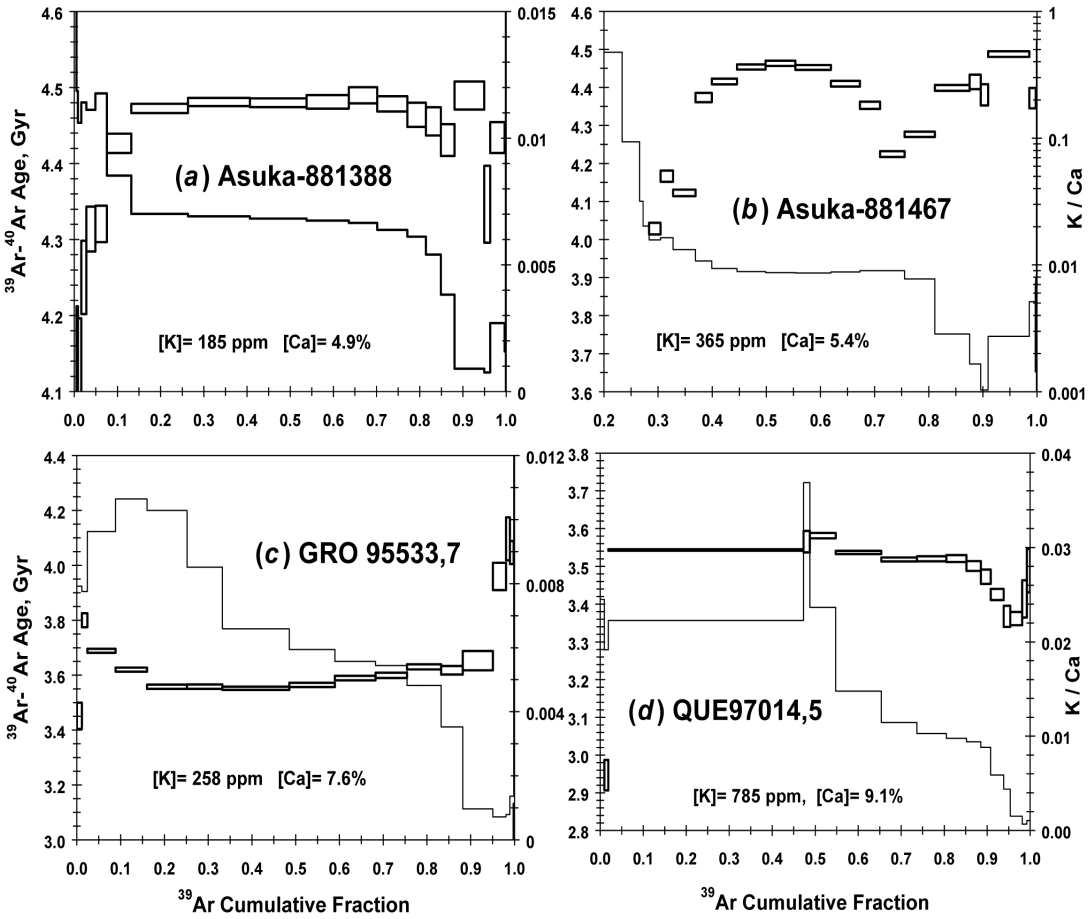

Fig. 2. ^{39}Ar-^{40}Ar ages and K/Ca ratios as a function of cumulative ^{39}Ar release for unbrecciated basaltic eucrites: a) Asuka-881388; b) Asuka-881467; c) GRO 95533; and d) QUE 97014.

the ^{39}Ar release are probably effects of terrestrial weathering. Six extractions releasing ~13–77% of the ^{39}Ar show constant K/Ca, give the same age within their uncertainties, and define an average Ar-Ar age of 4.480 ± 0.007 Gyr. If we include a seventh extraction at ~90% ^{39}Ar release, this age becomes 4.481 ± 0.007 Gyr. The small decrease in age at 77–88% ^{39}Ar release occurs from grain surfaces of a phase with much lower K/Ca and is most probably a small ^{39}Ar recoil effect.

Asuka-881467

This is a 38 g, unbrecciated, medium-grained, porphyritic eucrite (Yanai 1993) that was thermally annealed after brecciation (Yamaguchi and Misawa 2001). The Ar-Ar age spectrum is given in Fig. 2b. Much higher K/Ca ratios and very low apparent ages for the first 2 extractions (~0–26% ^{39}Ar release) are terrestrial weathering effects probably caused by mobilization and deposition of K on grain surfaces. The ^{36}Ar/^{37}Ar/^{38}Ar ratios indicate that the first two extractions also released significant amounts of adsorbed terrestrial Ar, and atmospheric ^{40}Ar probably accounts for all of the ^{40}Ar measured in these 2 extractions. Extractions releasing ~28–40% ^{39}Ar suggest a modest amount of ^{40}Ar diffusive loss. Three extractions (~45–62% ^{39}Ar release) give the same age of 4.45 Gyr within their uncertainties. A decrease in age at ~71–81% ^{39}Ar release occurs just before the point at which K/Ca decreases and suggests release of recoil-implanted ^{39}Ar. Ten extractions releasing ~40–100% ^{39}Ar, but omitting the 3 extractions with the youngest ages, give an average age of 4.42 ± 0.04 Gyr. However, the highest observed age is 4.465 ± 0.008 Gyr for a single extraction at 91–99% ^{39}Ar release. Because diffusive ^{40}Ar loss and recoiled ^{39}Ar have probably affected much of the age spectrum, ~4.46 Gyr is probably a better estimate of the time of K-Ar closure.

GRO 95533

This 613 g eucrite (weathering category A/B) is unbrecciated, but pyroxene crystals have been granulated (Antarctic Meteorite Newsletter). The Ar-Ar age spectrum is shown in Fig. 2c. The ^{36}Ar/^{37}Ar and ^{36}Ar/^{38}Ar ratios are nearly constant after the first extraction and indicate that only the first extraction released adsorbed terrestrial Ar. This means that the slightly higher ages at ~1–16% ^{39}Ar release are not produced by terrestrial ^{40}Ar, and the lower Ar-Ar ages at intermediate extraction temperatures cannot be the result of ^{40}Ar loss caused by weathering. Consequently, we interpret the higher ages at 1–16% ^{39}Ar release to be the result of the loss of recoiled ^{39}Ar. The shape of the age spectrum over 16–100% ^{39}Ar release resembles that expected if the sample had been extensively degassed of ^{40}Ar by impact heating (Turner 1969). The time of this degassing event is approximately determined by the minimum in the age spectrum. Four extractions, showing the same age within their mutual uncertainties and releasing ~16–58% of the ^{39}Ar, give an average age of 3.557 ± 0.016 Gyr. The ^{39}Ar that implanted into pyroxene grain surfaces after recoil is expected to degas around 80–95% ^{39}Ar release, where the K/Ca ratio substantially decreases and the age sharply increases. This implanted ^{39}Ar probably has depressed the smooth curvature of the expected age spectrum in this region. We infer that the degassing event seen by GRO 95533 occurred 3.55 ± 0.02 Gyr ago, which places it in the range of eucrite degassing ages previously documented for the HED parent body (Bogard 1995).

QUE 97014

The Ar-Ar age spectrum for this 142 g unbrecciated eucrite (weathering category A) is shown in Fig. 2d. The third extraction was accidentally overheated and released ~45% of the total ^{39}Ar. The ^{36}Ar/^{37}Ar/^{38}Ar ratios indicate that only the first extraction released a significant amount of terrestrial Ar. Several extractions releasing ~88–98% of the ^{39}Ar show a decrease in age and K/Ca ratios, probably due to the release of recoil-implanted ^{39}Ar. Although the 3.544 ± 0.007 Gyr age of the third extraction could be influenced by ^{39}Ar recoil loss, 6 subsequent extractions give nearly the same age. The Ar age of 7 extractions releasing ~2–85% of the ^{39}Ar is 3.540 ± 0.026 Gyr. We conclude that 3.54 ± 0.03 Gyr is the time of the impact event that totally reset K-Ar in this meteorite. This degassing time is the same as that for GRO 95533, although the 2 meteorites were recovered at different Antarctic locations.

Ibitira and EET 90020

The ^{39}Ar-^{40}Ar age spectra we measured for these 2 unbrecciated eucrites were reported previously (Table 1). Ibitira is fine-grained, vesicular, and shows a metamorphic grade of 5 (Steele and Smith 1976; Takeda and Graham 1991). In the Ar-Ar age spectrum (Bogard and Garrison 1995), 5 extractions releasing ~14–89% of the ^{39}Ar define an age of 4.487 ± 0.016 Gyr. (Note that this age differs slightly from that previously reported because of a change in the manner in which we calculate plateau ages.) Although not vesicular, EET 90020 contains 2 phases, separated by vugs, having different grain sizes and also shows type 5 metamorphism (Yamaguchi et al. 2001). The 2 phases yield essentially identical Ar-Ar age spectra, and no significant ^{39}Ar recoil effects are apparent in either age spectrum (Yamaguchi et al. 2001). For the fine-grained sample, 8 extractions releasing ~14–98% of the ^{39}Ar define an age of 4.489 ± 0.013 Gyr. For the coarse-grained sample, 8 of 9 extractions releasing ~8–95% of the ^{39}Ar define an age of 4.486 ± 0.008 Gyr. No evidence exists in either EET 90020 age spectrum for significant amounts of additional ^{40}Ar loss.

Cumulate Eucrites

Cumulate eucrites are coarse-grained gabbros principally composed of low-Ca pyroxene and calcic plagioclase. They are believed to have formed at some depth in their parent body. Extensive annealing has caused the original pigeonite to

Table 1. ^{39}Ar-^{40}Ar, Pb-Pb, ^{147}Sm-^{144}Nd, and Pu-Xe age summary (Gyr) of some eucrites.[a]

Meteorite	Ar-Ar	Pb-Pb	Sm-Nd	Pu-Xe	Reference[b]
Unbrecciated basaltic					
EET 90020	–	–	4.51 ± 0.04	–	(a)
Fine-grain	4.489 ± 0.013 (±0.035)	–	–	–	–
Coarse-grain	4.486 ± 0.008 (±0.030)	–	–	–	–
Ibitira	4.486 ± 0.016 (±0.038)	4.556 ± 0.006[c]	4.46 ± 0.02	4.581 ± 0.025	(b, c, m)
			4.41–4.57	–	(d)
QUE 97053	4.480 ± 0.015 (±0.037)	–	–	–	–
GRA 98098	4.45 ± 0.01, 4.49 ± 0.02 (±0.03 and ±0.04)	–	–	–	–
PCA 82502	4.506 ± 0.009 (±0.033)	–	–	4.559 ± 0.025	(m)
A-881388	4.480 ± 0.007 (±0.029)	–	–	–	–
PCA 91007	≥4.444	–	–	–	–
Caldera	4.493 ± 0.012 (±0.034)	4.516 ± 0.003	4.544 ± 0.019	~4.513	(e, m)
A-881467	~4.46	4.562 ± 0.011	–	–	(l)
GRO 95533	3.55 ± 0.02 (±0.04)	–	–	–	–
QUE 97014	3.54 ± 0.03 (±0.05)	–	–	–	–
Y-7308	4.48 ± 0.03 (±??)	–	–	–	(f)
Cumulate					
Moama	4.48 ± 0.01 (±0.03)	4.426 ± 0.092	4.46 ± 0.03	–	(g, h)
EET 87520	4.473 ± 0.011 (±0.032)	4.420 ± 0.020	4.547 ± 0.009	–	(i)
Moore County	4.25 ± 0.03 (±0.05)	4.484 ± 0.019	4.456 ± 0.025	~4.548	(g, m)
Serra de Magé	3.38 ± 0.03 (±0.05)	4.399 ± 0.035	4.41 ± 0.02	–	(g, j)
EET 87548	3.4 ± 0.1 (±0.12)	–	–	–	–
ALH 85001	3.6–3.7	–	–	–	–
Brecciated basaltic					
Piplia Kalan	3.5 ± 0.1 (±0.12)	(Rb-Sr = 3.96)	4.57 ± 0.023	–	(k)
Sioux County	~3.55	–	–	4.499 ± 0.017	(m)
A-87272	≤3.6	–	–	–	–
Macibini	~3.7–4.2	–	–	–	–
Eucritic clasts from howardites					
QUE 94200,13	~3.7	–	–	–	–
EET 87509,24	4.05 ± 0.02 (±0.04)	–	–	–	–
EET 87509,71	4.0 ± 0.1 (±0.12)	–	–	–	–
EET 87509,74	~4.0	–	–	–	–
EET 87531,21	3.81 ± 0.05 (±0.07)	–	–	–	–
EET 87503,53	3.70 ± 0.03 (±0.05)	–	–	–	–
EET 87503,23	~4.41	–	–	–	–

[a]All ^{39}Ar-^{40}Ar ages are JSC data, except that for Y-7308. The 2 Ar ages listed for GRA 98098 are discussed in the text. The first Ar-Ar age uncertainty given should be used when making comparisons among these Ar-Ar ages. The Ar-Ar age uncertainty given in parentheses contains an additional factor based on the uncertainty in the NL-25 hornblende monitor age and should be used when comparing these Ar-Ar ages with ages based on other chronometers. Pb-Pb and Sm-Nd isochron ages are taken from the cited references.

[b]References: (a) Yamaguchi et al. 2001; (b) Chen and Wasserburg 1985; (c) Prinzhofer et al. 1992; (d) Nyquist et al. 1999; (e) Carlson and Lugmair 2000; (f) Kaneoka 1981; (g) Tera et al. 1997; (h) Jacobsen and Wasserburg 1984; (i) Lugmair et al. 1991; (j) Lugmair et al. 1977; (k) Kumar et al. 1999; (l) Misawa and Yamaguchi 2001; (m) Shukolyukov and Begemann 1996.

[c]The Pb age for Ibitira is a model age.

undergo complex subsolidus exsolution of augite and sometimes inversion to orthopyroxene, with the result that some meteorites contain multiple pyroxene phases (see Mittlefehldt et al. 1998a). Pyroxene textures generally suggest very slow subsolidus cooling. Plagioclase in cumulates is more calcic (generally $An_{91–95}$) compared to plagioclase in basaltic eucrites, and consequently, the K concentrations in cumulates are lower. Many cumulate eucrites are unbrecciated, and plagioclase generally does not show zoning or shock effects. However, 2 of the specimens discussed below (ALH 85001 and EET 87548) do show signs of brecciation (Mittlefehldt et al. 1998a). As we shall see, these 2 cumulate eucrites also show younger Ar ages reset by later impacts.

Moama

The sample of Moama that we analyzed was received courtesy of M. Grady and the British Natural History Museum. The Ar-Ar age spectrum shows significant effects

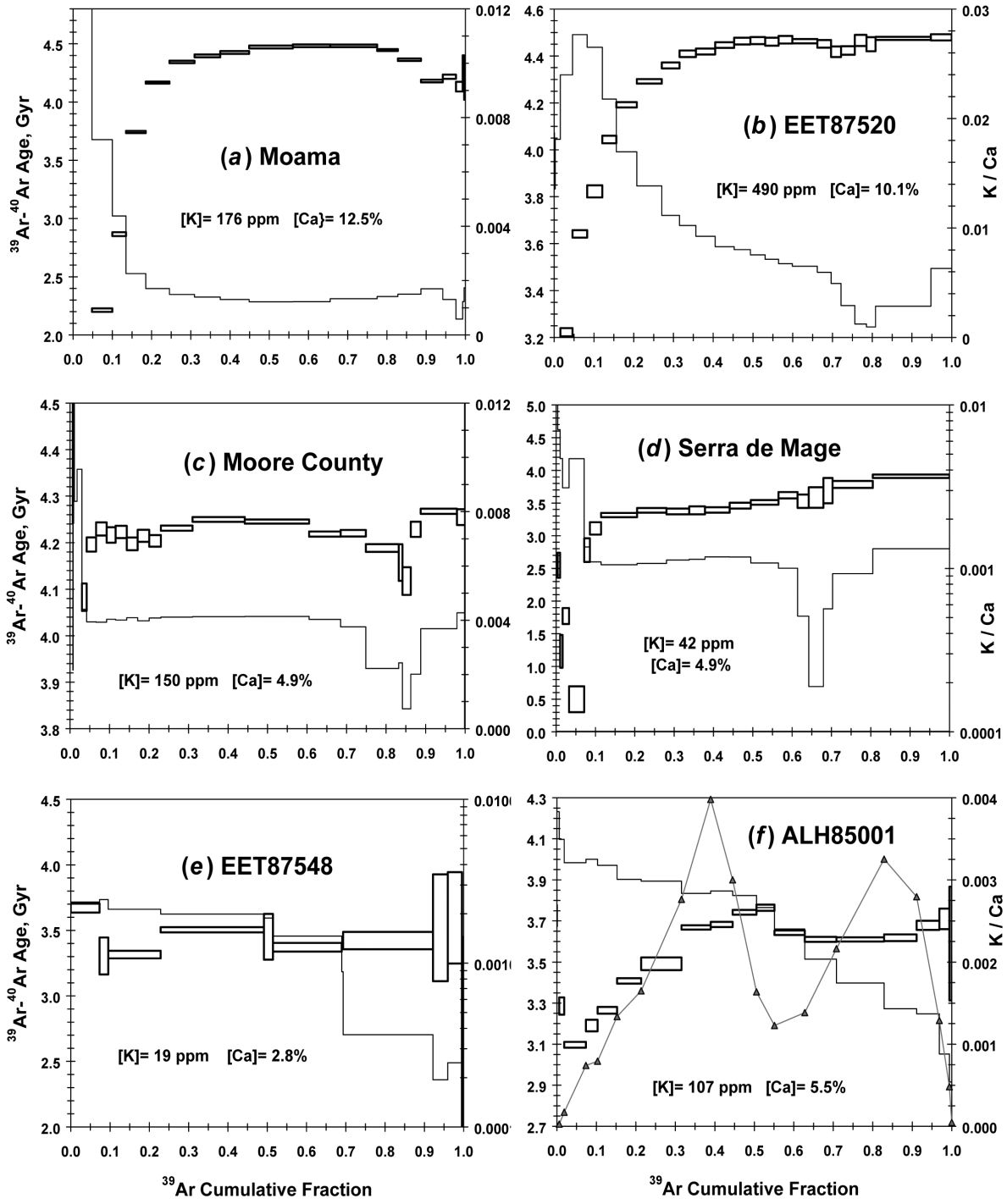

Fig. 3. ^{39}Ar-^{40}Ar ages and K/Ca ratios as a function of cumulative ^{39}Ar release for cumulate eucrites: a) Moama; b) EET 87520; c) Moore County; d) Serra de Magé; e) EET 87548; and f) ALH 85001. For ALH 85001, the two-phase, differential release of ^{39}Ar (in relative units) is also indicated.

of both ^{40}Ar diffusive loss and ^{39}Ar recoil (Fig. 3a). The K/Ca ratios are considerably higher for the first few extractions, but the ^{36}Ar/^{37}Ar/^{38}Ar ratios indicate that very small amounts of adsorbed terrestrial Ar were released only in the first 2 extractions. The Ar-Ar age spectrum up to ~45% ^{39}Ar release resembles that expected for a sample that has lost a portion of its radiogenic ^{40}Ar by diffusion from low temperature sites in relatively recent times (Turner 1969). The average age of 3 extractions releasing ~45–78% of the ^{39}Ar and showing the same age within their uncertainties is 4.480 ± 0.007 Gyr. Above 78% ^{39}Ar release, the age decreases, possibly due to release of recoil-implanted ^{39}Ar, although the K/Ca ratio does

not show a correlated decrease. We adopt 4.48 ± 0.01 Gyr as a minimum age for the time of K-Ar closure. With the reasonable assumption that these 3 extractions have lost little ^{40}Ar by diffusion and were not affected by ^{39}Ar recoil, 4.48 ± 0.01 Gyr could also date the last closure time. Tera et al. (1997) reported a four-point Pb-Pb isochron age of 4.416 ± 0.092 (some phases lay off this isochron) for Moama. Jacobson and Wasserburg (1984) reported a Sm-Nd isochron age for Moama of 4.46 ± 0.03 Gyr. These 3 ages agree within their relative uncertainties.

EET 87520

This 52 g eucrite (weathering category B) was classified as Mg-rich and described as possessing a cumulate-like composition and Mg-rich pyroxene unlike that in diogenites (Grossman 1994). However, the 490 ppm K concentration for our sample seems high for a cumulate. The Ar-Ar age spectrum (Fig. 3b) closely resembles that expected for a sample that has lost some of its radiogenic ^{40}Ar by diffusion from low temperature sites in relatively recent times (Turner 1969). The ^{36}Ar/^{37}Ar/^{38}Ar ratios indicate that only the first 2 extractions released significant amounts of adsorbed terrestrial Ar. The overall decrease in K/Ca ratios throughout most of the extraction, followed by an increase in K/Ca above 80% ^{39}Ar release, suggests overlapping degassing of multiple mineral phases. The small decrease in age and K/Ca ratio at ~70–75% ^{39}Ar release is probably due to release of recoil-implanted ^{39}Ar from surfaces of pyroxene grains. Twelve extractions releasing ~45–100% ^{39}Ar show relatively constant ages with an average age of 4.463 ± 0.020 Gyr. However, this average age may be a lower limit because of the small ^{39}Ar recoil effect and because a small amount of ^{40}Ar diffusive loss may have occurred from some of the intermediate temperature sites. If we omit the 2 extractions that suggest ^{39}Ar recoil (~70–75% ^{39}Ar release), then 10 extractions releasing 49% of the total ^{39}Ar define an age of 4.468 ± 0.011 Gyr. The last 4 extractions (~76–100% ^{39}Ar release) are the least likely to have been affected by Ar diffusive loss and give identical ages within their respective uncertainties. The weighted age of these 4 extractions is 4.473 ± 0.011 Gyr. We conclude that the last K-Ar closure time for EET 87520 was 4.471 ± 0.011 Gyr ago.

Lugmair et al. (1991) reported variable disturbance in the ages of EET 87520 obtained using other isotopic chronometers. Rb-Sr was highly disturbed and no age was reported. The Sm-Nd data defined ages of 4.598 ± 0.007 Gyr or 4.547 ± 0.009 Gyr, depending on the specific mineral separates included in the isochron. The Pb-Pb was described as being "decidedly younger than the Sm-Nd age" but disturbed and imprecise. However, Carlson and Lugmair (2000) report a Pb-Pb age for EET 87520 of 4.420 ± 0.020 Gyr (and a Sm-Nd age of 4.547 Gyr). Possible explanations for these age variations are given in the section, Discussion of Ages of Cumulate and Unbrecciated Eucrites.

Moore County

The Ar-Ar age spectrum for this cumulate eucrite is shown in Fig. 3c. The ^{36}Ar/^{37}Ar/^{38}Ar ratios indicate that only the first 2 extractions (<1% of the ^{39}Ar) released significant amounts of adsorbed terrestrial Ar. The K/Ca ratio is constant except for a small K enhancement in the first few extractions and a decrease in K/Ca at ~75–89% ^{39}Ar release. This K/Ca decrease is accompanied by a decrease in Ar-Ar age and probably reflects the release of recoil-implanted ^{39}Ar from pyroxene grain surfaces. The summed Ar age above 4% ^{39}Ar release is 4.227 Gyr. The age defined by 12 extractions releasing ~4–75% ^{39}Ar is essentially the same at 4.230 ± 0.006 Gyr. If we also include the 3 extractions releasing over ~86–100% ^{39}Ar release in this average, the age becomes 4.235 ± 0.007 Gyr. However, ages of extractions releasing ~5–45% of the ^{39}Ar are slightly lower, suggesting a small amount of ^{40}Ar diffusive loss, and the age shown by 2 extractions at >89% ^{39}Ar release is slightly higher at 4.26 Gyr. For the time of last significant Ar degassing of Moore County, we adopt an age of 4.25 ± 0.03 Gyr, where the error overlaps all these age combinations. Tera et al. (1997) reported a six-point Pb-Pb isochron age for Moore County of 4.484 ± 0.019 Gyr (data for some phases lay off this isochron) and a Sm-Nd isochron age (pyroxene, plagioclase, and whole rock) of 4.456 ± 0.025 Gyr (95% uncertainties). Thus the Ar-Ar age of Moore County seems to have been reset more recently than these other 2 chronometers.

Serra de Magé

Chemically, this is a cumulate eucrite, but its mineral texture is unlike that of most other cumulate eucrites, and after igneous formation, it was metamorphosed to ~838°C (Treiman and Goldman 2002). Our sample was received courtesy of B. Zanda and the Museum National D'Histoire Naturelle in Paris. The Ar-Ar age spectrum is shown in Fig. 3d. Although our sample contained only 42 ppm K, analytical uncertainties in calculated ages are relatively small. The ^{36}Ar/^{37}Ar/^{38}Ar ratios indicate that only the first 2 extractions released significant amounts of adsorbed terrestrial Ar. Significant diffusive loss of ^{40}Ar is shown by the first few extractions (0–8% ^{39}Ar release) from a phase with slightly higher K/Ca ratios, which suggests some concentration of K on grain surfaces. The decrease in K/Ca at ~61–70% ^{39}Ar release probably represents the degassing of ^{37}Ar from pyroxene grain surfaces, but the age spectrum in this region gives no indication of ^{39}Ar recoil effects. (The larger age uncertainties for these 3 extractions is due to the larger applied ^{39}Ar/^{37}Ar corrections.) The age spectrum over ~11–100% ^{39}Ar release resembles that expected from a sample strongly, but not completely, degassed by an impact heating event <3.5 Gyr ago (Turner 1969). Even the very retentive ^{40}Ar degassed in the 1500°C extraction (releasing ~20% of the total ^{39}Ar) gives an age of only 3.9 Gyr. Four extractions releasing ~21–45% of the ^{39}Ar have the same age within their individual uncertainties and give an average age of 3.386 ±

0.007 Gyr. From these data, we suggest that Serra de Magé was strongly degassed by an impact event 3.38 ± 0.03 Gyr ago. The Pb-Pb age (4.399 ± 0.035 Gyr; Tera et al. 1997) and the Sm-Nd age (4.41 ± 0.02 Gyr; Lugmair et al. 1977) are also considerably younger than a canonical age of 4.55 Gyr.

EET 87548

This 560 g eucrite (weathering category B/C) was classified as Mg-rich and described as possessing a cumulate-like composition and Mg-rich pyroxene unlike that in diogenites (Grossman 1994). The Ar-Ar age spectrum (Fig. 3e) is relatively flat. The relatively larger uncertainties and scatter among individual ages are due to the fact that our sample contained only 19 ppm K. (Blank corrections to ^{40}Ar, typically, were only a few percent, and those to ^{39}Ar were even smaller. Correction for ^{39}Ar produced from Ca in the reactor is the major contributor to the error in ages.) The average age, omitting 2 extractions releasing very small amounts of ^{40}Ar, is 3.44 ± 0.13 Gyr. If we omit the first extraction, the age is 3.42 ± 0.10 Gyr. (Only the first extraction suggests very small amounts of adsorbed terrestrial Ar.) We conclude that this meteorite was completely degassed by an impact event 3.4 ± 0.1 Gyr ago.

ALH 85001

This 212 g eucrite (weathering category A/B) was classified as Mg-rich and described as having a cumulate-like composition and Mg-rich pyroxene unlike that in diogenites (Grossman 1994; Warren and Ulff-Møller 1999). The Ar-Ar age spectrum is given in Fig. 3f. The ^{39}Ar/^{37}Ar/^{38}Ar ratios indicate that only the first 2 extractions released significant amounts of terrestrial Ar. The age spectrum appears complex in part because K was released in 2 distinct phases that might represent 2 different grain-size populations of feldspar possessing different Ar diffusion properties. These 2 phases are shown in Fig. 3f by the curve giving the relative rate of release of ^{39}Ar as a function of temperature, which defines 2 distinct peaks at ~39% and ~83% of the ^{39}Ar release. The Ar age spectrum needs to be interpreted independently for these 2 K-bearing phases. We interpret the age spectrum over ~2–55% ^{39}Ar release as a diffusion loss profile from the first K-bearing phase and the age spectrum over ~55–100% ^{39}Ar release as a separate diffusion loss profile from the second phase. The reasonable presumption is that the original meteorite age was ~4.5 Gyr and that both phases were strongly degassed. The age spectrum for the first, lower temperature phase indicates degassing by an event <3.1 Gyr ago, but part of this ^{40}Ar loss might have been produced by diffusive loss of ^{40}Ar during Antarctic weathering, as is observed commonly in Antarctic meteorites. The age spectrum for the second, higher temperature phase shows 3 extractions (63–83% ^{39}Ar release) having a common age with an average value of 3.613 ± 0.005 Gyr. The oldest age shown by this phase is only 3.71 ± 0.05 Gyr. Thus, we interpret these data to indicate almost complete degassing of this high temperature phase 3.61 ± 0.01 Gyr ago. The time of the impact event is unlikely to exceed the oldest age of ~3.7 Gyr. Whether a younger event occurred <3.1 Gyr ago and degassed only the low temperature phase cannot be determined from the data.

Brecciated Basaltic Eucrites

In addition to showing varying degrees of metamorphism, basaltic and brecciated eucrites have experienced impact heating and brecciation on their parent body (Mittlefehldt et al. 1998a). Bogard (1995) summarized available Ar-Ar, Rb-Sr, and Pb-Pb impact-reset ages of eucrites and concluded that most impact heating occurred over the relatively limited time interval of ~4.1–3.4 Gyr ago. Bogard (1995) suggested that this epoch constituted an impact cataclysm on the HED parent body analogous to the impact cataclysm that occurred on the moon ~3.8–4.0 Gyr ago (Tera et al. 1974). Since this review of HED impact ages, we have obtained Ar-Ar ages on several additional brecciated basaltic eucrites. Further, we report here the Ar-Ar age spectra for eucritic clasts in some howardites for which only the derived age was presented earlier. The impact heating experienced by most eucrites probably was not sufficient to significantly alter mineral textural evidence of an earlier period of metamorphism, as is discussed below.

Piplia Kalan

This equilibrated, monomict breccia (1996 fall) is related to main group eucrites and could represent a single lava flow or a shallow intrusive body. Piplia Kalan gives evidence of extensive thermal metamorphism, and transecting veins of glass document a later shock event (Buchanan et al. 2000a). Piplia Kalan is the first eucrite to show evidence of excess ^{26}Mg derived from extinct ^{26}Al, which requires that melting and basalt formation occurred on the parent body within a few million years after solar system formation (Srinivasan et al. 1999). Our sample was obtained from G. Srinivasan of the Physical Research Laboratory, India. The Ar-Ar age spectrum of Piplia Kalan (Fig. 4a) clearly shows the effects of impact heating. The ^{36}Ar/^{37}Ar and ^{36}Ar/^{38}Ar ratios are relatively constant, except for the first extraction, which alone shows the presence of terrestrial Ar. Higher ages for 4 extractions releasing ~2–30% of the ^{39}Ar are not produced by terrestrial Ar contamination but may be the consequence of recoil loss of ^{39}Ar from feldspar grain surfaces. In this case, recoiled ^{39}Ar could reside in those extractions releasing at ~80–90% ^{39}Ar release, where the K/Ca ratio and the age decrease. This suggests that the upward slope of the true age spectrum at higher extraction temperatures could be much steeper than that shown in Fig. 4a and that the impact degassing event could be younger than the youngest measured age of 3.54 Gyr. On the other hand, the higher ages at lower extraction temperatures may be caused by trapped radiogenic ^{40}Ar

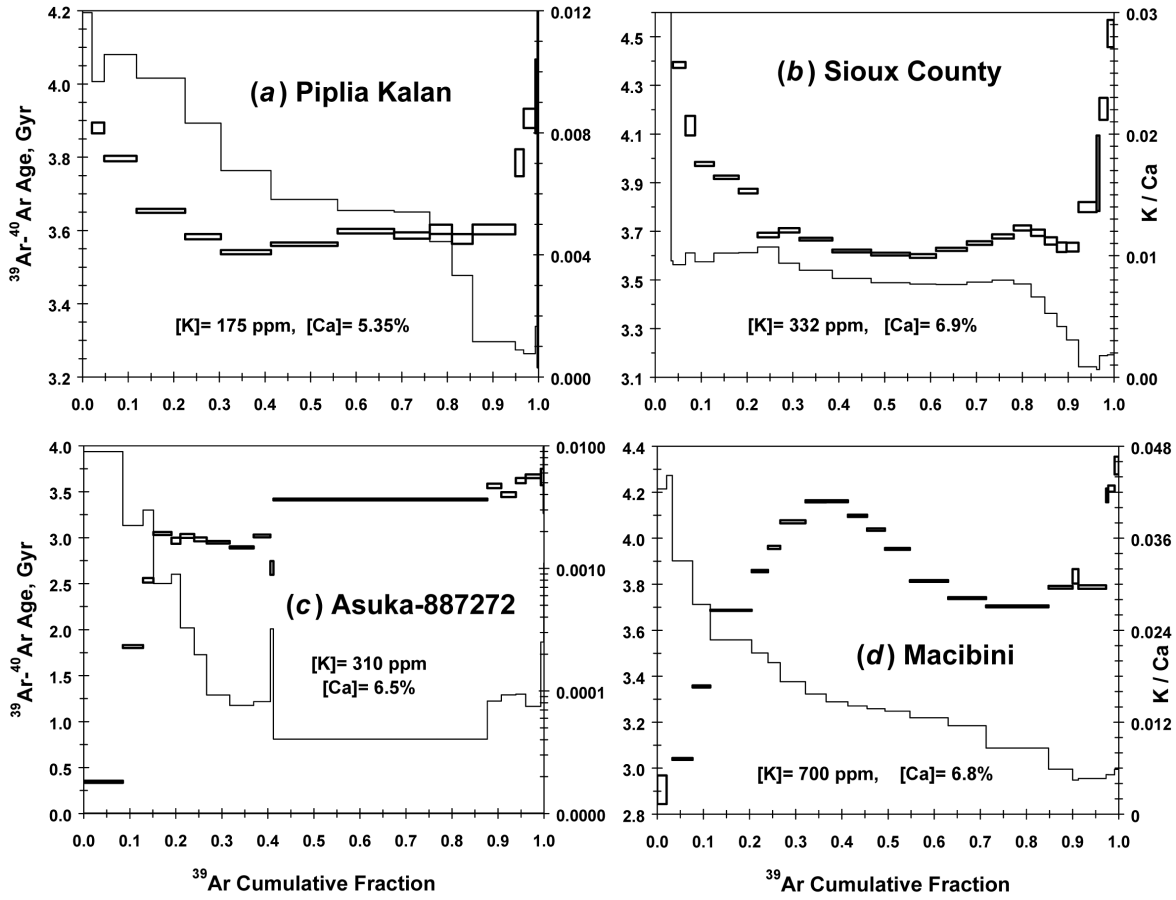

Fig. 4. ^{39}Ar-^{40}Ar ages and K/Ca ratios as a function of cumulative ^{39}Ar release for brecciated basaltic eucrites: a) Piplia Kalan; b) Sioux County; c) Asuka-887272; and d) Macibini.

mobilized by the shock event. Such "saddle-shaped" Ar age spectra are observed in some strongly shocked chondrites (Bogard and Hirsch 1980) and some terrestrial samples (McDougall and Harrison 1999). Isochron plots (^{40}Ar/^{36}Ar versus ^{39}Ar/^{36}Ar) for Piplia Kalan seem to support the second interpretation over the first. An isochron plot of 11 extractions releasing 30–100% of the ^{39}Ar (R^2 = 0.997) gives an age of 3.51 ± 0.03 Gyr and a ^{40}Ar/^{36}Ar intercept of 34 ± 10. An isochron plot of 7 extractions releasing 30–95% of the ^{39}Ar (R^2 = 0.999) gives an age of 3.55 ± 0.03 Gyr and a ^{40}Ar/^{36}Ar intercept of 11 ± 11. These positive intercepts suggest the presence of ^{40}Ar not degassed by the impact rather than a gain of recoiled ^{39}Ar. We conclude that the impact heating occurred 3.5 ± 0.1 Gyr ago and, possibly, ~3.55 Gyr ago.

Piplia Kalan gives a Sm-Nd whole rock isochron age of 4.57 ± 0.023 Gyr (Kumar et al. 1999) and a very old Pu-Xe age (Bhandari et al. 1998). A Rb-Sr whole rock isochron gives an apparent age of 3.963 ± 0.119 Gyr (Kumar et al. 1999). The Rb-Sr age is similar to the Ar-Ar age of ~3.9 Gyr shown by 3 extractions releasing ~97–100% of the ^{39}Ar, but whether this age of ~3.9 Gyr represents an earlier heating event or incomplete chronometer resetting cannot be determined. Some other shock-heated meteorites also indicate greater ease of resetting of Ar-Ar and Rb-Sr ages by shock heating in comparison to Sm-Nd and Pu-Xe ages.

Sioux County

Some controversy exists as to whether this main group eucrite is a primary partial melt, an orthocumulate, or a polymict breccia (Mittlefehldt et al. 1998b; Yamaguchi et al. 1997). The dominant lithic clast in Sioux County is a basalt or diabase, but less common gabbro clasts also exist. Several of the basalt clasts weighing ~4 g were crushed and homogenized to obtain material for various studies (D. Mittlefehldt 1997, personal communication), and we analyzed a sample of this powder. The Ar-Ar age spectrum of Sioux County (Fig. 4b) clearly shows the effects of impact heating, which would be consistent with a brecciation history. Eight extractions releasing ~22–74% of the ^{39}Ar define a broad age minimum and an average age of 3.64 ± 0.04 Gyr. The first extraction, with much higher K/Ca, has lost much of its ^{40}Ar. Several extractions releasing ~4–22% ^{39}Ar show higher ages. The ^{36}Ar/^{37}Ar ratios for the first 12 extractions systematically decrease by a factor of 15 and suggest the release of adsorbed terrestrial Ar. (This relatively large amount of terrestrial Ar is probably the result of our sample having been a powder.)

When an air-Ar correction is applied using the minimum measured $^{36}Ar/^{37}Ar$ ratio (see Garrison et al. 2000), the average age of those extractions releasing ~3–74% ^{39}Ar becomes 3.57 ± 0.08 Gyr. However, an isochron plot of those 6 extractions releasing ~4–22% ^{39}Ar gives an age of 3.19 ± 0.08 Gyr and a trapped $^{40}Ar/^{36}Ar$ intercept of 282 ± 21, which is in agreement with the terrestrial atmospheric ratio. This isochron age is younger than the minimum in the measured age spectrum and suggests some diffusive loss of ^{40}Ar at lower temperature. Some ^{39}Ar recoil loss possibly has occurred as well, and the slight drop in age at ~85–92% ^{39}Ar release (where a decrease in K/Ca suggests that pyroxene starts to degas Ar) may reflect the release of recoil-implanted ^{39}Ar. Although the time of major impact heating of Sioux County is uncertain because of the significant terrestrial Ar component, it is unlikely to have occurred earlier than 3.64 Gyr ago and probably occurred 3.5–3.6 Gyr ago. Tatsumoto et al. (1973) reported a Pb-Pb age for Sioux County of 4.526 ± 0.01 Gyr, which is similar to the Ar-Ar age of the 1400°C extraction.

Asuka-87272

This 5.7 kg eucrite is a monomict breccia consisting of coarse pyroxene and plagioclase grains set in a finer-grained ground mass that has been recrystallized to a granulitic texture (Takeda et al. 1997). The composition of the pyroxenes resembles that of ordinary eucrites, but the possible inversion to orthopyroxene suggests extensive metamorphism. The Ar-Ar age spectrum (Fig. 4c) indicates extensive resetting by impact heating. Overall, the age spectrum suggests a modest amount of recent diffusive loss of ^{40}Ar, but the shape is distorted because of the accidental overheating of the 1075°C extraction (41–87% ^{39}Ar release). None of the extractions suggest a significant release of adsorbed terrestrial Ar, and no obvious ^{39}Ar recoil effects are observed, although, the slightly higher ages at ~15–32% ^{39}Ar release may be due to ^{39}Ar recoil loss. The last 4 extractions (releasing ~94–100% of the ^{39}Ar) give ages of 3.60–3.65 Gyr, which may be an upper limit to the time of impact heating. The several extractions showing ages of ~3.0 Gyr (~15–40% ^{39}Ar release) may represent a second, later heating event.

Macibini

This fragmental, polymict eucrite breccia (1936 fall) was described by Buchanan et al. (2000b). The clasts display a variety of postcrystallization metamorphism, and some clasts are impact-melt breccias with a devitrified groundmass. The sample we analyzed (obtained from P. Buchanan) was largely impact glass, incorporating some melt matrix, from one of these impact-melt breccias. The Ar age spectrum (Fig. 4d) is complex and may indicate that 2 or more heating events are recorded in the sample. Ar degassing ages between ~3.7 and ~4.2 Gyr are suggested, but specific degassing events cannot be uniquely identified.

Howardites

We also have analyzed several eucritic clasts extracted from a few Antarctic howardites. One (QUE 94200) was analyzed recently, but several Elephant Moraine samples were analyzed during the period of 1990–92. Based on chemical composition, Mittlefehldt and Lindstrom (1991) suggested that these EET meteorites contained ~15–35% diogenetic component. Because howardites are brecciated mixtures of eucritic and diogenitic material originating from different depths within the parent body, they, obviously, have experienced multiple impacts. One purpose of these studies was to compare reset Ar ages of eucrites with those of individual howardite clasts. These samples also showed varying degrees of terrestrial weathering. The Ar-Ar data for EET howardites discussed below have not been reported in detail. A few of the ages reported here differ slightly, but not significantly, from those used by Bogard (1995).

QUE 94200,13

This is a 165 g howardite (weathering class A/B) from which we analyzed a clast consisting of pyroxene phenocrysts set in a fine-grained groundmass of pyroxene and plagioclase (Mittlefehldt and Lindstrom 1998). This clast has a bulk composition intermediate between howardites and polymict eucrites and may represent an impact melt of a trace element-rich polymict eucritic target rock (Mittlefehldt and Lindstrom 1998). The Ar-Ar age spectrum (Fig. 5a) over ~0–52% ^{39}Ar release indicates modest amounts of diffusive loss of ^{40}Ar possibly caused by weathering. A small decrease in age where the K/Ca falls sharply (~85–95% ^{39}Ar release) suggests the release of recoil-implanted ^{39}Ar, and the higher age seen in the third extraction (~2–11% ^{39}Ar release) may be the source of this recoiled ^{39}Ar. The $^{36}Ar/^{37}Ar/^{38}Ar$ ratios are relatively flat across all extractions and indicate that only the first extraction released measurable amounts of terrestrial Ar. The approximate time of impact degassing is probably given by 2 extractions releasing ~53–83% of the total ^{39}Ar, which give the same age of 3.71 ± 0.01. We assign a degassing age of ~3.7 Gyr.

EET 87509

We analyzed 3 clasts from this meteorite. Clast Q (24) shows skeletal phenocrysts in a fine-grained groundmass; Clast D (71) is very fine-grained and has a texture indicative of rapid cooling with no evidence of subsequent annealing; and Clast E (74) is porphyritic in a fine-grained groundmass (Buchanan and Reid 1990, 1991). The clasts show varying degrees of quench textures (some suggesting rapid cooling), and the matrix contains glass fragments (Buchanan et al. 1999). These authors suggested that the matrix contains <10% diogenitic material and that the meteorite should be classified as a polymict eucrite.

The Ar-Ar age spectra for 3 different eucritic clasts (24,

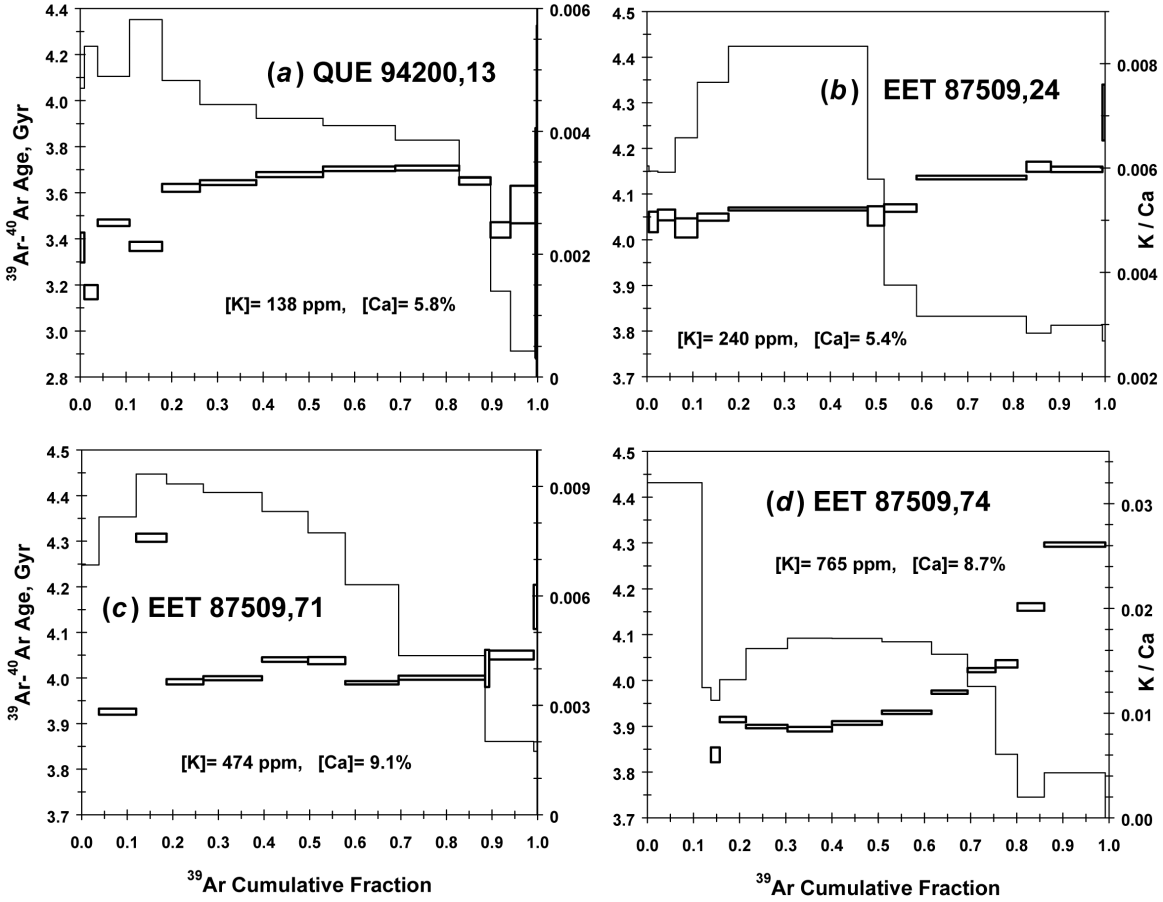

Fig. 5. ^{39}Ar-^{40}Ar ages and K/Ca ratios as a function of cumulative ^{39}Ar release for eucritic clasts in howardites: a) QUE 94200; b) EET 87509,24; c) EET 87509,71; and d) EET 87509,74.

71, and 74) are given in Figs. 5b–5d, all to the same age scale. All 3 clasts have been impact degassed. The age spectrum for EET 87509,24 shows a step in age at ~58% ^{39}Ar release, which correlates with a decrease in K/Ca ratio and with evidence from the rate of release of ^{39}Ar for distinct K-bearing phases. The ^{36}Ar/^{37}Ar ratios suggest that only the first extraction released significant amounts of terrestrial ^{40}Ar. The age of 7 extractions releasing ~1–58% of the ^{39}Ar is 4.059 ± 0.016 Gyr, and the age of 3 extractions releasing ~58–99% of the ^{39}Ar is 4.144 ± 0.013 Gyr. The lower age plateau may itself consist of 2 separate age plateaus of 4.043 ± 0.014 (1–17% ^{39}Ar release) and 4.067 ± 0.011 Gyr (17–58% ^{39}Ar release). We conclude that the time of the most recent heating of this clast was 4.05 ± 0.02 Gyr ago. The older plateau age at higher extraction temperatures may represent an early heating event or incomplete ^{40}Ar degassing during the ~4.05 Gyr event.

The Ar age spectrum for EET 87509,71 (Fig. 5c) shows a similar degree of degassing. The average age for 8 extractions releasing 4–99% of the ^{39}Ar is 4.013 ± 0.025 Gyr. We offer 3 possible interpretations for this age spectrum and the separate, upward slope in age over ~4–58% ^{39}Ar release and ~58–99% ^{39}Ar release. First, extractions releasing 58–89% of the ^{39}Ar may contain small amounts of recoiled ^{39}Ar that originated from extractions releasing <18% ^{39}Ar. This explanation suggests that the time of last impact heating was 4.0–4.1 Gyr ago. Secondly, these separate age slopes may represent small amounts of ^{40}Ar diffusion loss over time, possibly caused by terrestrial weathering, from distinct K-bearing domains degassing at different extraction temperatures (cf. Fig. 3f). This explanation also implies that the last time of impact degassing was ~4.0–4.1 Gyr ago. Thirdly, the age slopes may have been produced by severe but not quite complete Ar loss during impact heating ~3.9–4.0 Gyr ago. Thus, we adopt an impact degassing age of 4.0 ± 0.1 Gyr for clast 71. This age could be identical to that derived for clast 24.

The first extraction of EET 87509,74 shows significant ^{39}Ar release, a relatively large K/Ca ratio, and an apparent age of ~0.7 Gyr (Fig. 5d). These observations suggest that some K was mobilized during terrestrial weathering and was deposited on grain surfaces. Atmospheric ^{40}Ar corrections were applied to the first few extractions (0–30% ^{39}Ar release). The resulting Ar age spectrum indicates partial ^{40}Ar degassing from an initial age of >4.3 Gyr, with an age plateau suggested at intermediate temperatures. Four extractions releasing ~15–51% of the ^{39}Ar have similar ages, give an

average age of 3.90 ± 0.01 Gyr, and may define the time of last impact degassing for this clast. Given the complexity of the age spectrum, the Ar degassing age of this clast may or may not be different from the other 2 EET 87509 clasts.

EET 87531,21

This sample derived from a large eucritic clast (J) that appears moderately recrystallized and contains inhomogeneous pyroxenes (Buchanan and Reid 1991). Buchanan et al. (1999) concluded that EET 87531 is paired with EET 87509. The Ar age spectrum for our sample (Fig. 6a) suggests a ^{40}Ar degassing profile from an initial age of >4.3 Gyr. The ^{36}Ar/^{37}Ar ratios indicate that only the first extraction released significant terrestrial Ar. Five extractions releasing ~3–67% of the ^{39}Ar give an average age of 3.81 ± 0.03 Gyr, and 3 extractions releasing ~14–55% of the ^{39}Ar give an age of 3.817 ± 0.010. We conclude that the time of the last impact degassing of this clast occurred at 3.81 ± 0.03 Gyr. Likely, this degassing age is distinct from that determined above for EET 87509,24.

EET 87503

Buchanan et al. (1999) suggested that this meteorite is a howardite and is paired with EET 87513. Nyquist et al. (1994) reported concordant Rb-Sr and Sm-Nd isochron ages of ~4.5 Gyr for one clast from EET 87513. However, these isotopic systems for clast EET 87503,53 were severely disturbed, although, apparently not by terrestrial weathering. The ^{36}Ar/^{37}Ar/^{38}Ar ratios for our sample of clast EET 87503,53 indicate that only the first extraction released significant terrestrial Ar. The Ar-Ar age (Fig. 6b) indicates extensive impact heating. Four extractions releasing ~31–76% of the ^{39}Ar give the same age within their uncertainties and an average value of 3.682 ± 0.008 Gyr. Likely, slightly higher ages for 3 extractions releasing ~2–31% of the ^{39}Ar and slightly lower ages for 2 extractions releasing ~76–87% of the ^{39}Ar are caused by ^{39}Ar recoil redistribution. The total age (all extractions) is 3.74 Gyr, and the age for ~2–95% ^{39}Ar release is 3.70 Gyr. We conclude that the time of impact degassing of this clast occurred at 3.70 ± 0.03 Gyr ago, with a most probable time of 3.68 Gyr.

The Ar age spectrum for clast EET 87503,23 (Fig. 6c) is very different from that for clast 53, which implies different thermal histories. Extractions releasing <65% of the ^{39}Ar show major losses of ^{40}Ar. However, 5 extractions of clast 23, releasing ~65–100% of the ^{39}Ar, show nearly the same age and give an average value of 4.407 ± 0.013 Gyr. The ^{36}Ar/^{37}Ar/^{38}Ar ratios are relatively constant throughout the extraction and indicate that the elevated ages over ~0–16% release are not due to adsorbed terrestrial Ar. No obvious evidence exists for ^{39}Ar recoil redistribution. We suggest that this clast has experienced 2 degassing events. One occurred ~4.407 Gyr ago, and a second, less severe degassing occurred much more recently and affected only low and intermediate

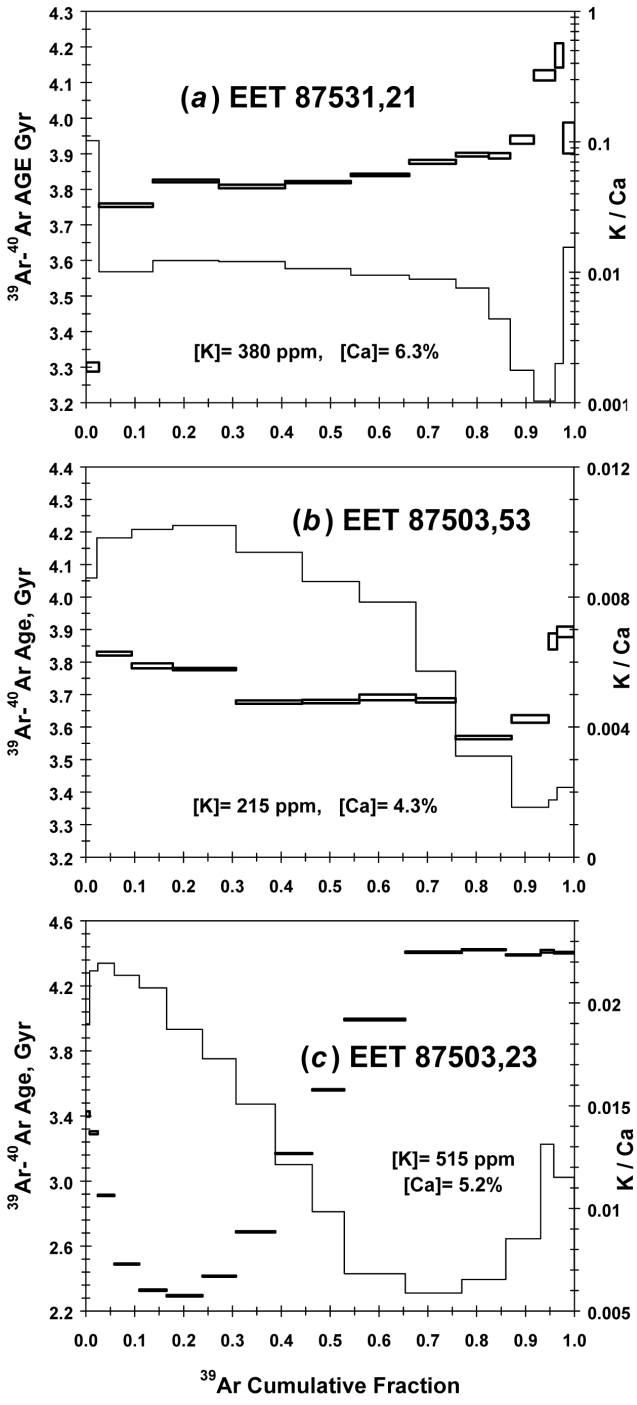

Fig. 6. ^{39}Ar-^{40}Ar ages and K/Ca ratios as a function of cumulative ^{39}Ar release for eucritic clasts in howardites: a) EET 87531,21; b) EET 87503,53; and c) EET 87503,23.

temperature sites. The second degassing event for clast 23 probably occurred on the parent body before breccia assembly. This second event only degassed ^{40}Ar from low temperature diffusion sites, and rapid cooling trapped some of this mobilized ^{40}Ar. Similar "saddle-shaped" Ar age spectra are observed in strongly shocked chondrites and in some

terrestrial samples containing excess ^{40}Ar (Bogard and Hirsch 1980; McDougall and Harrison 1999).

DISCUSSION OF AGES OF CUMULATE AND UNBRECCIATED EUCRITES

Age Comparisons

A summary of available radiometric ages of individual cumulate and unbrecciated eucrites is given in Table 1. All such ages ≥4.3 Gyr are compared in Fig. 7. We also plot the Ar-Ar age of 4.48 ± 0.03 Gyr reported for a clast from howardite Y-7308 (Kaneoka 1981), which is the only additional "precise" Ar-Ar age >4.3 Gyr of which we are aware. When comparing the Ar-Ar ages determined at JSC, the smaller age uncertainties that do not consider error in the NL-25 monitor age should be used (Table 1). When comparing these Ar-Ar ages with the ages determined using other isotopic chronometers, one should use the larger Ar age uncertainties that do consider the monitor age.

The ^{39}Ar-^{40}Ar ages of unbrecciated and cumulate eucrites having an age greater than ~4.3 Gyr cluster within a narrow age range of ~4.46–4.51 Gyr. Six such meteorites with relatively small and overlapping Ar-Ar age uncertainties (Ibitira, EET 90020, QUE 97053, A-881388, Moama, and EET 87520) define an age of 4.48 ± 0.01 Gyr. The higher temperature plateau age of GRA 98098 (4.49 ± 0.02 Gyr) is consistent with this age cluster, while the age of PCA 82502 (4.506 ± 0.009 Gyr) is slightly older. Further, the Ar-Ar ages of the 4 other meteorites (Caldera, A-881467, PCA 91007, and Y-7308) could well be consistent with an age of 4.48 ± 0.01 Gyr, given their larger uncertainties. Five eucrites (GRO 95533, QUE 97014, Serra de Magé, EET 87548, and ALH 81005) give much younger Ar-Ar ages (Table 1), and these probably have been reset by later impact heating. The Ar-Ar age of Moore County also may have been reset by impact heating. These impact-reset ages will be discussed in the section, Impact Ages of Brecciated Eucrites.

In contrast to the Ar-Ar ages, available Pb-Pb and Sm-Nd isochron ages of unbrecciated and cumulate eucrites show a wider distribution for a smaller number of dated meteorites and range from ~4.4 Gyr up to ~4.55 Gyr (Table 1; Fig. 7). Some of these Pb-Pb and Sm-Nd ages have relatively large uncertainties, but these do not seem sufficient to explain the wider range in these ages. Individual ages for a specific meteorite do not always agree (Fig. 8; Table 1). For several

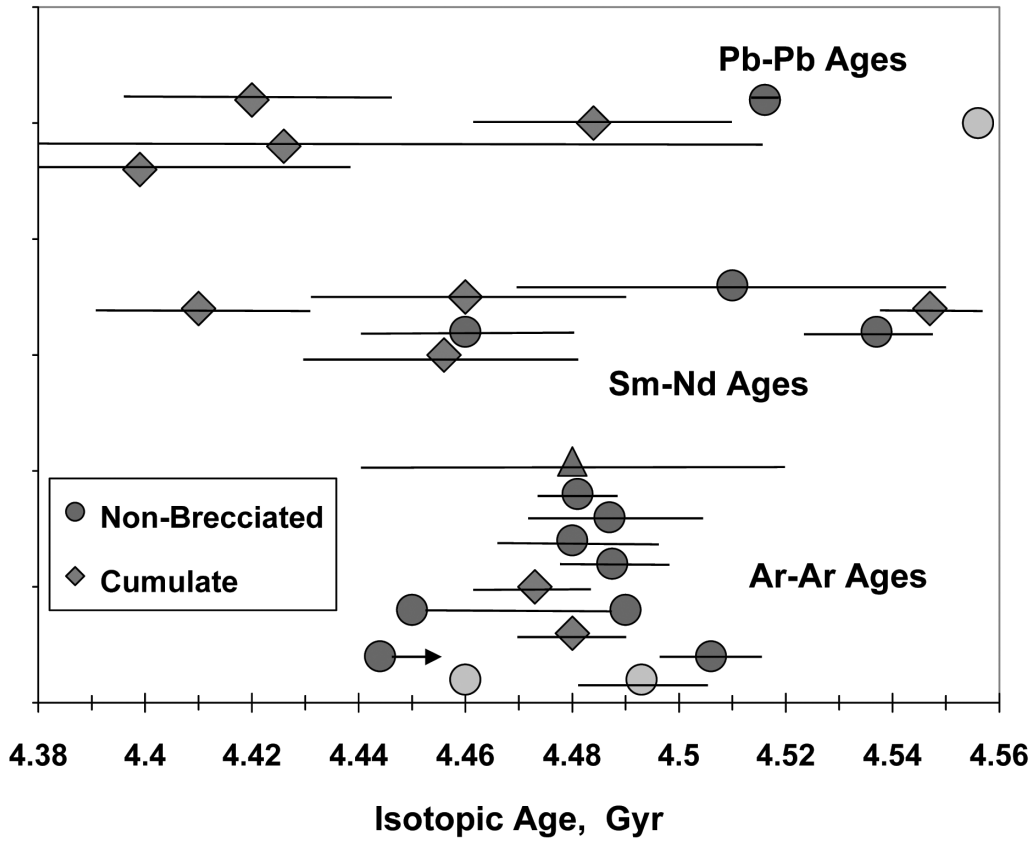

Fig. 7. ^{39}Ar-^{40}Ar, Pb-Pb, and ^{147}Sm-^{143}Nd ages for cumulate and unbrecciated basaltic eucrites (Table 1). All Ar-Ar ages are from JSC, except that for unbrecciated Y-7308 (triangle). Pb-Pb and Sm-Nd ages are isochron ages, except the Pb age for unbrecciated Ibitira (light-colored point), which is a model age. Two Ar-Ar ages shown as light symbols have greater uncertainties, a third age is a lower limit, and the 2 connected points represent the 2 plateau ages of GRA 98098.

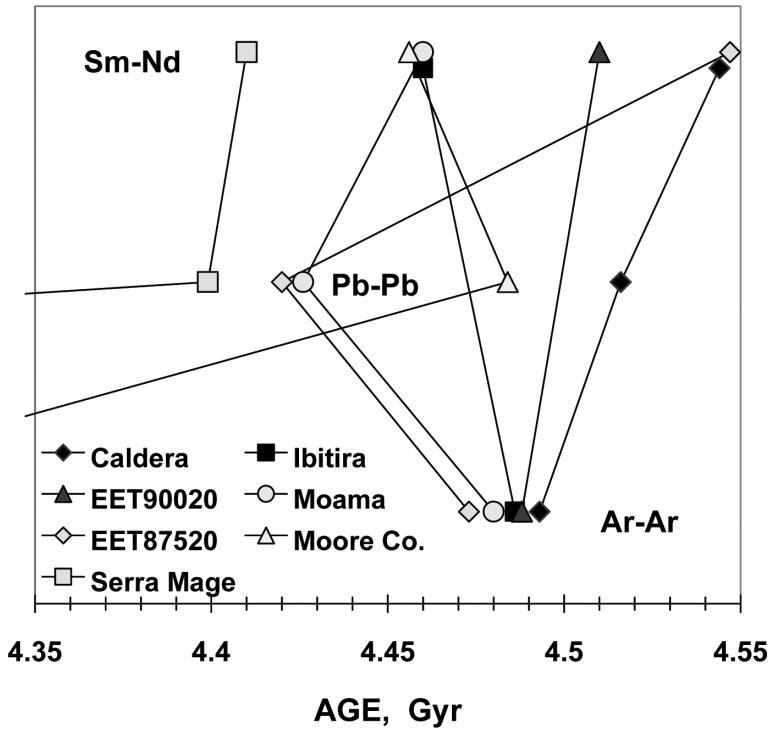

Fig. 8. To permit comparisons, Ar-Ar, Pb-Pb, and Sm-Nd ages for individual cumulate and unbrecciated basaltic eucrites are connected by line segments. The Ar-Ar ages for Moore County and Serra de Magé would plot below the lower scale.

meteorites, the Ar-Ar age is within combined uncertainties of either the Pb-Pb age (Caldera) or the Sm-Nd age (Moama, EET 90020, and possibly Ibitira). The Ar-Ar ages of only 2 eucrites (Moore County and Serra de Magé) are clearly younger than both the Pb-Pb and Sm-Nd age, and the much younger Ar-Ar age of Serra de Magé was almost certainly reset by later impact heating (see the subsection, Distribution of Eucrite Impact-Reset Ages). The Ar-Ar age for EET 87520 only appears older than the Pb-Pb age, within mutual uncertainties. The Pb-Pb ages are apparently younger than the Sm-Nd ages for 2 eucrites (EET 87520 and Caldera), and in no case is a Pb-Pb isochron age older than a Sm-Nd age (within mutual uncertainties). Further, 2 different laboratories reported a range of possible ^{147}Sm-^{143}Nd ages for Ibitira, although, the ^{146}Sm-^{142}Nd decay system in both studies suggested an old age. Because Sm-Nd data for some minerals implied a younger age, Nyquist et al. (1999) suggested metamorphism of Ibitira at the time of the Ar-Ar age.

The parent bodies of many meteorites, including HEDs, formed earlier than 4.55 Gyr ago and probably ~4.56 Gyr ago. Evidence for this comes from the existence in meteorites, including a few eucrites, of decay products of short-lived, nuclides such as ^{53}Mn, ^{26}Al, and ^{60}Fe (Carlson and Lugmair 2000; Nyquist et al. 2001; Srinivasan et al. 2002; Shukolyukov and Lugmair 1993), and from old radiometric ages of several meteorite types (e.g., Carlson and Lugmair 2000; Tera et al. 1997). Further, precise Pb-Pb model ages of 4.556 ± 0.006 and 4.560 ± 0.003 Gyr were reported for Ibitira (Chen and Wasserburg 1985; Manhès et al. 1987). What, then, is the explanation for the younger radiometric ages of unbrecciated and cumulate eucrites documented in Table 1 and Fig. 7? Bogard (1995) summarized the measured ages of many eucrites (almost all basaltic breccias) and noted that essentially all Ar-Ar ages and many Rb-Sr and Pb-Pb ages had been partially or totally reset ~4.1–3.4 Gyr ago. He suggested that this resetting was the result of heating during a period of impact bombardment possibly related to the lunar impact cataclysm. However, 17 of the eucrites listed in Table 1 are classified as unbrecciated or cumulate, and most show little to no textural evidence of significant impact heating. Two cumulate and 2 unbrecciated meteorites listed in Table 1 do give much younger Ar-Ar ages that are consistent with the impact-reset ages of brecciated eucrites (discussed in the section, Impact Ages of Brecciated Eucrites). However, to conclude that the Ar-Ar ages of the rest of the listed samples were not affected by the same impact history that reset the ages of most brecciated basalts seems reasonable. However, this does not mean that impact heating is ruled out for these samples. We now discuss 3 possible explanations for the radiometric ages of cumulate and unbrecciated eucrites: young formation, metamorphism, and early impact heating.

Young Formation Ages

One possible explanation for the distribution of younger ages of the cumulate and unbrecciated eucrites shown in Fig. 7 is that these ages represent the actual formation times

of these eucrites. From their study of Pb-Pb ages of cumulate and basaltic eucrites, Tera et al (1997) concluded that magmatic activity on the eucrite parent body(ies) continued for nearly 150 Myr and that cumulate eucrites are tens of millions of years younger than noncumulate eucrites. They further noted that the primitive U/Pb ratios differed substantially between cumulate and non-cumulate eucrites, and from this, they suggested that these 2 types of eucrites might derive from different parent bodies. In a study of ^{176}Lu-^{176}Hf whole rock samples of 16 basaltic and 5 cumulate eucrites (including Moama, Moore County, and Serra de Magé), Blichert-Toft et al. (2002a) conclude that cumulate eucrites are ~100 Myr younger than basaltic eucrites. (However, this conclusion seems at odds with the statement by Blichert-Toft et al. (2002b) that "cumulates Moore County, Serra de Magé, and Moama do not seem to be younger than the basaltic eucrites.")

However, arguments can be made against different formation times and separate parent bodies for cumulate and basaltic eucrites. The strong Ar-Ar age cluster at ~4.48 Gyr (Fig. 7) is comprised of several unbrecciated basaltic eucrites and 2 cumulate eucrites that have identical Ar ages. Also, Tera et al (1997) noted that a whole rock Pb-Pb isochron of their 3 cumulate eucrites defined an age of 4.483 ± 0.057 Gyr, which is identical to the average value of the Ar-Ar age cluster. Thus, if cumulate and basaltic eucrites derive from different parent bodies, they must have produced cumulate and basaltic eucrites at about the same time, a time that is younger than the formation age of most other meteorite types. Although some other meteorite types give evidence for extensive metamorphic heating, no compelling evidence exists for formation of such asteroidal meteorites at times <4.5 Gyr.

Production of eucrites over a relatively long time period of ~150 Myr would imply either an extended source of heat beyond that produced by short-lived nuclides such as ^{26}Al or very deep burial in the parent body so as to retain that heat for a significant time. Although late formation of cumulate eucrites at depth may be less of an issue, basaltic eucrites formed as surface flows or as shallow intrusive bodies that were later metamorphosed (Stolper 1977; Taylor et al. 1993; Takeda and Graham 1991). In their thermal modeling of the HED parent body, Ghosh and McSween (1998) concluded that, assuming initial heating from short-lived nuclides and a parent body the size of 4 Vesta, the mantle could be kept hot for ~100 Myr, volcanism could sustain for this time period, and the observed difference in ages between cumulate and non-cumulate eucrites could, thereby, be explained. But, if unbrecciated basaltic eucrites also formed 4.5 Gyr ago, does that imply that brecciated and unbrecciated basaltic eucrites have different formation times even though they are not obviously different in other basic properties? Evidence for the existence of short-lived nuclides (e.g., ^{26}Al and ^{53}Mn) in some brecciated basaltic eucrites precludes their late formation. Further, if unbrecciated eucrites formed later, how do we explain the old Pb-Pb model age and ^{146}Sm-^{142}Nd age for Ibitira?

If we assume that the eucrite ages shown in Fig. 7 represent actual formation times, what were these times? The strong tendency of the Ar-Ar ages to cluster might permit all dated samples to have a common age of ~4.48 Gyr. The reason that Pb-Pb ages of 3 out of 4 dated cumulates should be younger than this value (including two cumulates with both Ar and Pb ages measured) is not clear. Perhaps, the whole rock Pb-Pb isochron age of 4.483 ± 0.053 reported by Tera et al. (1997) is the actual formation time, and 3 individual meteorites have been disturbed to suggest younger Pb-Pb ages. If so, interestingly, the Ar-Ar ages, which are usually more sensitive to thermal events, were not also disturbed. The Sm-Nd age of Serra de Magé is significantly younger than 4.48 Gyr and agrees with the Pb-Pb age. However, the impact event at ~3.4 Gyr that reset the Ar-Ar age of Serra de Magé possibly also disturbed the Pb-Pb and Sm-Nd age (see later discussion). Further, while the Ar-Ar and Sm-Nd ages of Moama, EET 90020, and Ibitira could be the same within their uncertainties, the Sm-Nd ages for EET 87520 and Caldera are older than the Ar-Ar and Pb-Pb ages. Thus, while the Ar-Ar ages could be consistent with a common formation time for several cumulate and unbrecciated eucrites, the Pb-Pb and Sm-Nd ages seem only partially consistent with a range of formation ages. We do not believe that variable formation times is the explanation for the radiometric ages of cumulate and unbrecciated eucrites.

Metamorphism Ages

As mentioned earlier, most eucrites have been metamorphosed to varying degrees (many ≥800°C), cations in their pyroxenes have chemically equilibrated, and/or pyroxenes have undergone equilibrium phase changes (Takeda and Graham 1991; Yamaguchi et al. 1997). This type of metamorphism likely occurred at depth, implying relatively deep burial of even those basaltic eucrites that initially solidified at the parent body surface. Arguments can be made that this metamorphism occurred very early and was not produced during later (i.e., <4.1 Gyr) impact heating. For example, some unbrecciated eucrites with old ages that did not experience later impact heating are also metamorphosed, e.g., Ibitira and EET 90020 show metamorphic grade #5 on a scale of 1–6, where 6 is the greatest (Takeda and Graham 1991). Further, a pristine, unmetamorphosed clast from the basaltic breccia Y-75011 did have its Ar-Ar age largely reset by impact ~3.95 Gyr ago, indicating that heating sufficient to reset Ar-Ar did not produce pyroxene metamorphism (Takeda et al. 1994; Bogard and Garrison 1995). What, then, was the heat source that metamorphosed basaltic eucrites? Takeda (1979) and Ikeda and Takeda (1985) suggested that the parent body produced a magma ocean that crystallized into layers corresponding to the various metamorphic grades, with

diogenites and cumulates near the bottom and low metamorphic grade basaltic eucrites near the top. Nyquist et al. (1986) suggested that metamorphism occurred from the heat produced by large impact craters. Yamaguchi et al. (1996, 1997) suggested that magmatic production of basalts on the parent body was so rapid that it produced a crust 15–25 km deep in a time period of only ~1 Myr and that metamorphism occurred when basalt came into the high thermal gradient existing at depth. Very early metamorphism times would be required by the first and third models.

If early eucrite metamorphism occurred at depth, the material likely remained hot for some considerable period of time. If the surface of the parent body was heavily brecciated into a megaregolith, heat loss could have been retarded (Warren et al. 1991). In their thermal modeling of the differentiation of 4 Vesta, Ghosh and McSween (1998) concluded that after 100 Myr much of the interior would remain above 1100°C, and the upper ~15 km would remain above 400°C. Such a thermal environment could permit isotopic chronometers to remain open for a considerable period of time after actual meteorite formation, and, thus, many ages could be younger than ~4.55 Gyr. As various eucrites would reside at different depths and temperatures, one might also expect cumulate eucrites to show younger ages than unbrecciated basaltic eucrites. Although the data base is sparse, the Pb-Pb and Sm-Nd ages in Fig. 7 might suggest such an age difference. Also, given the common observation that Ar-Ar is most easily reset by heating and Sm-Nd the least, this model might predict the Sm-Nd ages to be older than the other ages. Caldera and Moore County do show the expected age sequence of Sm-Nd >Pb-Pb >Ar-Ar.

Some additional data also suggest that isotopic chronometers closed at different times for various eucrites. The ^{244}Pu-fission-Xe ages for ~22 eucrites, including 5 eucrites listed in Table 1, vary by ~100 Myr, from ~4.56 Gyr to ~4.46 Gyr (Shukolyukov and Begemann 1996; Miura et al. 1998). These Pu-Xe ages are calculated assuming that the Angra dos Reis angrite has quantitatively retained fission Xe over its Pb-Pb age of 4.5578 Gyr. Both of these Pu-Xe investigations concluded that parent body metamorphism is a likely explanation for the younger Pu-Xe ages. Pedicting how easily Pu-Xe would be reset during metamorphic heating at depth is difficult. Although Xe is a gas, it diffuses less readily than Ar, and greater pressure at depth might enhance its retention in minerals, even when elements like Pb and Nd undergo isotopic exchange. For several brecciated basaltic eucrites showing Pb-Pb ages considerably younger than 4.55 Gyr, Shukolyukov and Begemann (1996) noted that the Pu-Xe ages were considerably older than the Pb-Pb ages, indicating a greater resistance to resetting during impact heating. These authors also noted that for most of these eucrites, Pu-Xe ages correlated with K-Ar and Ar-Ar ages, although the Ar-Ar ages were much younger and indicated a much greater ease of diffusion loss of Ar compared to Xe during shock heating.

To summarize the sections, Young Formation Ages and Metamorphism Ages, retention of considerable heat from early decay of short-lived nuclides might permit the formation of basaltic or cumulate eucrites at times considerably later than the formation of the parent body >4.555 Gyr ago. On the other hand, the presence of short-lived nuclides observed in some eucrites, along with the nature of likely models needed to produce the observed metamorphism in many basaltic eucrites, requires that they formed very early, i.e., >4.55 Gyr ago. If early metamorphism left eucrites in a hot environment at depth, their isotopic chronometers may have remained open for significant and variable periods of time. This might permit, in principle, an explanation for the apparent variation in ages among different eucrites and for different ages obtained by different chronometers for the same or similar eucrites, although, the specific ages are not always what is expected. However, one difficulty with this scenario is the strong clustering of Ar-Ar ages of both cumulate and unbrecciated eucrites at ~4.48 Gyr. Ar-Ar ages are expected to be the easiest to reset by metamorphic heating, and thus, we would expect them to yield the youngest values. Further, if variable Pb-Pb and Sm-Nd ages among these eucrites reflect slow cooling and different closure times, why do the Ar-Ar ages also not show greater variations among meteorites? Thus, we reject this scenario as the sole explanation of eucrite chronology and examine the possible role of early impact heating.

Impact-Produced Ages

We conclude that the strong clustering of Ar-Ar ages of both cumulate and unbrecciated eucrites (Fig. 7) is not accidental but, rather, dates some major, widespread event on the HED parent body. A prior multidiscipline study of the EET 90020 eucrite may offer an explanation for this age cluster. Yamaguchi et al (2001) concluded from mineral textures that this unbrecciated eucrite formed at the surface and later was metamorphosed at depth to grade 5. It was then briefly heated above the subsolidus temperature of ~1060°C, causing partial melting, followed by rapid cooling of several °C/day. The temperature of the rock just before this reheating could have been ~870°C, based on the two-pyroxene method. These authors suggested that this partial melting event was responsible for resetting the Ar-Ar and Sm-Nd ages (Table 1), as well as apparent disturbance of the Rb-Sr and Mn-Cr systems. They further suggested that this reheating event was the formation on Vesta of a very large impact crater ~4.50 Gyr ago, which excavated relatively hot material from considerable depths and caused it to cool quickly. Miyamoto et al. (2001) suggested a similar history for Ibitira.

Vesta presents several lines of evidence for early impact heating events that could have affected eucrite chronology. Study of Vesta using the Hubble Space Telescope indicates the existence of a few very large craters (Thomas et al. 1997). The largest crater near Vesta's south pole is ~460 km in diameter,

~13 km deep below the rim, and contains a central peak nearly as high. A second crater is ~160 km in diameter and ~6 km deep. Spectral studies suggest that, while much of Vesta's surface resembles howardites or basaltic eucrites, other areas likely associated with large impact structures suggest enrichment in pyroxene and/or olivine and may indicate exposure of Vesta's lower crust or mantle (Gaffey 1997; Thomas et al. 1997). Zappalá et al. (1995) concluded that Vesta possesses a dynamic family of ~240 small asteroids, which are closely associated with it physically and which may have derived from a large collision with Vesta. This Vesta family may have been ejected from one of these large craters (Sykes and Vilas 2001). In addition, observers have identified ~18 Vestoids, which are small (~4–10 km) asteroids with Vesta-like spectra and the orbits of which form a bridge connecting Vesta with the ν_6 resonance and the 3:1 Kirkwood gap (Binzel and Xu 1993). These Vestoids also may have been ejected from one of the large craters on Vesta. The orbital location of Vesta does not favor direct ejection of material to Earth. Gravitational perturbations by Jupiter from the ν_6 resonance and the 3:1 Kirkwood gap are thought to be "gates" through which objects pass on their way to Earth (Wisdom 1985; Binzel and Xu 1993; Wetherill 1985). Thus, eucrites in our collections likely derived originally from one or more large impacts on Vesta (or a similar body now disrupted) and were brought to Earth by further collisions on one of these smaller, secondary asteroids (Sykes and Vilas 2001).

We suggest that one of these very large impact events on Vesta occurred ~4.48 Gyr ago and excavated both basaltic and cumulate eucrites (and probably diogenites) from considerable depths. At the time of excavation, the temperature of most ejecta was above the closure temperature of the K-Ar chronometer. Rapid cooling immediately after the impact event produced closure of all isotopic chronometers, including all K-Ar ages. Older Sm-Nd and Pb-Pb ages for 2 dated meteorites can be explained if their ambient temperature had fallen sufficiently low before the impact, causing these chronometers to have already closed (e.g., both the Sm-Nd and Pb-Pb ages of Caldera and the Sm-Nd age of EET 87520). Early closure might also account for the slightly older Ar-Ar age for PCA 82502. Sm-Nd and Pb-Pb ages of ~4.46–4.51 Gyr for some other eucrites are sufficiently imprecise that they also could have closed during rapid cooling after the impact ejection 4.48 Gyr ago. The younger Pb-Pb ages for 2 cumulates, Moama and EET 87520, may require some additional explanation, although, the uncertainty in the Pb-Pb age for EET 87520 (±92 Myr) more than overlaps the postulated ~4.48 Gyr impact heating event. Subsequent impact heating of Moore County and Serra de Magé, as suggested by younger Ar-Ar ages (see the subsection, Distribution of Eucrite Impact-Reset Ages), could, conceivably, have caused the Lu-Hf ages of cumulate eucrites to appear slightly younger than the age of basaltic eucrites (Blichert-Toft et al. 2002a).

Another consideration in interpreting isotopic ages for slowly cooling systems, such as the Vesta crust before the ~4.48 Gyr impact, is that different minerals may close to diffusion at different times. If the impact event then imparted additional sudden heating as postulated for EET 90020, then Pb-Pb and Sm-Nd isochrons defined by mineral phases may partially reflect different closure times and differential disturbance rather than a true age. A similar kind of age disturbance was demonstrated for Rb-Sr and Sm-Nd ages of a lunar rock heated in the laboratory to temperatures up to 990°C for a time period of 170 hours (Nyquist et al. 1991). Further, in the various Pb-Pb isochrons for Moama (Tera et al. 1997), the whole rock, plagioclase, and pyroxene acid-treated samples that define the isochron are not completely linear. Thus, we suggest that those few ages in Fig. 7 that appear to be significantly younger than ~4.48 Gyr are not true closure ages.

Another question about the chronology of cumulate and unbrecciated eucrites is why their ages were not reset in the later cataclysmic bombardment that reset Ar-Ar ages of most brecciated eucrites (see the section, Impact ages of Brecciated Eucrites). One explanation might be statistical in that a few basaltic eucrites simply escaped such resetting, while ages of a few cumulate eucrites were later reset (Table 1). A second possible reason could be that the parent material of these meteorites remained deeply buried inside Vesta during this bombardment. This explanation seems incompatible with the ~4.48 Gyr event scenario postulated above, however, and would still require large impact events to uncover these eucrites from depth. The younger Pb-Pb and Sm-Nd ages (4.40–4.41 Gyr) for Serra de Magé may date resetting in a later impact event, and evidence presented in the section cited above argues for major impact events in the range of ~3.4–4.1 Gyr. A third possible explanation for the lack of brecciation among some eucrites is that a very large impact ~4.48 Gyr ago ejected the direct parent objects of cumulate and unbrecciated eucrites away from Vesta as km-sized Vestoids or the associated dynamical Vesta family. These smaller direct parent objects cannot suffer the large impacts necessary to heat crater deposits sufficiently to reset isotopic ages without destroying the parent asteroid (Bogard 1995). Thus, cumulate and unbrecciated eucrites might derive from smaller asteroids ejected from Vesta ~4.48 Gyr ago, asteroids that did not experience later impact heating. Since most brecciated basaltic eucrites did experience later impact heating, they presumably were ejected from Vesta at later times. Because the cosmic ray exposure ages of all eucrites are much younger than 0.1 Gyr (Eugster and Michel 1995), the eucrites must have resided in bodies at least several meters in diameter for most of their history.

Time of Early Impact Event

We now perform a test to examine whether all individual, older Ar-Ar ages of eucrites are consistent with the conclusion that these ages date a single thermal event. Figure

9 is an age probability plot for 10 Ar-Ar age analyses of 9 unbrecciated and cumulate eucrites (Table 1). Each curve represents a Gaussian probability distribution of an individual Ar-Ar age, assuming that the error reported for each age represents a one-sigma uncertainty in this age. These curves are constructed from the standard formula for normal distribution of measurements about a single true value (Bevington 1969). (Although the error we report for each age is not strictly a 1σ statistical error, it is approximately so. Because we compare only Ar-Ar ages, we use the smaller age uncertainties of Table 1.) For each curve, the Y-axis gives the probability of any given age (A) lying between A Myr and A + 1 Myr. A smaller age uncertainty yields a curve that is narrow in age and taller (greater probability). If two or more age probability curves overlap significantly, then they are consistent with a single heating event. In fact, with one possible exception (PCA 82502), all analyses of unbrecciated and cumulate eucrites show a significant overlap in their age probability curves. The solid, heavy curve in Fig. 9 is constructed by adding together the probability of all 10 individual curves in order to give a summed probability distribution, and then dividing this curve by 10, the number of individual curves. This permits one to read the summed probability for any age, to the nearest Myr, directly from the same probability scale as the individual curves. Obviously, this summed curve itself resembles a single probability distribution. The most probable age in this summed curve averages 4.48 Gyr, and to the extent that the shape of this summed curve itself resembles a Gaussian distribution, the one-sigma uncertainty in this most probable event age is ~20 Myr. This evaluation constitutes strong statistical evidence that at least 9 of these 10 Ar-Ar ages can readily be explained by a single degassing event ~4.48 Gyr ago.

We applied this same probability test to the 12 Pb-Pb and Sm-Nd isochron ages (Table 1) reported for 7 cumulate and unbrecciated eucrites (Fig. 10). (In this case, the summed probability curve was divided by 12. Note that the age range in Fig. 10 is more than a factor of 2 larger than that of Fig. 9.) The individual Pb-Pb and Sm-Nd age curves do not all overlap, and the summed probability curve in no way resembles a Gaussian curve indicative of a single event. This indicates either that several age resetting events are required, or that some of these individual meteorite ages do not represent real events. As mentioned above, we suggest that the 3 ages distinctly older than 4.50 Gyr represent isotopic closure during slow parent body cooling and that the 3 ages younger than ~4.44 Gyr represent partial disturbance rather than the times of resetting events. Five other Sm-Nd and Pb-Pb ages are consistent with the Ar-Ar age distribution (Fig. 9). Note that in Fig. 10, those 3 eucrites with accurately measured isochron ages of 4.516, 4.537, and 4.547 Gyr combine in the summed curve to give 2 peaks. However, there is no compelling reason to believe these 3 age distributions can be explained by 2 events occurring at ~4.52 and 4.54 Gyr. This

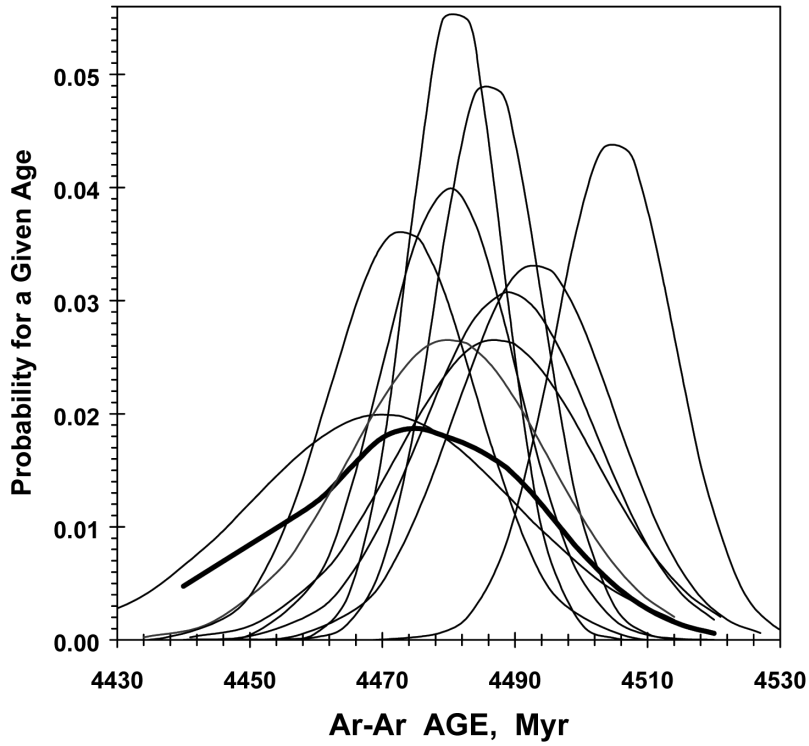

Fig. 9. Ar-Ar age probability curves (Gaussian) for 10 analyses of 9 cumulate and unbrecciated basaltic eucrites. For each curve, the Y-axis gives the probability of any given age (A), lying between A Myr and A + 1 Myr. The heavy-line curve is the summed age probability, which also resembles a Gaussian distribution. The mean summed age is 4.48 ± ~0.02 Gyr.

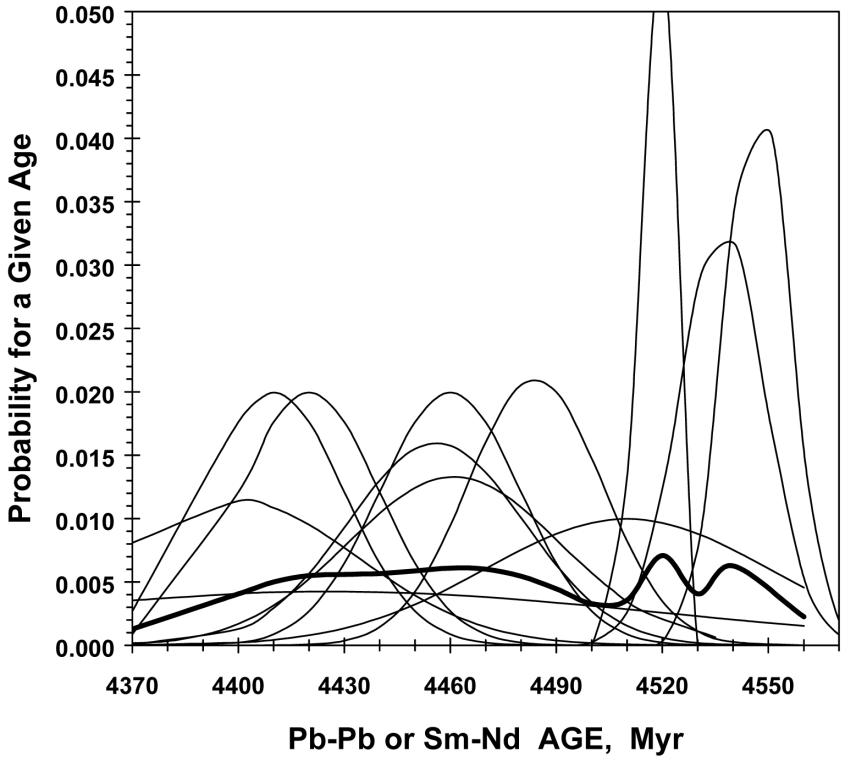

Fig. 10. Age probability curves (Gaussian) for Pb-Pb and Sm-Nd isochron ages (Table 1) of 7 cumulate and unbrecciated basaltic eucrites. The heavy-line curve is the summed age probability.

illustrates the point that one must be cautious in using summed probability curves to infer times of specific events when multiple events are involved.

IMPACT AGES OF BRECCIATED EUCRITES

Distribution of Eucrite Impact-Reset Ages

Bogard (1995) summarized available ^{39}Ar-^{40}Ar ages of eucrites, along with those Rb-Sr and Pb-Pb ages that are ≤4.3 Gyr. These ages gave a broad distribution, with most samples showing ages between ~3.4 and ~4.2 Gyr. Only 3 eucrites gave Ar-Ar ages of >4.3 Gyr and none gave Ar ages of <3 Gyr. These ages were all attributed to resetting during heating by relatively large impacts on the HED parent body, as only large craters and their ejecta deposits retain sufficient heat to cause such resetting. The existence of polymict eucrites and eucritic clasts in howardites implies multiple impact events, which would seem to be consistent with a distribution of impact ages. Bogard (1995) noted a general similarity between the distribution of eucrite ages and Ar-Ar, Rb-Sr, and Pb-Pb ages of lunar highland rocks returned by 3 Apollo missions. Tera et al. (1974) suggested that the resetting of these lunar rock ages was caused by an enhanced period of impact bombardment of the moon, for which they coined the term "lunar cataclysm." Bogard (1995) suggested that an analogous impact cataclysm occurred on the HED parent body and throughout the whole inner solar system. The reason that widespread age resetting occurred on the moon and the HED parent (but apparently not on some other meteorite parent bodies) was attributed to the larger size of the moon and the HED parent when compared to other meteorite parent bodies. Larger size permitted the generation of larger and hotter impact deposits without destroying the parent object.

The new data reported here furnish 22 additional Ar-Ar ages that can be added to the 46 Ar-Ar ages compiled by Bogard (1995). The updated histogram of Ar-Ar ages of eucrites is shown in Fig. 11. As done previously, Ar ages are plotted in 0.1 Gyr increments, and more precisely determined Ar ages are distinguished from approximate Ar ages. Precise Ar-Ar ages are somewhat arbitrarily defined as those for which a specific age uncertainty is reported. These individual age uncertainties ranged over 0.02–0.10 Gyr, but most were no greater than 0.05 Gyr. Generally speaking, the distribution of "precise" ages is similar to that of approximate Ar-Ar ages. The most obvious change in this age histogram, compared to the previous one, is the addition of several meteorites with ages of 4.50 ± 0.05 Gyr. These, of course, are the unbrecciated and cumulate samples discussed earlier. These older ages measure events that occurred much earlier than the lunar cataclysmic impacts, although, we argue above that they also date a single, large impact event. However, 9 new Ar-Ar ages plot in the age range of 3.4–3.7 Gyr, and the Moore County cumulate plots at 4.2 Gyr. Four of these 9 new Ar ages are

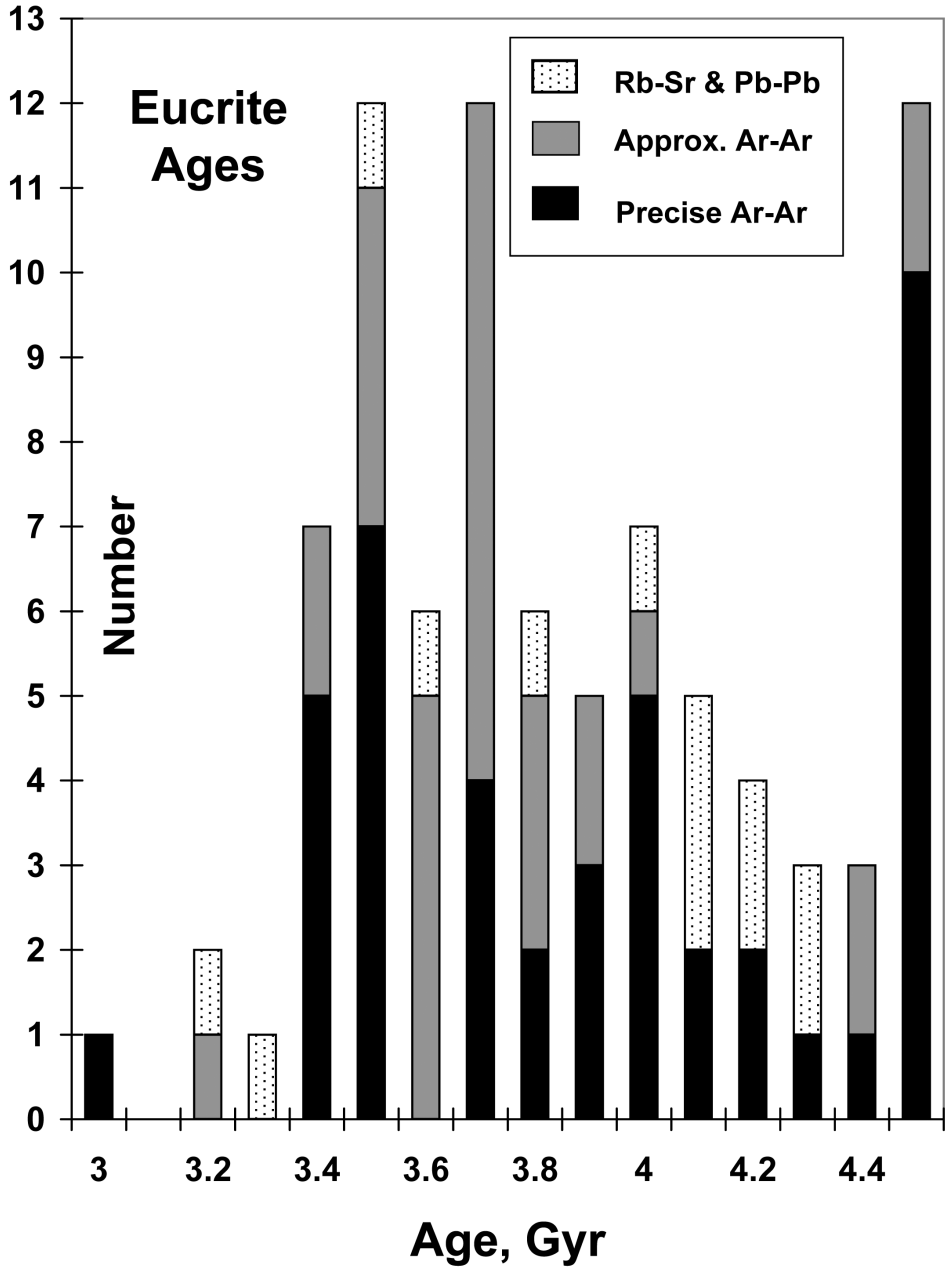

Fig. 11. Histogram of Ar-Ar impact-reset ages of eucrites. Rb-Sr and Pb-Pb ages of <4.3 Gyr are also shown.

considered to be "precise." The new distribution of eucrite impact ages below 4.4 Gyr is generally similar to that reported earlier, with a slightly greater relative weighing toward ages of <3.8 Gyr.

An age probability plot for 28 eucrite samples with reported age uncertainties and with Ar-Ar ages between 3.3 and 4.1 Gyr is shown in Fig. 12. In this case, the summed probability (heavy curve) was divided by 7 rather than the proper 28 to make the shape of the curve more discernable. Thus, the summed probability for a given age read on the Y-axis should be decreased by a factor of 4. This summed probability curve suggests heating events at ~3.45, 3.55, 4.0 Gyr, and possibly also at ~3.7, 4.05, and 3.8–3.9 Gyr. Seven samples give ages of ~3.95–4.05 Gyr, and 7 samples give ages of ~3.45–3.55 Gyr. Only 4 analyses give ages in the range of 3.80–3.95 Gyr, which is the time interval in which several large lunar basins probably were formed by impact (Stöffler and Ryder 2001). The few howardite clasts analyzed are not represented in the younger age peaks.

Nature of "Cataclysmic" Bombardment

The nature of the early lunar bombardment and whether a significant short-term increase in impactor flux existed over the decaying background flux is still under debate (e.g.,

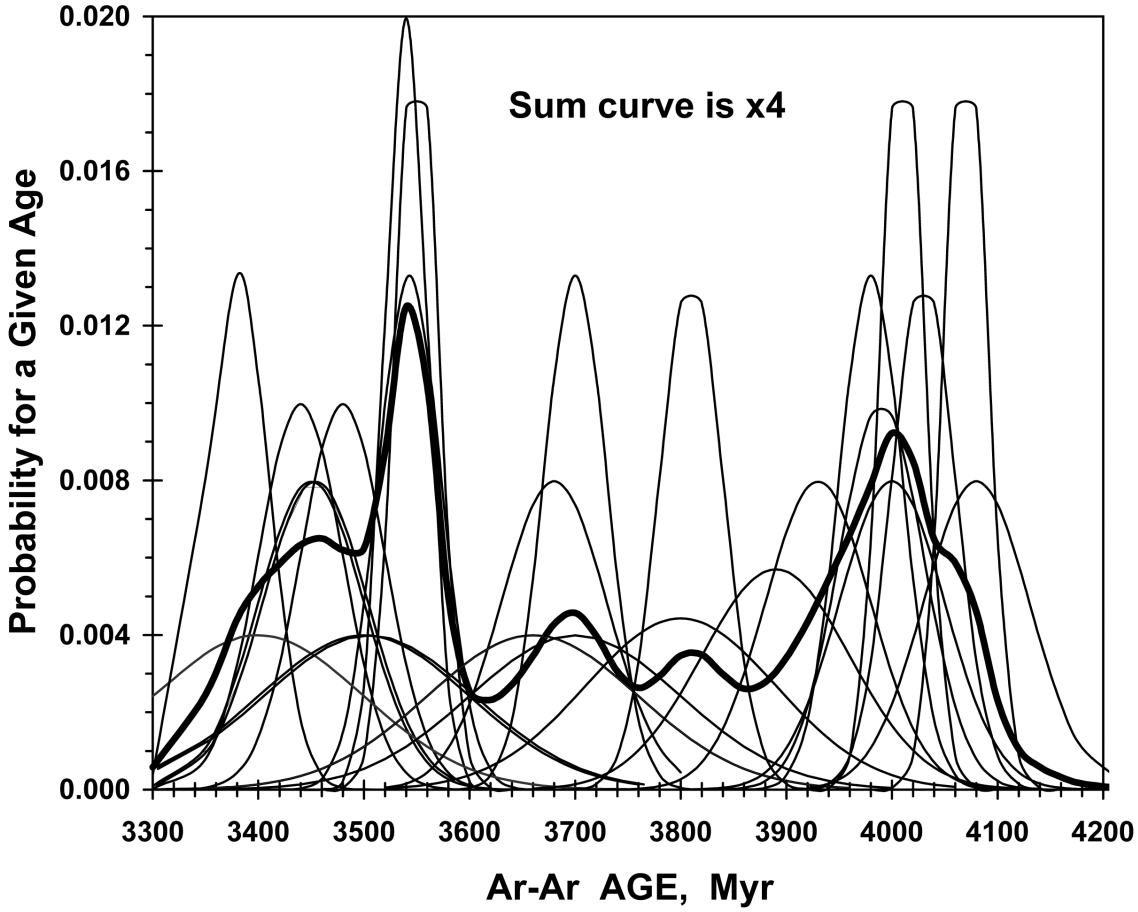

Fig. 12. Ar-Ar age probability curves (Gaussian) for 28 analyses of brecciated basaltic eucrites. The summed age probability (heavy-line curve) has been multiplied by a factor of four.

Hartmann et al. 2000; Ryder 2002). Ryder (2002) has argued that a distinct lunar cataclysm existed and that it was characterized by a significant increase in very large impacts. He also argued that this increase may have been relatively short-lived, perhaps ~0.2 Gyr in duration, and occurred ~4.0–3.8 Gyr ago. Ar-Ar and Rb-Sr ages of highland rocks from 3 Apollo lunar highland sites show a broad distribution of ~3.7–4.1 Gyr (Bogard 1995). However, good arguments have been presented regarding several of the younger, large impact basins on the moon formed in the narrow time interval of ~3.82–3.90 (Ryder 2002; Stöffler and Ryder 2001). (These basin ages were obtained by dating those impact melts for which a strong argument holds for their derivation from either the Imbrium, Serenitatis, or Nectaris basins.) However, whether the older (pre-Nectarian) lunar impact basins have ages of ~3.9–4.0 Gyr or are considerably older than 4.0 Gyr is still not clear. In the absence of good age estimates for the older lunar basins, we cannot know for certain when an increase in flux of large impactors actually began, or even if a dramatic increase above the background flux actually occurred.

Several workers have considered possible sources of objects that might have produced a cataclysmic bombardment ≥0.5 Gyr after the moon formed. (Objects with a total mass of ≥10^{22} g are apparently required to produce the lunar basins, and the source of these objects would have to be several orders of magnitude more massive.) Suggested sources include the breakup of a large body within the asteroid belt, gravitational scattering of objects near Neptune and Uranus, and perturbations of comets in the Oort cloud by close-passing stars (see Hartmann et al. 2000). Each of these suggested sources of objects implies that not just the moon, but the whole inner solar system, should have experienced this cataclysmic bombardment. Thus, evidence for impact-reset ages on the relatively large Vesta asteroid could be expected.

Because much lower crater densities exist on dated lunar mare surfaces compared to the lunar highlands, by ~3.7–3.5 Gyr ago, this early impactor flux, whatever its nature, is generally believed to have fallen to a value more comparable to the average flux over the past 3 Gyr of lunar history (Ryder 2002; Stöffler and Ryder 2001). The age of the youngest, large lunar basin (Orientale) is estimated at ~3.82 Gyr and certainly is not younger than 3.7 Gyr (Stöffler and Ryder 2001). However, the lunar rock chronology that defines the impact cataclysm is associated almost entirely with only 2–4

large and recent lunar near side basins, primarily Imbrium and Serenitatis, and less certainly Nectaris and Crisium. The time duration is still unclear for the cataclysmic bombardment involving smaller impactors that produced, not impact basins, but large lunar craters on the back side of the moon (and the largest craters on Vesta, which are much smaller than lunar basins). For example, 31 small impact melt clasts in 4 lunar meteorites (which may have originated from the lunar back side) show the wide distribution in Ar-Ar ages of ~2.4–4.1 Gyr, and fewer than half of these are older than 3.7 Gyr (Cohen et al. 2000). Those ages that are <3.7 Gyr may have been reset by the background impactor flux not the cataclysmic bombardment, and the case may be that few or none of the ages of these melt clasts were reset by an enhanced flux of large impactors. On the other hand, the existence of 4 extensive impact melt deposits, having an age of 3.47 Gyr, in South Africa and western Australia are interpreted to have formed in several large impacts of objects ~20 km in diameter (Byerly et al. 2002; Byerly and Lowe 1994). An object of such size could be expected to produce a very large crater on the moon or a basin on Vesta. On the moon, apparently, a relatively large crater is required to significantly reset Ar-Ar ages in rocks ejected outside the crater. Thus, a crater like Copernicus did reset Ar-Ar ages of ejected material (Bogard et al. 1994), but smaller craters like those visited at various Apollo landing sites did not. (Impact melt, which is largely contained within the crater, apparently, was not sampled for any of these smaller craters but was for the Imbrium and Serenitatis impacts.)

We suggest that a cataclysmic bombardment, as described for the moon from impact-reset ages of highland rocks, must satisfy 2 basic criteria: it must show an apparent increase in impactor flux compared to the decaying background flux, and this enhanced impactor flux must later decrease into the background flux. The distribution of impact-reset ages for eucrites (Figs. 11 and 12) appears to satisfy both of these criteria. The lunar impact cataclysm, as measured by formation times of large basins, began at an unknown time >3.9 Gyr ago and lasted until ~3.8 Gyr ago. The Vesta cataclysm (assuming the term applies) appears to have begun ~4.1 Gyr ago and lasted until ~3.4 Gyr ago. Fewer eucrite ages occur in the time interval of 4.1–4.4 Gyr than in the interval 4.0–3.4 Gyr, and this suggests that the impact cataclysm did involve a significant increase in impactor flux. This observation is consistent with the lunar impact cataclysm, as its upper time bound is not well constrained. On the other hand, impact-reset ages of eucrites in the time interval of 3.4–3.7 Gyr appear to be at least as numerous as those in the interval of 3.7–4.0 Gyr. Whether we consider only "precise" Ar-Ar ages or both precise and approximate ages, the distribution is continual across 4.3–3.7 Gyr but suggests an enhancement at ~4.0 and ~3.5 Gyr. Thus, the distribution of impact-reset ages of eucrites (Fig. 11) shows a broader range than that postulated by Ryder (2002) for the lunar cataclysm, which may be in conflict with the lunar observation that the impact cataclysm flux had fallen to the background flux level by 3.7–3.5 Gyr ago and that no large lunar basins formed after ~3.8 Gyr ago. However, the enhanced number of reset eucrite ages at ~3.4–3.5 Gyr is consistent with the evidence for several large impacts on Earth 3.47 Gyr ago (Byerly et al. 2002).

We can offer 3 possible explanations for the difference in the distribution of impact-reset ages between eucrites and lunar highland rocks. One explanation is that the timing of the bombardment on Vesta somehow lasted longer than that on the moon, although, it is difficult to explain why this should be the case. Another explanation is that the late stages of the bombardment may have consisted of smaller impacting objects than those which formed the lunar basins—smaller impactors which may have persisted in the inner solar system until ~3.4 Gyr ago. Presumably, the flux of later arriving objects was not high, or we would observe more ages of <3.7 Gyr among lunar highland rocks. The third and related explanation is the possibility that both eucrites and returned lunar highland rocks represent an incomplete sampling of the full range of reset ages on these bodies. Above, we suggested that the cluster of ages at ~4.48 Gyr for unbrecciated and cumulate eucrites may represent resetting by the largest crater observed on Vesta. Possibly, two other large craters on Vesta formed at times of ~4.0 and ~3.5 Gyr and caused resetting of many of the basaltic eucrite ages. Lunar highland rocks were all returned from a limited area of the moon, and many of these had their ages reset by 3 large impacts (Imbrium, Serenitatis, and Nectaris, out of ~30 recognized large basins) that occurred in this same area of the moon. The distribution of ages of large impactors across the whole surface of the moon is not accurately known. In any case, both the lunar and eucrite ages indicate that after ~3.4 Gyr ago, large scale impact heating apparently ceased on both bodies. Clearly, our understanding of the nature of the early bombardment of the inner solar system by relative large objects remains incomplete.

VESTA'S THERMAL HISTORY

Similarities between the spectral signatures of the asteroid 4 Vesta and of eucritic meteorites suggest that Vesta is the original parent body of eucrites (McCord et al. 1970). Several quite large impact craters apparently exist on Vesta (Thomas et al. 1997; Gaffey 1997). These may have been the source of the relatively large asteroidal family dynamically associated with Vesta and those asteroids with eucrite-like spectra, which are distributed in space between the ν_6 resonance and the 3:1 Kirkwood gap, likely making them direct parent objects for meteorites that fall on Earth (Zappalá et al. 1995; Binzel and Xu 1993; Sykes and Vilas 2001).

The eucrite parent body, which we assume to be Vesta, probably formed earlier than 4.56 Gyr ago (Lugmair and Shukolyukov 1998). Soon thereafter, decay of short-lived

radionuclides such as ^{26}Al (Srinivasan et al. 1999; Nyquist et al. 2001) caused extensive melting, likely core formation, and the generation of large quantities of surface basalt flows. The presence of decay products of short-lived nuclides and old Pb-Pb radiometric ages for a few eucrites (e.g., Carlson and Lugmair 2000), implies that this basalt production occurred relatively rapidly. However, modeling of the early thermal history of Vesta from decay of ^{26}Al indicates that the interior of Vesta likely remained hot for a substantial period of time. Much of the asteroid may have remained near the basaltic melting point for a time of ~10^8 years (Ghosh and McSween 1998). Most eucrites give evidence of thermal annealing during this period, many to temperatures ≥800°C (Yamaguchi et al. 1996, 1997). For example, the pyroxenes in many eucrites have been heated sufficiently to homogenize concentrations of cations such as Fe and Mg (Takeda and Graham 1991). This metamorphism probably occurred soon after eucrites formed, either through formation of a deep layered crust (Ikeda and Takeda 1985) or by rapid burial of many successive basalt flows (Yamaguchi et al. 1997). Cumulate eucrites show evidence of even greater heating than basaltic eucrites (Mittlefehldt et al. 1998a) and probably resided at greater depths.

Most eucrites are breccias formed by surface impacts and give ample evidence in their radiometric chronology for impact mixing and heating that occurred long after Vesta formed. With the reasonable assumption that eucrite metamorphism occurred at some depth in the parent body, impacts of significant size are required to bring these meteorites to the near-surface. However, most cumulate eucrites and a few basaltic eucrites are unbrecciated and apparently were not affected by these later impacts. For example, 12 Pb-Pb and Sm-Nd isochron ages of 4 cumulate and 3 unbrecciated basaltic eucrites lie between ~4.4 Gyr and ~4.55 Gyr (Tera et al. 1997; Carlson and Lugmair 2000). In contrast, we show in this work that the ^{39}Ar-^{40}Ar ages of 2 cumulate eucrites and 7 unbrecciated basaltic eucrites cluster rather tightly about an age of 4.48 Gyr. Although the younger Pb-Pb and Sm-Nd ages were suggested previously to indicate late formation of these eucrites, possibly on separate parent bodies (Tera et al. 1997), we argue that this explanation cannot account for diverse data sets. More likely, the younger ages of cumulate and unbrecciated basaltic eucrites are the result of residence at depth in a common parent where elevated temperatures kept isotopic systems open for a significant time after the eucrites actually formed. However, if this were the only explanation for the younger radiometric ages, we might expect to see variable ages among different meteorites. We would also expect to see Sm-Nd ages older than Pb-Pb ages and older than Ar-Ar ages, which reflect the relative ease in the resetting of these radiometric chronometers. Residence at depth alone cannot explain the tight clustering of Ar-Ar ages, which appear older than a few Pb-Pb ages.

Thus, we suggest that the distribution of radiometric ages of cumulate eucrites and unbrecciated basaltic eucrites (Fig. 7) has 2 related explanations. These samples did reside under elevated temperatures at depth for a significant time period after their formation. However, ~4.48 Gyr ago, a very large impact on Vesta, possibly the one that formed the largest (~460 km diameter) crater believed to exist on its surface, ejected these meteorites from depth and quenched their temperatures. These ejected objects may have produced the Vestoids. Because the K-Ar system was open in all meteorites, this ejection and cooling event set the Ar-Ar ages to a common value. The Sm-Nd and Pb-Pb ages of some of these eucrites were also set by the large impact ejection event. Because the Sm-Nd system closes at higher temperatures than does K-Ar, the Sm-Nd ages of some other eucrites (i.e., those with ages older than 4.48 Gyr) had already closed. The younger Sm-Nd and Pb-Pb ages, and much younger Ar-Ar age, for cumulate Serra de Magé (and the younger Ar-Ar age for Moore County) are probably due to a much later impact disturbance.

Significantly later than this ~4.48 Gyr impact event, the surface of Vesta suffered additional large impacts which affected radiometric chronometers. The K-Ar ages of essentially all brecciated basaltic eucrites (and howardites) were partially or totally reset during this period, and Rb-Sr and Pb-Pb ages of some eucrites were disturbed or partially reset. Bogard (1995) suggested that the source of these impactors was related to the impact cataclysm on the moon, which reset the ages of most lunar highland rocks. This period of impact-resetting on Vesta, about 4.1 to 3.4 Gyr ago, appears to have lasted longer than the lunar cataclysm, and apparently required several distinct impact heating events. Parent bodies of most other meteorite types do not show the same degree of chronometer impact-resetting because they were smaller than Vesta and, thus, could not sustain an impact of sufficient size to produce chronometer resetting. Details of the origin and nature of these impactors and their actual flux over time remains unknown.

Acknowledgments–This research was supported by NASA's Cosmochemistry Program under RTOP 344–31–30–01. We appreciate constructive reviewer comments by T. Swindle, R. Burgess, and R. Wieler and informative discussions with D. Mittlefehldt about some of these eucrites. We thank the following for furnishing samples: R. Haag, M. Grady, B. Zanda, G. Srinivasan, D. Mittlefehldt, P. Buchanan, H. Takeda, the Japanese National Institute of Polar Research, and the U.S. Antarctic Meteorite Curation Program.

Editorial Handling—Dr. Rainer Wieler

REFERENCES

Alexander E. C. and Davis P. K. 1974. ^{40}Ar-^{39}Ar ages and trace element contents of Apollo 14 breccias: An interlaboratory cross-calibration of ^{40}Ar-^{39}Ar standards. *Geochimica et Cosmochimica Acta* 38:911–928.

Antarctic Meteorite Newsletter, http://www-curator.jsc.nasa.gov/antmet/antmet.htm.

Bevington P. R. 1969. Data reduction and error analysis for the physical sciences. New York: McGraw-Hill. 336 p.

Bhandari N., Murty S. V. S., Suthar K. M., Shukla A. D., Ballabh G. M., Sosodia M. S., and Vaya V. K. 1998. The orbit and exposure history of the Piplia Kalan eucrite. *Meteoritics & Planetary Science* 33:455–461.

Binzel R. P. and Xu S. 1993. Chips off of asteroid 4 Vesta: Evidence for the parent body of basaltic achondrite meteorites. *Science* 260:186–191.

Blichert-Toft J., Boyet M., Télouk P., and Albarède F. 2002a. ^{147}Sm-^{143}Nd and ^{176}Lu-^{176}Hf in eucrites and the differentiation of the HED parent body. *Earth and Planetary Science Letters* 204:167–181.

Blichert-Toft J., Boyet M., and Albarède F. 2002b. ^{147}Sm-^{143}Nd, ^{176}Lu-^{176}Hf, and ^{92}Zr in eucrites (abstract). *Meteoritics & Planetary Science* 37:A19.

Boctor N. Z., Palme H., Spettel B., El Goresy A., and MacPherson G. J. 1994. Caldera: A second unbrecciated noncumulate eucrite (abstract). *Meteoritics* 29:445.

Bogard D. D. 1995. Impact ages of meteorites: A synthesis. *Meteoritics* 30:244–268.

Bogard D. D. and Hirsch W. C. 1980. ^{40}Ar-^{39}Ar dating, Ar diffusion properties, and cooling rate determinations of severely shocked chondrites. *Geochimica et Cosmochimica Acta* 44:1667–1682.

Bogard D. D. and Garrison D. H. 1995. ^{39}Ar-^{40}Ar age of the Ibitira eucrite and constraints on the time of pyroxene equilibration. *Geochimica et Cosmochimica Acta* 59:4317–4322.

Bogard D. D., Garrison D. H., Shih C. Y., and Nyquist L. E. 1994. ^{39}Ar-^{40}Ar dating of two lunar granites: The age of Copernicus. *Geochimica et Cosmochimica Acta* 58:3093–3100.

Bogard D. D., Garrison D. H., Norman M., Scott E. R. D., and Keil K. 1995. ^{39}Ar-^{40}Ar age and petrology of Chico: Large-scale impact melting on the L chondrite parent body. *Geochimica et Cosmochimica Acta* 59:1383–1400.

Bogard D. D., Garrison D. H., and McCoy T. J. 2000. Chronology and petrology of silicates from IIE iron meteorites: Evidence of a complex parent body evolution. *Geochimica et Cosmochimica Acta* 64:2133–2154.

Buchanan P. C. and Reid A. M. 1990. Clast populations in three Antarctic achondrites. Proceedings, 21st Lunar and Planetary Science Conference. pp. 141–142.

Buchanan P. C. and Reid A. M. 1991. Eucrite and diogenite clasts in three Antarctic achondrites. Proceedings, 22nd Lunar and Planetary Science Conference. pp. 149–150.

Buchanan P. C., Lindstrom D. J., and Mittlefehldt D. W. 1999. Pairing among the EET 87503 group of howardites and polymict eucrites. Workshop on Extraterrestrial Materials from Hot and Cold Deserts. *LPI Contribution No. 997.* pp. 21–24.

Buchanan P. C., Mittlefehldt D. W., Hutchison R., Koeberl C., Lindstrom D. J., and Pandit M. K. 2000a. Petrology of the Indian eucrite Piplia Kalan. *Meteoritics & Planetary Science* 35:609–616.

Buchanan P. C., Lindstrom D. J., Mittlefehldt D. W., Koeberl C., and Reimold W. U. 2000b. The South African polymict eucrite Macibini. *Meteoritics & Planetary Science* 35:1321–1331.

Byerly G. R. and Lowe D. R. 1994. Spinel from Archean impact spherules. *Geochimica et Cosmochimica Acta* 58:3469–3486.

Byerly G. R., Lowe D. R., Wooden J. L., and Xie X. 2002. An Archean impact layer from the Pilbara and Kaapvaal cratons. *Science* 297:1325–13227.

Carlson R. W. and Lugmair G. W. 2000. Timescales of planetesimal formation and differentiation based on extinct and extant radioisotopes. In *Origin of the earth and moon,* edited by Canup R. and Righter K. Tucson: University of Arizona Press. pp. 25–44.

Chen J. H. and Wasserburg G. J. 1985. U-Th-Pb isotopic studies on meteorite ALHA81005 and Ibitira. Proceedings, 16th Lunar and Planetary Science Conference. pp. 119–120.

Cohen B. A., Swindle T. D., and Kring D. A. 2000. Support for the lunar cataclysm hypothesis from lunar meteorite impact ages. *Science* 290:1754–1756.

Eugster O. and Michel T. 1995. Common asteroid break-up events of eucrites, diogenites, and howardites and cosmic-ray production rates for noble gases in achondrites. *Geochimica et Cosmochimica Acta* 59:177–199.

Gaffey M. J. 1997. Surface lithologic heterogeneity of asteroid 4 Vesta. *Icarus* 127:130–157.

Garrison D., Hamlin S., and Bogard D. 2000. Chlorine abundances in meteorites. *Meteoritics & Planetary Science* 35:419–429.

Ghosh A. and McSween H. Y. 1998. A thermal model for the differentiation of asteroid 4 Vesta, based on radiogenic heating. *Icarus* 134:187–206.

Grossman J. N. 1994. The Meteoritical Bulletin No. 76: The U.S. Antarctic meteorite collection. *Meteoritics* 29:100–143.

Hartmann W. K., Ryder G., Dones L., and Grinspoon D. 2000. The time-dependent intense bombardment of the primordial Earth/moon system. In *Origin of the earth and moon,* edited by Canup R. M. and Righter K. Tucson: University of Arizona. pp. 493–512.

Ikeda Y. and Takeda H. 1985. A model for the origin of basaltic achondrites based on the Yamato-7308 howardite. Proceedings, 15th Lunar and Planetary Science Conference. *Journal of Geophysical Research* 90:C649–C663.

Jacobson S. B. and Wasserburg G. J. 1984. Sm-Nd isotopic evolution of chondrites and achondrites, II. *Earth and Planetary Science Letters* 67:137–150.

Kaneoka I. 1981. ^{39}Ar-^{40}Ar ages of Antarctic meteorites Y-74191, Y-75258, Y-7308, Y-74450, and ALH 763. *Proceedings of the 6th Symposium on Antarctic meteorites* 20:250–263.

Keil K. 2002. Geological history of asteroid 4 Vesta: The smallest terrestrial planet. In *Asteroids III,* edited by Bottke W., Cellino A. Paolicchoi P., and Binzel R. P. Tucson: University of Arizona Press. 1025 p.

Kumar A., Gopalan K., and Bhandari N. 1999. ^{147}Sm-^{143}Nd and ^{87}Rb-^{87}Sr ages of the eucrite Piplia Kalan. *Geochimica et Cosmochimica Acta* 63:3997–4001.

Kunz J., Trieloff M., Bobe K. D., Metzler K., Stöffler D., and Jessberger E. K. 1995. The collisional history of the HED parent body inferred from ^{39}Ar-^{40}Ar ages of eucrites. *Planetary and Space Science* 43:527–543.

Lugmair G. W., Scheinin N. B., and Carlson R. W. 1977. Sm-Nd systematics of the Serra de Magé eucrite (abstract). *Meteoritics* 12:300–301.

Lugmair G. W., Galer S. J. G., and Carlson R. W. 1991. Isotope systematics of cumulate eucrite EET 87520 (abstract). *Meteoritics* 26:368.

Lugmair G. W. and Shukolyukov A. 1998. Early solar system timescales according to ^{53}Mn-^{53}Cr systematics. *Geochimica et Cosmochimica Acta* 62:2863–2886.

Manhès G., Göpel C., and Allègre C. J. 1987. High resolution chronology of the early solar system based on lead isotopes (abstract). *Meteoritics* 22:453–454.

Mason B., MacPherson G., Score R., Schwartz C., and Delaney J. 1989. Descriptions of stony meteorites. In *Smithsonian Contributions to the Earth Sciences* 28:52.

McCord T. B., Adams J. B., and Johnson T. V. 1970. Asteroid Vesta: Spectral reflectivity and compositional implications. *Science* 168:1445–1447.

McDougall I. and Harrison T. M. 1999. *Geochronology and*

Thermochronology by the ^{39}Ar-^{40}Ar Method. New York: Oxford University Press. 288 p.

Misawa K. and Yamaguchi A. 2001. U-Pb isotopic systematics of zircons from basaltic eucrites (abstract). *Antarctic Meteorites* 26: 83–84.

Mittlefehldt D. W. and Lindstrom M. M. 1991. Geochemistry of 5 Antarctic howardites and their clasts. Proceedings, 22nd Lunar and Planetary Science Conference. pp. 901–902.

Mittlefehldt D. W. and Lindstrom M. M. 1998a. Black clasts from howardite QUE 94200. Impact melts not primary magnesian basalts (abstract #1832). Proceedings, 24th Lunar and Planetary Science Conference.

Mittlefehldt D. W. and Lee M. T. 2001. Petrology and geochemistry of unusual eucrite GRA 98098 (abstract). *Meteoritics & Planetary Science* 36:A136.

Mittlefehldt D. W., McCoy T. J., Goodrich C. A., and Kracher A. 1998a. Non-chondritic meteorites from asteroidal bodies. In *Planetary materials,* edited by Papike J. J. Washington D.C.: Mineralogical Society of America. *Reviews in Mineralogy* 36.

Mittlefehldt D. W., Jones J. H., Palme H., Jarosewich E., and Grady M. M. 1998b. Sioux County. A study in why sleeping dogs are best left alone (abstract #1220). Proceedings, 29th Lunar and Planetary Science Conference.

Miura Y. N., Nagao K., Sugiura N., Fujitani T., and Warren P. H. 1998. Noble gases, ^{81}Kr-Kr exposure ages, and ^{244}Pu-Xe ages of six eucrites, Béréba, Binda, Camel Donga, Juvinas, Millbillillie, and Stannern. *Geochimica et Cosmochimica Acta* 62:2369–2388.

Miyamoto M., Mikouchi T., and Kaneda K. 2001. Thermal history of the Ibitira noncumulate eucrite as inferred from pyroxene exsolution lamella: Evidence for reheating and rapid cooling. *Meteoritics & Planetary Science* 36:231–237.

Nyquist L. E., Takeda H., Bansal B., Shih C. Y., Wiesmann H., and Wooden J. L. 1986. Rb-Sr and Sm-Nd internal isochron ages of a subophitic basalt clast and a matrix sample from the Y75011 eucrite. *Journal of Geophysical Research* 91:8137–8150.

Nyquist L. E., Bogard D. D., Garrison D. H., Bansal B. M., Wiesmann H., and Shih C. Y. 1991. Thermal resetting of radiometric ages. I. Experimental Investigation; II. Modeling and applications. Proceedings, 22nd Lunar and Planetary Science Conference. pp. 985–988.

Nyquist L. E., Shih C. Y., Wiesmann H., and Bansal B. M. 1994. Pre-bombardment crystallization ages of basaltic clasts from Antarctic howardites EET 87503 and EET 87513. Proceedings, 25th Lunar and Planetary Science Conference. pp. 1015–1016.

Nyquist L. E., Reese Y. D., Wiesmann H., and Shih C. Y. 1999. Two ages for Ibitira: A record of crystallization and recrystallization? (abstract). *Meteoritics & Planetary Science* 34:A87–88

Nyquist L. E., Reese Y., Wiesmann H., Shih C. Y., and Takeda H. 2001. Live ^{53}Mn and ^{26}Al in an unique cumulate eucrite with very calcic feldspar (An98) (abstract). *Meteoritics & Planetary Science* 36:A151–152.

Prinzhofer A., Papanastassiou D. A., and Wasserburg G. J. 1992. Sm-Nd evolution of meteorites. *Geochimica et Cosmochimica Acta* 56:797–815.

Renne P. R. 2000. ^{39}Ar-^{40}Ar age of plagioclase from Acapulco meteorite and the problem of systematic errors in cosmochronology. *Earth and Planetary Science Letters* 175:13–26.

Ryder G. 2002. Mass flux in the ancient Earth-Moon system and benign implications for the origin of life on Earth. *Journal of Geophysical Research* 107:1–14.

Srinivasan G. 2002. ^{26}Al-^{26}Mg systematics in eucrites A-881394, A-87122, and Vissannapetta (abstract). *Meteoritics & Planetary Science* 37:A135.

Srinivasan G., Goswami J. N., and Bhandari N. 1999. ^{26}Al in eucrite Piplia Kalan: Plausible heat source and formation chronology. *Science* 284:1348–1350.

Shukolyukov A. and Begemann F. 1996. Pu-Xe dating of eucrites. *Geochimica et Cosmochimica Acta* 60:2453–2480.

Shukolyukov A. and Lugmair G. W. 1993. ^{60}Fe in eucrites. *Earth and Planetary Science Letters* 119:159–166.

Steele I. M. and Smith J. V. 1976. Mineralogy of the Ibitira eucrite and comparison with other eucrites and lunar samples. *Earth and Planetary Science Letters* 33:67–78.

Steiger R. and Jäger E. 1977. Subcommission on geochronology; Convention on the use of decay constants in geo- and cosmochronology. *Earth and Planetary Science Letters* 36:359–362.

Stöffler D. and Ryder G. 2001. Stratigraphy and isotopic ages of lunar geologic units: Chronological standard for the inner solar system. *Space Science Reviews* 95:1–47.

Stolper E. 1977. Experimental petrology of eucrite meteorites. *Geochimica et Cosmochimica Acta* 41:587–612.

Sykes M. V. and Vilas F. 2001. Closing in on HED meteorite sources. *Earth, Planets, and Space* 53:1077–1083.

Takeda H. 1979. A layered crust model of a howardite parent body. *Icarus* 40:445–470.

Takeda H. 1997. Mineralogical records of early planetary processes on the howardite, eucrite, diogenite parent body with reference to Vesta. *Meteoritics & Planetary Science* 32:841–853.

Takeda H. and Graham A. L. 1991. Degree of equilibration of eucritic pyroxenes and thermal metamorphism of the earliest planetary crust. *Meteoritics* 26:129–134.

Takeda H., Mori H., and Bogard D. D. 1994. Mineralogy and ^{39}Ar-^{40}Ar age of an old pristine basalt: Thermal history of the HED parent body. *Earth and Planetary Science Letters* 122:183–194.

Takeda H., Ishi T., Arai T., and Miyamoto M. 1997. Mineralogy of the Asuka-87 and -88 eucrites and crustal evolution of the HED parent body. *Antarctic Meteorite Research* 10:401–413.

Tatsumoto M., Knight R. J., and Allègre C. J. 1973. Time differences in the formation of meteorites as determined from the ratio of lead-207 to lead-206. *Science* 180:1279–1283.

Taylor G. J., Keil K., McCoy T., Haack H., and Scott E. R. D. 1993. Asteroid differentiation: Pyroclastic volcanism to magma oceans. *Meteoritics* 28:34–52.

Tera F., Papanastassiou D. A., and Wasserburg G. J. 1974. Isotopic evidence for a terminal lunar cataclysm. *Earth and Planetary Science Letters* 22:1–21.

Tera F., Carlson R. W., and Boctor N. Z. 1997. Radiometric ages of basaltic achondrites and their relation to the early solar system. *Geochimica et Cosmochimica Acta* 61:1713–1731

Thomas P. C., Binzel R. P., Gaffey M. J., Storrs A. D., Wells E. N., and Zellner B. H. 1997. Impact excavation on asteroid 4 Vesta: Hubble Space Telescope results. *Science* 277:1492–1495.

Treiman A. H. and Goldman K. 2002. Petrology of the cumulate eucrite Serra de Magé (abstract# 1191). Proceedings, 23rd Lunar and Planetary Science Conference.

Turner G. 1969. Thermal histories of meteorites by the ^{39}Ar-^{40}Ar method. In *Meteorite research,* edited by Milliman P. M. New York: Springer-Verlag. pp. 407–417.

Wadhwa M. and Lugmair G. W. 1996. Age of the eucrite Caldera from convergence of long-lived and short-lived chronometers. *Geochimica et Cosmochimica Acta* 60:4889–4893.

Warren P. H. and Ulff-Møller F. 1999. A compositional-petrologic study of diverse cumulate eucrites (abstract #2054). Proceedings, 30th Lunar and Planetary Science Conference.

Warren P. H., Haack H., and Rasmussen K. L. 1991. Megaregolith insulation and the duration of cooling to isotopic closure within differentiated asteroids and the moon. *Journal of Geophysical Research* 96:5909–5923.

Warren P. H., Kallemeyn G. W., Arai T., and Kaneda K. 1996.

Compositional–petrologic investigations of eucrites and the QUE 94201 shergottite. *Antarctic Meteorites* 21:195–197.

Wetherill G. W. 1985. Asteroidal source of ordinary chondrites. *Meteoritics* 20:1–22.

Wisdom J. 1985. Meteorites may follow a chaotic route to Earth. *Nature* 315:731–733.

Yamaguchi A. and Misawa K. 2001. Occurrence and possible origin of zircon in basaltic eucrites (abstract). *Antarctic Meteorites* 26: 165–166.

Yamaguchi A., Taylor G. J., and Keil K. 1996. Global crustal metamorphism of the eucrite parent body. *Icarus* 124:97–112.

Yamaguchi A., Taylor G. J., and Keil K. 1997. Metamorphic history of the eucritic crust of 4 Vesta. *Journal of Geophysical Research* 102:13381–13386.

Yamaguchi A., Taylor G. J., and Keil K. 1997. Not all eucrites are monomict breccias (abstract). Proceedings, 28th Lunar and Planetary Science Conference. pp. 1601–1602.

Yamaguchi A., Taylor G. J., and Keil K., Floss C., Crozaz G., Nyquist L. E., Bogard D. D., Garrison D. H., Reese Y., Wiesmann H., and Shih C. Y. 2001. Post-crystallization reheating and partial melting of eucrite EET 90020 by impact into the hot crust of asteroid 4 Vesta ~4.50 Ga ago. *Geochimica et Cosmochimica Acta* 65:3577–3599.

Yanai K. 1993. The Asuka-87 and Asuka-88 collections of Antarctic meteorites. *Proceedings of NIPR Symposium on Antarctic Meteorites* 6:148-170.

Zappalá V., Bendjoya P., Cellino A., Farinella P., and Froeschlé C. 1995. Asteroid families: Search of a 12,487-asteroid sample using two different clustering techniques. *Icarus* 116:291–314.

APPENDIX

Argon Isotopic Data

In the following table, the columns, left to right, give the extraction temperature in °C, the ^{39}Ar concentration in units of 10^{-11} cm^3 STP/g, the calculated age in Gyr, the K/Ca ratio, and the ^{40}Ar/^{39}Ar, ^{38}Ar/^{39}Ar, ^{37}Ar/^{39}Ar, and ^{36}Ar/^{39}Ar isotopic ratios. The data in several columns have been multiplied by the factors indicated. The uncertainties in the age and all ratios are listed beneath the values. The sample weights in g and irradiation constants (J values) are also given. All age uncertainties include the error in J.

Table 1A.

Temp (°C)	^{39}Ar cc/g ×10^{11}	Age (Gyr)	K/Ca ratio ×1000	40/39 ± ×1	38/39 ± ×10	37/39 ± ×1	36/39 ± ×10
QUE 97053,8 (0.0439 g) J = 0.02094 ± 0.00008							
350	0.3	9.669	8.55	10105	89.83	64.3	346.83
		0.316	1.51	1776	16.31	11.3	61.14
450	0.7	3.749	4.82	333.8	20.22	114.0	4.89
		0.249	0.76	52.6	3.89	18.0	1.10
525	3.8	4.043	5.36	401.4	11.40	102.5	3.83
		0.074	0.25	18.4	0.63	4.8	0.26
575	5.5	4.202	5.72	442.7	6.63	96.2	3.87
		0.055	0.20	14.8	0.31	3.4	0.19
625	7.6	4.348	6.30	483.9	5.99	87.3	3.63
		0.041	0.17	12.0	0.21	2.3	0.14
675	8.9	4.389	6.94	496.3	5.75	79.3	3.57
		0.069	0.30	20.7	0.28	3.4	0.18
720	20.9	4.460	7.57	517.9	5.08	72.6	3.24
		0.017	0.11	5.1	0.08	1.0	0.05
750	25.1	4.456	7.90	516.9	4.75	69.6	3.08
		0.015	0.10	4.3	0.07	0.9	0.05
775	34.5	4.491	7.96	527.7	4.66	69.1	3.05
		0.012	0.09	3.2	0.05	0.8	0.04
800	42.9	4.479	8.03	524.1	4.69	68.5	3.03
		0.010	0.09	2.6	0.04	0.8	0.03
825	45.7	4.475	7.97	522.6	4.84	69.0	3.03
		0.010	0.09	2.4	0.04	0.8	0.03
850	35.2	4.460	8.03	518.1	5.11	68.5	3.03
		0.012	0.09	3.0	0.05	0.8	0.04
875	25.9	4.465	8.16	519.5	5.47	67.4	3.02
		0.015	0.10	4.1	0.07	0.9	0.04
900	15.5	4.450	8.37	514.9	5.81	65.7	3.02
		0.022	0.14	6.6	0.11	1.1	0.07
950	15.9	4.427	8.34	507.8	6.37	66.0	3.13
		0.022	0.13	6.4	0.11	1.1	0.07
1000	28.7	4.440	7.55	511.8	6.85	72.9	3.62
		0.013	0.09	3.6	0.06	0.9	0.04

Table 1A. *Continued.*

Temp (°C)	^{39}Ar cc/g ×10^{11}	Age (Gyr)	K/Ca ratio ×1000	40/39 ± ×1	38/39 ± ×10	37/39 ± ×1	36/39 ± ×10
1040	24.4	4.430	7.08	508.6	6.75	77.7	4.05
		0.015	0.09	4.4	0.07	1.0	0.05
1080	34.2	4.466	5.93	520.0	9.33	92.7	4.92
		0.012	0.07	3.2	0.07	1.1	0.05
1110	31.0	4.466	4.86	520.0	10.61	113.1	6.31
		0.013	0.06	3.5	0.08	1.4	0.06
1140	24.8	4.467	3.34	520.1	14.22	164.7	8.86
		0.016	0.04	4.5	0.13	2.2	0.10
1180	20.5	4.464	2.26	519.2	18.78	243.0	12.24
		0.019	0.03	5.5	0.21	3.6	0.16
1250	17.4	4.496	2.72	529.5	15.65	202.3	10.31
		0.021	0.04	6.5	0.21	3.2	0.15
1350	45.6	4.488	5.30	527.1	7.55	103.8	4.98
		0.010	0.06	2.6	0.05	1.2	0.04
1425	53.2	4.481	6.16	524.8	6.19	89.2	4.11
		0.010	0.07	2.5	0.04	1.0	0.04
1500	2.4	4.579	6.52	556.8	6.10	84.4	5.81
		0.107	0.42	35.8	0.45	5.5	0.43
1600	0.1	5.817	9.59	1152.5	11.50	57.3	28.04
		0.542	3.00	360.2	4.16	17.9	9.78
GRA 98098,26 WR (0.0424 g) J = 0.02094 ± 0.00008							
350	2.1	7.008	33.62	2275.5	44.62	16.4	78.36
		0.119	2.29	152.9	3.07	1.1	5.30
450	1.2	3.239	23.01	239.8	28.56	23.9	6.01
		0.183	2.81	29.2	4.29	2.9	1.01
525	5.7	3.872	17.99	360.7	15.67	30.6	4.35
		0.049	0.58	11.1	0.57	1.0	0.19
600	20.7	4.368	18.84	490.1	7.86	29.2	3.87
		0.016	0.25	4.4	0.10	0.4	0.05
635	16.1	4.487	24.65	526.6	4.72	22.3	2.84
		0.021	0.39	6.4	0.10	0.4	0.08
675	36.4	4.345	24.76	483.0	4.99	22.2	2.92
		0.086	1.32	25.2	0.27	1.2	0.16
700	29.9	4.438	23.68	511.2	4.99	23.2	3.16
		0.013	0.29	3.4	0.06	0.3	0.05
725	34.8	4.458	19.53	517.4	5.87	28.2	3.81
		0.011	0.22	2.9	0.05	0.3	0.03
750	37.3	4.458	16.56	517.5	6.87	33.2	4.51
		0.011	0.19	2.7	0.05	0.4	0.04
775	45.1	4.466	13.62	520.1	8.03	40.4	5.27
		0.010	0.15	2.3	0.05	0.4	0.04
800	68.5	4.452	11.42	515.6	9.69	48.2	6.26
		0.011	0.13	2.8	0.06	0.5	0.04

Table 1A. *Continued.*

Temp (°C)	^{39}Ar cc/g ×10^{11}	Age (Gyr)	K/Ca ratio ×1000	40/39 ± ×1	38/39 ± ×10	37/39 ± ×1	36/39 ± ×10
825	46.2	4.428	10.51	508.1	10.57	52.3	6.79
		0.009	0.11	2.1	0.06	0.6	0.04
850	38.5	4.467	9.39	520.3	12.00	58.6	7.69
		0.010	0.11	2.6	0.08	0.7	0.05
875	39.8	4.456	8.68	516.8	13.69	63.4	8.42
		0.010	0.10	2.4	0.08	0.7	0.05
900	29.7	4.459	7.96	517.8	16.27	69.1	9.38
		0.012	0.09	3.3	0.12	0.8	0.07
925	21.6	4.433	7.46	509.6	19.44	73.7	10.32
		0.016	0.10	4.4	0.18	1.0	0.10
950	12.3	4.483	6.97	525.2	21.96	78.9	11.10
		0.025	0.12	7.6	0.33	1.4	0.17
1000	23.3	4.475	6.74	522.8	24.86	81.6	11.78
		0.015	0.09	4.1	0.22	1.0	0.11
1050	22.1	4.481	6.80	524.7	28.48	80.9	12.25
		0.016	0.09	4.5	0.25	1.1	0.11
1100	22.6	4.474	6.38	522.5	34.58	86.1	13.91
		0.015	0.08	4.5	0.30	1.1	0.13
1150	19.3	4.454	3.85	516.1	51.97	142.8	23.06
		0.017	0.05	5.0	0.52	2.0	0.24
1225	19.4	4.466	1.52	520.0	91.24	361.6	54.70
		0.020	0.02	6.0	1.06	5.5	0.64
1325	26.9	4.478	1.86	523.9	79.18	296.2	46.02
		0.015	0.02	4.5	0.70	3.9	0.41
1425	62.8	4.511	3.23	534.1	54.23	170.3	27.04
		0.010	0.04	2.5	0.29	1.9	0.15
1575	7.7	4.384	2.92	494.6	41.79	188.3	27.32
		0.042	0.08	12.6	1.09	5.1	0.72
GRA 98098,29 Vein (0.0163 g) J = 0.02094 ± 0.00008							
1000	1403.2	4.403	25.36	500.6	4.27	21.7	2.75
		0.006	0.25	0.4	0.02	0.2	0.01
1100	45.4	4.462	10.16	518.8	12.44	54.1	7.28
		0.018	0.15	5.4	0.16	0.8	0.09
1200	88.8	4.473	10.26	522.0	11.85	53.6	7.28
		0.011	0.12	2.9	0.08	0.6	0.05
1275	32.2	4.512	5.05	534.6	23.86	108.9	15.14
		0.025	0.09	7.9	0.38	1.9	0.25
1375	141.5	4.483	5.81	525.3	20.40	94.7	12.81
		0.009	0.06	2.0	0.09	1.0	0.07
1450	15.1	4.467	5.88	520.4	17.93	93.5	12.21
		0.054	0.20	16.8	0.65	3.2	0.45
1575	1.5	4.219	6.94	447.3	16.07	79.3	13.46
		0.291	1.24	79.9	3.75	14.2	3.13

Table 1A. *Continued.*

Temp (°C)	^{39}Ar cc/g ×10^{11}	Age (Gyr)	K/Ca ratio ×1000	40/39 ± ×1	38/39 ± ×10	37/39 ± ×1	36/39 ± ×10
PCA 82502,81 (0.0473 g) J = 0.03087 ± 0.00012							
350	5.4	3.348	20.78	174.8	1.56	26.5	4.66
		0.031	0.47	3.5	0.07	0.6	0.14
450	11.7	3.300	8.64	169.4	2.27	63.7	1.80
		0.019	0.13	2.0	0.05	1.0	0.06
550	21.5	4.061	7.22	275.2	3.02	76.2	2.27
		0.012	0.09	1.8	0.04	0.9	0.05
600	30.5	4.301	7.46	319.1	3.01	73.8	2.16
		0.011	0.08	1.7	0.03	0.8	0.04
650	33.5	4.416	8.42	342.1	2.67	65.3	1.86
		0.012	0.10	2.0	0.03	0.8	0.05
700	77.5	4.475	9.15	354.6	2.46	60.1	1.80
		0.008	0.10	1.0	0.02	0.6	0.02
720	29.9	4.505	9.60	361.1	2.35	57.3	1.66
		0.010	0.11	1.8	0.03	0.6	0.03
745	43.0	4.507	9.49	361.5	2.37	58.0	1.69
		0.009	0.10	1.4	0.02	0.6	0.03
775	63.5	4.510	9.43	362.2	2.38	58.3	1.70
		0.008	0.10	1.1	0.02	0.6	0.02
800	66.7	4.512	9.52	362.6	2.37	57.8	1.69
		0.008	0.10	1.1	0.02	0.6	0.02
825	55.2	4.495	9.45	359.0	2.40	58.2	1.69
		0.008	0.10	1.2	0.02	0.6	0.03
850	41.7	4.465	9.09	352.4	2.51	60.5	1.79
		0.010	0.10	1.5	0.02	0.7	0.03
900	51.4	4.400	8.42	338.8	2.80	65.3	2.01
		0.009	0.09	1.3	0.02	0.7	0.03
950	55.3	4.341	7.17	327.0	3.51	76.7	2.52
		0.009	0.08	1.3	0.03	0.8	0.03
1000	66.5	4.362	5.67	331.0	4.82	97.1	3.50
		0.010	0.06	1.5	0.03	1.1	0.04
1050	52.8	4.403	2.97	339.5	9.28	184.9	6.65
		0.014	0.04	2.5	0.08	2.3	0.08
1100	13.4	4.408	1.46	340.6	18.37	375.5	13.22
		0.032	0.03	6.5	0.39	8.1	0.32
1200	30.3	4.451	2.26	349.5	12.01	243.1	8.68
		0.018	0.03	3.6	0.13	3.5	0.13
1300	39.3	4.488	2.19	357.3	12.60	251.1	9.13
		0.017	0.03	3.5	0.13	3.5	0.13
1400	0.7	5.341	2.12	592.9	15.94	258.9	22.27
		0.125	0.16	43.2	1.41	19.0	2.06
1575	0.4	4.614	4.21	385.5	8.28	130.5	13.93
		0.200	0.51	46.3	1.35	15.7	2.36

Table 1A. *Continued.*

Temp (°C)	^{39}Ar cc/g ×10^{11}	Age (Gyr)	K/Ca ratio ×1000	40/39 ± ×1	38/39 ± ×10	37/39 ± ×1	36/39 ± ×10
PCA 91007,26 (0.0443 g) J = 0.03074 ± 0.00012							
350	60.6	1.560	87.76	44.7	0.44	6.3	1.20
		0.006	0.95	0.2	0.02	0.1	0.01
450	16.0	2.973	14.24	136.5	1.58	38.6	1.24
		0.015	0.20	1.3	0.04	0.5	0.04
550	30.6	3.697	10.26	220.0	2.17	53.6	1.56
		0.013	0.13	1.5	0.03	0.7	0.03
600	33.9	4.166	8.90	295.0	2.50	61.8	1.78
		0.011	0.10	1.5	0.03	0.7	0.03
650	39.9	4.335	9.27	327.1	2.37	59.3	1.72
		0.011	0.10	1.7	0.03	0.7	0.04
700	45.0	4.424	9.25	345.2	2.40	59.4	1.68
		0.009	0.10	1.3	0.02	0.6	0.03
725	62.1	4.445	9.17	349.7	2.41	60.0	1.69
		0.009	0.10	1.2	0.02	0.6	0.03
750	70.5	4.446	9.18	350.0	2.39	59.9	1.71
		0.008	0.10	1.1	0.02	0.6	0.02
775	51.2	4.441	9.40	348.7	2.38	58.5	1.66
		0.009	0.10	1.3	0.02	0.6	0.03
850	84.4	4.366	9.03	333.4	2.53	60.9	1.82
		0.008	0.09	1.0	0.02	0.6	0.02
900	58.0	4.213	8.75	303.5	2.61	62.8	1.89
		0.009	0.09	1.1	0.02	0.7	0.03
950	55.6	4.051	8.50	274.8	2.86	64.7	2.05
		0.009	0.09	1.0	0.02	0.7	0.03
1000	55.2	4.242	6.85	308.9	3.71	80.3	2.68
		0.010	0.08	1.4	0.03	0.9	0.04
1050	49.5	4.311	4.21	322.4	6.34	130.6	4.55
		0.012	0.05	1.9	0.05	1.5	0.06
1100	12.3	4.317	1.98	323.4	13.28	277.9	9.79
		0.030	0.04	5.7	0.28	5.7	0.24
1200	96.6	4.360	2.49	332.1	10.63	221.1	7.63
		0.015	0.03	2.8	0.10	2.9	0.10
1300	5.7	4.460	2.88	352.9	9.39	191.3	7.45
		0.054	0.10	11.4	0.39	6.5	0.39
1550	8.3	4.312	3.02	322.6	8.73	182.3	6.05
		0.067	0.13	13.1	0.48	7.6	0.43
Caldera (0.0442 g) J = 0.07630 ± 0.00025							
350	138.3	3.517	220.48	79.0	5.53	2.49	2.68
		0.005	2.22	0.1	0.02	0.03	0.01
450	33.9	3.422	131.65	74.2	3.84	4.18	2.40
		0.010	1.52	0.4	0.04	0.05	0.03
550	7.6	3.541	31.14	80.2	5.62	17.7	2.12
		0.041	0.88	2.1	0.22	0.5	0.14

Table 1A. *Continued.*

Temp (°C)	^{39}Ar cc/g ×10^{11}	Age (Gyr)	K/Ca ratio ×1000	40/39 ± ×1	38/39 ± ×10	37/39 ± ×1	36/39 ± ×10
650	25.4	2.819	18.95	49.4	2.29	29.0	0.55
		0.021	0.33	0.7	0.06	0.5	0.04
750	32.1	3.763	9.52	92.4	0.99	57.8	0.38
		0.014	0.12	0.8	0.03	0.7	0.04
800	25.4	4.184	6.44	120.2	0.88	85.4	0.41
		0.016	0.09	1.1	0.03	1.1	0.05
850	47.4	4.317	5.81	130.3	0.84	94.6	0.44
		0.011	0.07	0.8	0.03	1.1	0.04
900	64.8	4.379	5.94	135.3	0.77	92.5	0.44
		0.009	0.06	0.6	0.02	1.0	0.03
950	85.2	4.378	6.16	135.3	0.71	89.3	0.40
		0.008	0.07	0.5	0.02	1.0	0.03
975	91.2	4.403	5.95	137.3	0.73	92.4	0.40
		0.008	0.06	0.5	0.02	1.0	0.03
1000	132.5	4.443	5.32	140.7	0.80	103.4	0.44
		0.008	0.06	0.5	0.02	1.1	0.04
1025	155.8	4.458	4.94	142.0	0.87	111.4	0.48
		0.008	0.05	0.5	0.02	1.2	0.04
1050	72.1	4.443	5.26	140.7	0.83	104.6	0.45
		0.010	0.06	0.7	0.02	1.2	0.04
1150	134.8	4.404	2.76	137.4	1.82	199.4	1.03
		0.013	0.03	0.9	0.03	2.4	0.07
1250	74.4	4.428	0.97	139.4	5.78	566.7	3.31
		0.030	0.02	2.5	0.12	11.7	0.20
1400	249.7	4.493	2.87	145.0	1.71	191.4	0.97
		0.012	0.03	0.9	0.03	2.3	0.06
1550	15.0	4.480	4.25	143.9	1.34	129.4	1.56
		0.090	0.71	7.9	0.11	21.6	0.21
Asuka-881388,55 (0.0486 g) J = 0.02193 ±0.00004							
350	1.5	3.250	17.55	230.6	77.14	31.3	3.60
		0.094	1.11	14.4	5.31	2.0	0.44
450	0.8	4.070	11.87	389.7	46.99	46.4	3.88
		0.142	1.05	34.2	4.44	4.1	0.66
500	2.2	4.128	10.61	403.8	14.23	51.8	5.02
		0.069	0.46	17.1	0.70	2.3	0.37
550	3.2	4.250	11.41	435.3	7.36	48.2	5.26
		0.048	0.36	12.8	0.30	1.5	0.26
600	5.7	4.314	11.12	452.6	6.29	49.5	4.97
		0.030	0.23	8.1	0.16	1.0	0.15
650	7.1	4.320	11.77	454.4	6.01	46.7	4.26
		0.024	0.21	6.6	0.13	0.8	0.12
700	15.4	4.427	8.52	484.7	7.14	64.5	5.12
		0.013	0.11	3.7	0.07	0.8	0.07

Table 1A. *Continued.*

Temp (°C)	^{39}Ar cc/g ×10^{11}	Age (Gyr)	K/Ca ratio ×1000	40/39 ± ×1	38/39 ± ×10	37/39 ± ×1	36/39 ± ×10
735	35.6	4.473	7.01	498.4	8.37	78.4	5.68
		0.007	0.07	1.8	0.04	0.8	0.04
760	38.9	4.481	6.91	500.9	8.48	79.6	5.62
		0.006	0.07	1.7	0.04	0.8	0.04
790	35.7	4.480	6.83	500.6	8.64	80.6	5.74
		0.006	0.07	1.7	0.04	0.9	0.04
825	26.6	4.481	6.75	501.0	8.79	81.5	5.89
		0.009	0.08	2.7	0.06	0.9	0.05
850	17.8	4.490	6.66	503.6	8.99	82.6	5.99
		0.011	0.08	3.2	0.07	1.0	0.06
900	19.0	4.479	6.38	500.2	9.59	86.2	6.26
		0.010	0.07	3.0	0.07	1.0	0.06
925	11.6	4.464	6.11	495.8	10.33	90.0	6.64
		0.016	0.08	4.8	0.12	1.2	0.10
955	9.5	4.455	5.40	493.3	12.04	101.8	7.94
		0.019	0.08	5.6	0.16	1.5	0.13
1010	8.5	4.431	3.82	486.0	17.92	143.8	11.78
		0.021	0.06	6.2	0.24	2.3	0.17
1100	18.7	4.489	0.90	503.5	82.60	612.6	54.19
		0.019	0.01	5.6	0.93	9.2	0.64
1175	3.7	4.346	0.75	461.6	94.14	728.9	62.12
		0.051	0.02	14.2	2.98	23.6	1.99
1300	9.1	4.434	2.70	486.9	25.69	203.6	16.88
		0.021	0.04	6.0	0.32	3.2	0.23
1450	0.8	4.853	1.58	625.9	47.14	347.6	34.93
		0.168	0.16	62.4	4.79	34.8	3.56
1600	0.2	4.444	2.95	489.9	30.33	186.7	31.93
		0.427	0.76	126.7	8.32	48.3	8.78
Asuka-881467,42 (0.0513 g) J = 0.02191 ± 0.00004							
350	124.9	0.202	475.51	5.4	3.84	1.16	0.13
		0.003	8.25	0.1	0.08	0.02	0.01
400	17.2	0.684	93.72	21.0	3.90	5.9	0.86
		0.021	3.54	0.8	0.22	0.2	0.05
450	3.4	2.363	31.77	123.5	25.91	17.3	0.77
		0.052	1.30	4.9	1.29	0.7	0.14
500	5.9	3.369	20.22	249.8	13.28	27.2	1.26
		0.030	0.44	4.9	0.33	0.6	0.11
575	11.4	4.007	15.77	375.2	3.68	34.9	1.64
		0.016	0.22	3.6	0.08	0.5	0.07
625	12.1	4.145	16.36	408.6	2.79	33.6	1.64
		0.015	0.22	3.7	0.07	0.5	0.06
675	22.3	4.101	13.20	397.6	2.70	41.7	1.56
		0.009	0.15	2.1	0.04	0.5	0.04
700	16.1	4.351	10.75	463.6	2.85	51.2	1.79
		0.012	0.13	3.4	0.06	0.6	0.05

Table 1A. *Continued.*

Temp (°C)	^{39}Ar cc/g ×10^{11}	Age (Gyr)	K/Ca ratio ×1000	40/39 ± ×1	38/39 ± ×10	37/39 ± ×1	36/39 ± ×10
725	24.7	4.394	9.37	475.7	3.17	58.7	2.02
		0.008	0.10	2.2	0.04	0.6	0.04
750	28.3	4.432	8.88	486.8	3.24	62.0	2.10
		0.007	0.10	2.0	0.04	0.7	0.04
775	29.3	4.441	8.71	489.7	3.28	63.2	2.13
		0.008	0.09	2.1	0.04	0.7	0.04
800	35.2	4.430	8.64	486.4	3.34	63.6	2.17
		0.007	0.09	1.9	0.03	0.7	0.03
825	28.7	4.388	8.81	473.9	3.34	62.4	2.11
		0.008	0.10	2.2	0.04	0.7	0.04
850	19.8	4.331	9.02	457.9	3.35	61.0	2.07
		0.010	0.10	2.6	0.05	0.7	0.05
900	24.2	4.203	9.03	423.4	3.97	60.9	2.18
		0.008	0.10	2.0	0.05	0.7	0.04
975	29.9	4.255	7.76	437.1	4.30	70.9	2.67
		0.008	0.08	1.9	0.03	0.8	0.03
1050	34.4	4.377	2.85	470.8	12.37	193.0	8.21
		0.008	0.03	2.2	0.07	2.1	0.08
1080	10.8	4.392	1.66	475.3	22.04	331.6	14.66
		0.019	0.03	5.5	0.28	5.1	0.22
1140	7.4	4.358	1.03	465.5	35.04	532.7	23.25
		0.028	0.02	7.9	0.61	10.5	0.44
1250	40.7	4.465	2.74	496.8	12.45	201.0	8.27
		0.008	0.03	2.2	0.06	2.2	0.08
1300	6.3	4.350	5.12	463.1	6.23	107.4	4.12
		0.027	0.10	7.6	0.13	2.1	0.10
1400	1.2	3.748	7.87	318.9	4.53	69.9	3.46
		0.115	0.58	23.3	0.42	5.2	0.35
1600	0.02	3.940	blank	359.8	blank	blank	blank
		0.560		125.8			
GRO 95533,7 (0.0478 g) J = 0.03036 ± 0.00029							
350	5.8	3.452	7.92	190.2	3.64	69.4	12.39
		0.050	5.02	5.9	0.30	43.9	1.18
450	6.2	3.796	7.76	237.2	1.74	70.8	1.37
		0.029	0.15	3.8	0.07	1.3	0.09
550	32.1	3.689	9.63	221.6	1.46	57.1	1.03
		0.017	0.11	1.1	0.02	0.6	0.03
600	36.2	3.620	10.65	212.1	1.41	51.7	0.98
		0.017	0.12	1.0	0.02	0.6	0.03
650	45.7	3.557	10.29	203.7	1.42	53.4	1.06
		0.017	0.11	1.0	0.02	0.6	0.03
700	40.4	3.558	8.52	203.8	1.73	64.6	1.23
		0.017	0.10	1.0	0.02	0.7	0.03
750	76.6	3.552	6.59	203.0	2.24	83.5	1.61
		0.016	0.07	0.8	0.02	0.9	0.03

Table 1A. *Continued.*

Temp (°C)	^{39}Ar cc/g ×10^{11}	Age (Gyr)	K/Ca ratio ×1000	40/39 ± ×1	38/39 ± ×10	37/39 ± ×1	36/39 ± ×10
775	52.2	3.564	5.94	204.6	2.51	92.5	1.79
		0.017	0.07	1.0	0.03	1.0	0.04
800	46.3	3.589	5.57	207.9	2.66	98.7	1.91
		0.017	0.06	1.1	0.03	1.1	0.04
850	36.0	3.599	5.44	209.3	2.77	101.0	1.98
		0.018	0.06	1.3	0.03	1.2	0.04
925	39.2	3.630	4.83	213.4	3.37	114.0	2.44
		0.018	0.06	1.3	0.04	1.3	0.05
1000	24.7	3.618	3.53	211.8	5.23	155.6	3.76
		0.022	0.05	2.1	0.07	2.2	0.08
1100	34.3	3.652	0.97	216.5	20.40	568.0	14.54
		0.038	0.02	4.9	0.47	14.0	0.39
1200	15.2	3.959	0.72	262.8	24.74	767.4	17.65
		0.052	0.02	8.2	0.79	25.1	0.62
1300	4.4	4.096	0.79	286.1	21.53	695.2	15.25
		0.080	0.04	13.8	1.17	34.3	0.90
1400	4.4	4.047	1.36	277.4	13.57	403.5	9.28
		0.044	0.04	7.2	0.41	11.2	0.33
1550	0.8	2.823	20.08	124.6	8.22	27.4	4.79
		0.308	4.34	26.9	2.49	5.9	1.60
QUE 97014,5 (0.0398 g) J = 0.02094 ± 0.00008							
350	8.7	4.553	24.48	547.9	43.03	22.5	15.41
		0.039	0.62	12.7	1.04	0.6	0.38
450	8.8	2.947	19.17	196.8	15.76	28.7	1.25
		0.041	0.57	5.5	0.53	0.8	0.09
550	425.9	3.544	22.27	292.7	2.75	24.7	0.82
		0.006	0.22	0.4	0.02	0.2	0.01
600	13.6	3.566	36.88	296.9	1.06	14.9	0.55
		0.029	0.77	5.5	0.08	0.3	0.05
700	56.5	3.582	23.64	300.0	1.42	23.3	0.78
		0.009	0.26	1.4	0.03	0.3	0.02
750	99.4	3.537	14.77	291.4	2.40	37.2	1.29
		0.007	0.15	0.8	0.02	0.4	0.04
775	77.5	3.518	11.45	287.9	3.13	48.0	1.68
		0.008	0.12	1.0	0.03	0.5	0.02
800	64.1	3.520	10.28	288.3	3.53	53.5	1.87
		0.009	0.11	1.2	0.03	0.6	0.03
825	44.0	3.521	9.78	288.4	3.88	56.2	1.99
		0.011	0.11	1.7	0.04	0.7	0.03
860	31.5	3.501	9.41	284.8	4.49	58.5	2.12
		0.014	0.12	2.4	0.06	0.8	0.04
925	21.3	3.473	8.81	279.6	5.35	62.5	2.40
		0.020	0.14	3.4	0.10	1.0	0.06
1000	28.4	3.426	5.88	271.2	8.45	93.6	3.97
		0.016	0.08	2.6	0.11	1.3	0.06

Table 1A. *Continued.*

Temp (°C)	^{39}Ar cc/g ×10^{11}	Age (Gyr)	K/Ca ratio ×1000	40/39 ± ×1	38/39 ± ×10	37/39 ± ×1	36/39 ± ×10
1050	14.4	3.368	4.38	261.1	9.66	125.6	5.16
		0.028	0.09	4.8	0.23	2.6	0.14
1150	26.1	3.362	1.52	260.1	26.66	360.9	15.51
		0.019	0.02	3.0	0.35	5.5	0.24
1250	9.7	3.442	0.68	274.0	51.53	812.5	31.84
		0.047	0.02	8.3	1.70	25.8	1.09
1350	7.4	3.501	1.04	284.8	34.17	527.3	20.98
		0.059	0.04	10.7	1.34	20.6	0.84
1500	1.3	3.577	1.09	299.1	33.29	505.4	22.82
		0.010	0.16	1.6	5.05	74.2	3.48
1625	0.1	3.563	8.48	296.4	5.10	64.8	13.40
		0.841	4.60	160.4	4.02	35.2	10.13
Moama (0.0621 g) J = 0.02229 ± 0.00005							
350	4.3	0.866	75.30	27.7	79.87	7.3	0.94
		0.070	7.75	2.8	11.47	0.8	0.16
400	3.3	1.441	31.43	54.9	77.18	17.5	1.80
		0.073	2.34	4.0	7.92	1.3	0.22
500	4.9	1.439	15.99	54.7	45.06	34.4	1.62
		0.052	0.86	2.9	3.32	1.9	0.15
600	13.4	2.213	7.19	108.2	8.72	76.5	3.40
		0.015	0.11	1.3	0.14	1.2	0.07
675	9.0	2.865	4.38	174.8	10.23	125.5	5.62
		0.017	0.07	2.0	0.16	1.9	0.11
725	12.9	3.743	2.26	312.4	15.72	243.2	9.92
		0.010	0.03	1.9	0.12	2.8	0.12
775	15.7	4.167	1.71	407.1	19.43	321.3	12.86
		0.010	0.02	2.3	0.13	3.7	0.14
810	16.4	4.345	1.49	453.8	22.11	369.7	14.78
		0.011	0.02	3.0	0.16	4.4	0.16
847	17.0	4.396	1.40	468.3	23.49	393.4	15.66
		0.012	0.02	3.2	0.18	4.8	0.18
880	19.0	4.426	1.31	476.9	24.82	420.0	16.61
		0.012	0.02	3.3	0.19	5.1	0.19
900	28.8	4.473	1.22	490.7	26.57	449.8	17.61
		0.012	0.02	3.5	0.20	5.5	0.20
915	24.6	4.484	1.23	493.7	26.97	448.4	17.95
		0.012	0.02	3.5	0.20	5.5	0.20
925	30.9	4.483	1.33	493.5	24.92	412.3	16.50
		0.011	0.02	3.2	0.17	4.9	0.18
940	13.7	4.447	1.42	482.8	23.60	388.1	15.61
		0.009	0.02	2.3	0.14	4.3	0.16
975	15.2	4.363	1.50	459.0	22.40	366.1	14.65
		0.011	0.02	2.9	0.16	4.3	0.16
1025	14.4	4.181	1.70	410.5	19.99	323.8	13.22
		0.012	0.02	2.9	0.15	4.0	0.15

Table 1A. *Continued.*

Temp (°C)	^{39}Ar cc/g ×10^{11}	Age (Gyr)	K/Ca ratio ×1000	40/39 ± ×1	38/39 ± ×10	37/39 ± ×1	36/39 ± ×10
1100	8.6	4.217	1.31	419.8	28.81	421.3	18.98
		0.018	0.02	4.6	0.33	6.2	0.26
1200	4.5	4.133	0.58	398.5	67.90	941.7	45.00
		0.042	0.02	10.2	1.94	25.9	1.34
1350	1.0	4.294	1.23	439.9	29.44	447.2	19.65
		0.107	0.08	28.8	2.06	29.7	1.41
1600	0.8	4.209	1.74	417.5	24.21	316.3	18.39
		0.188	0.20	48.1	3.02	36.7	2.33
EET 87520 (0.0445 g) J = 0.02094 ± 0.00008							
350	0.5	5.481	18.68	948.9	87.35	29.4	32.49
		0.246	2.69	136.0	13.39	4.2	5.06
450	1.1	2.004	13.58	97.2	49.95	40.5	0.60
		0.224	2.52	18.0	12.20	7.5	0.24
550	7.4	2.671	18.10	162.2	18.33	30.4	0.25
		0.042	0.57	4.9	0.68	1.0	0.05
600	17.8	3.222	23.99	237.2	0.96	22.9	0.19
		0.018	0.37	2.8	0.05	0.4	0.03
650	21.7	3.642	27.67	311.7	0.41	19.9	0.17
		0.017	0.40	3.2	0.04	0.3	0.03
685	22.2	3.823	26.52	349.7	0.57	20.7	0.17
		0.027	0.51	5.7	0.05	0.4	0.04
710	20.7	4.044	21.78	401.5	0.46	25.3	0.21
		0.017	0.31	4.0	0.04	0.4	0.03
735	30.1	4.192	16.97	439.9	0.56	32.4	0.30
		0.013	0.21	3.0	0.04	0.4	0.03
760	36.6	4.292	13.84	467.7	0.69	39.8	0.37
		0.011	0.16	2.7	0.03	0.5	0.02
782	26.3	4.360	11.15	487.5	0.85	49.3	0.47
		0.014	0.14	3.8	0.04	0.6	0.03
799	24.0	4.410	10.23	502.6	0.92	53.8	0.49
		0.015	0.13	4.3	0.04	0.7	0.04
822	28.3	4.419	9.24	505.3	1.04	59.5	0.56
		0.014	0.12	3.8	0.04	0.7	0.03
850	27.7	4.447	8.30	513.9	1.21	66.2	0.64
		0.014	0.10	3.7	0.04	0.8	0.04
875	23.8	4.463	8.03	519.1	1.23	68.5	0.64
		0.016	0.11	4.5	0.05	0.9	0.04
900	21.9	4.465	7.55	519.8	1.37	72.9	0.68
		0.017	0.10	4.9	0.05	1.0	0.04
935	19.6	4.461	7.15	518.3	1.50	76.9	0.71
		0.018	0.10	5.4	0.04	1.1	0.03
975	20.5	4.469	6.74	521.0	1.63	81.6	0.78
		0.017	0.09	5.1	0.04	1.1	0.04
1010	36.5	4.463	6.51	519.0	1.68	84.4	0.81
		0.011	0.07	2.9	0.04	1.0	0.04

Table 1A. *Continued.*

Temp (°C)	^{39}Ar cc/g ×10^{11}	Age (Gyr)	K/Ca ratio ×1000	40/39 ± ×1	38/39 ± ×10	37/39 ± ×1	36/39 ± ×10
1040	20.2	4.452	5.96	515.5	2.13	92.3	0.90
		0.018	0.08	5.2	0.04	1.3	0.04
1085	14.8	4.418	4.94	505.1	3.15	111.4	1.17
		0.023	0.08	6.9	0.06	1.9	0.05
1150	20.2	4.423	2.92	506.7	6.83	188.4	2.09
		0.019	0.04	5.5	0.09	2.8	0.07
1200	17.0	4.466	1.24	520.1	9.76	444.8	5.15
		0.024	0.02	7.4	0.15	7.7	0.17
1275	13.4	4.450	0.96	514.9	11.49	570.5	6.49
		0.031	0.02	9.3	0.22	11.8	0.23
1400	81.4	4.476	2.85	523.0	3.61	192.7	2.09
		0.009	0.03	2.1	0.03	2.1	0.06
1600	30.7	4.479	6.30	524.2	1.54	87.3	0.97
		0.014	0.08	4.1	0.03	1.1	0.03
Moore County (0.0461 g) J = 0.02187 ± 0.00008							
350	1.7	6.742	623.57	1873.1	456.95	0.88	60.78
		0.020	10.50	20.4	5.74	0.01	0.86
425	0.2	4.541	2.16	520.8	211.77	254.4	23.16
		0.300	0.39	94.0	50.86	46.0	5.82
500	0.4	2.102	17.70	100.8	175.71	31.1	0.25
		0.315	4.50	25.6	62.74	7.9	0.15
550	0.4	1.827	12.80	80.2	71.79	43.0	0.88
		0.348	3.88	24.3	30.38	13.0	0.45
625	1.8	3.210	8.38	225.2	13.16	65.6	0.47
		0.074	0.42	11.0	0.90	3.3	0.14
700	3.0	3.029	9.56	199.3	5.19	57.5	0.67
		0.049	0.33	6.6	0.25	2.0	0.16
750	3.1	4.083	4.41	393.7	3.57	124.8	1.18
		0.030	0.09	7.2	0.11	2.6	0.42
800	6.0	4.196	3.94	422.2	2.64	139.6	1.19
		0.016	0.05	3.9	0.05	1.9	0.09
830	6.6	4.230	3.93	431.0	2.33	140.1	1.16
		0.015	0.05	3.7	0.05	1.9	0.09
852	5.7	4.217	4.04	427.6	2.29	136.3	1.13
		0.018	0.06	4.4	0.05	1.9	0.09
875	7.1	4.223	4.01	429.3	2.25	137.2	1.13
		0.014	0.05	3.5	0.04	1.8	0.08
895	6.9	4.197	4.09	422.6	2.17	134.5	1.07
		0.015	0.05	3.5	0.05	1.7	0.08
920	7.4	4.215	3.97	427.1	2.19	138.4	1.06
		0.014	0.05	3.4	0.04	1.8	0.08
950	7.4	4.204	4.08	424.2	2.09	134.8	1.02
		0.014	0.05	3.3	0.04	1.7	0.08
975	20.1	4.231	4.12	431.4	2.08	133.6	1.05
		0.008	0.04	1.5	0.03	1.4	0.05

Table 1A. *Continued.*

Temp (°C)	^{39}Ar cc/g ×10^{11}	Age (Gyr)	K/Ca ratio ×1000	40/39 ± ×1	38/39 ± ×10	37/39 ± ×1	36/39 ± ×10
1000	33.3	4.250	4.13	436.4	2.10	133.1	1.05
		0.008	0.04	1.3	0.03	1.4	0.05
1025	40.8	4.245	4.14	435.1	2.12	132.9	1.06
		0.007	0.04	1.2	0.02	1.4	0.04
1050	20.1	4.218	4.03	428.1	2.20	136.5	1.11
		0.008	0.04	1.5	0.03	1.4	0.05
1100	16.0	4.220	3.76	428.5	2.42	146.4	1.25
		0.009	0.04	1.8	0.03	1.6	0.05
1150	20.9	4.189	2.22	420.3	5.38	247.7	3.06
		0.010	0.02	2.2	0.05	2.8	0.09
1155	2.4	4.157	2.43	412.2	4.40	226.5	2.16
		0.040	0.06	10.0	0.14	5.9	0.15
1225	5.3	4.117	0.73	402.3	15.72	751.0	9.16
		0.030	0.02	7.4	0.31	15.7	0.31
1325	6.3	4.229	2.01	430.8	5.77	273.1	3.30
		0.017	0.03	4.3	0.08	3.9	0.11
1425	23.0	4.267	3.69	441.1	2.60	149.1	1.41
		0.008	0.04	1.5	0.03	1.6	0.05
1500	5.1	4.255	4.27	437.7	2.04	128.8	1.15
		0.018	0.06	4.6	0.04	1.9	0.07
1600	0.1	4.272	14.86	442.4	2.38	37.0	blank
		0.610	5.55	165.0	1.13	13.8	
Serra de Mage (0.0455 g) J = 0.02081 ± 0.00008							
350	0.3	6.100	25.73	1365.1	181.27	21.4	43.40
		0.114	1.71	89.2	14.04	1.4	3.82
450	0.4	2.548	7.06	149.2	65.52	77.9	4.18
		0.191	0.99	20.9	12.45	11.0	0.97
525	0.4	1.231	4.70	47.0	16.89	116.9	0.64
		0.250	1.32	13.2	6.45	32.8	0.38
600	1.1	1.770	3.11	80.1	4.76	176.6	0.99
		0.122	0.34	8.7	0.71	19.2	0.25
650	2.7	0.499	4.70	15.3	2.81	117.1	0.81
		0.199	2.14	7.0	1.86	53.4	0.62
700	1.0	2.779	1.35	176.2	5.40	406.4	2.63
		0.180	0.17	22.4	0.90	51.8	0.59
775	2.0	3.112	1.10	221.7	6.70	501.8	3.57
		0.093	0.07	13.9	0.54	32.0	0.40
825	6.4	3.316	1.05	253.9	6.93	522.1	4.11
		0.033	0.03	5.5	0.19	12.5	0.22
875	5.2	3.387	1.07	266.1	6.76	513.2	3.90
		0.037	0.03	6.4	0.21	13.3	0.22
925	4.0	3.372	1.13	263.5	6.45	488.1	3.63
		0.045	0.03	7.7	0.24	15.0	0.24
975	2.8	3.388	1.14	266.2	6.33	483.9	3.51
		0.060	0.05	10.5	0.32	19.7	0.28

Table 1A. *Continued.*

Temp (°C)	^{39}Ar cc/g ×10^{11}	Age (Gyr)	K/Ca ratio ×1000	40/39 ± ×1	38/39 ± ×10	37/39 ± ×1	36/39 ± ×10
1025	4.4	3.395	1.18	267.4	6.14	466.9	3.48
		0.041	0.03	7.0	0.21	13.2	0.22
1075	3.7	3.461	1.17	279.2	6.17	468.5	3.67
		0.045	0.04	8.1	0.23	14.4	0.24
1125	4.9	3.511	1.08	288.4	6.83	508.7	3.84
		0.037	0.03	6.8	0.21	13.0	0.22
1175	3.4	3.619	1.00	309.2	7.62	548.7	4.36
		0.048	0.03	9.5	0.30	17.8	0.28
1225	2.0	3.528	0.51	291.7	15.67	1077.1	8.80
		0.103	0.03	19.3	1.08	72.2	0.72
1275	2.6	3.585	0.19	302.4	44.89	2902.1	26.15
		0.158	0.02	30.7	4.61	295.8	2.85
1325	1.6	3.689	0.57	323.2	14.35	972.0	8.46
		0.193	0.07	39.7	2.06	119.8	1.36
1400	7.1	3.783	0.93	343.2	8.35	592.0	4.84
		0.053	0.03	11.4	0.30	20.5	0.26
1500	13.6	3.910	1.32	371.7	5.46	417.0	3.21
		0.028	0.03	6.3	0.11	8.2	0.15
EET 87548 (0.0508 g) J = 0.02234 ± 0.00005							
350	2.0	3.674	2.36	298.2	96.97	233.1	11.95
		0.035	0.06	6.6	2.79	5.7	0.46
450	0.6	3.309	2.44	235.4	48.56	225.1	9.07
		0.141	0.23	21.9	5.91	21.1	1.37
550	3.7	3.320	2.13	237.1	31.70	258.1	10.65
		0.029	0.05	4.5	0.77	5.6	0.32
650	7.2	3.509	1.99	268.3	20.79	275.8	12.59
		0.021	0.03	3.5	0.35	4.6	0.25
800	0.6	3.455	1.89	259.0	21.55	291.7	13.80
		0.175	0.22	29.5	3.20	33.4	2.22
900	4.8	3.376	1.46	245.9	31.39	376.0	22.64
		0.034	0.04	5.4	0.85	9.1	0.64
1000	0.1	2.610	0.89	145.5	53.74	620.7	39.11
		0.748	0.48	78.9	35.35	337.1	26.31
1100	6.3	3.426	0.37	254.3	128.05	1504.0	83.97
		0.073	0.02	12.0	6.45	72.9	4.28
1200	1.0	3.523	0.19	270.8	237.36	2833.3	160.72
		0.412	0.05	72.1	66.27	755.0	45.03
1350	1.0	3.599	0.25	284.2	193.60	2230.1	127.62
		0.352	0.06	64.1	46.56	503.7	30.84
1600	0.1	1.738	0.17	72.5	284.83	3249.3	191.30
		1.715	0.26	111.5	456.26	4994.7	307.34
ALH 85001,32 (0.0530 g) J = 0.02226 ± 0.00005							
350	1.0	4.754	3.83	581.6	284.74	143.5	18.45
		0.041	0.10	14.2	8.56	3.8	0.77

Table 1A. *Continued.*

Temp (°C)	^{39}Ar cc/g $\times 10^{11}$	Age (Gyr)	K/Ca ratio $\times 1000$	40/39 $\pm \times 1$	38/39 $\pm \times 10$	37/39 $\pm \times 1$	36/39 $\pm \times 10$
450	2.0	3.286	3.50	232.7	54.72	157.4	6.79
		0.042	0.10	6.4	2.02	4.6	0.36
550	8.6	3.097	3.21	205.2	18.77	171.3	4.89
		0.015	0.04	2.0	0.24	2.4	0.11
600	4.6	3.191	3.25	218.6	11.15	169.1	4.82
		0.028	0.07	4.1	0.29	3.6	0.18
650	7.8	3.265	3.18	229.6	10.69	173.0	5.19
		0.017	0.05	2.5	0.16	2.6	0.12
700	9.6	3.408	3.01	252.2	10.24	182.9	5.59
		0.014	0.04	2.2	0.12	2.4	0.11
750	16.1	3.491	2.99	266.3	9.68	184.1	5.38
		0.031	0.07	5.3	0.20	4.1	0.13
775	11.6	3.669	2.84	298.4	9.93	193.8	5.69
		0.011	0.03	2.0	0.09	2.3	0.09
800	8.7	3.683	2.87	301.1	9.96	191.8	5.70
		0.013	0.04	2.5	0.11	2.5	0.11
850	9.5	3.742	2.81	312.7	10.72	195.7	5.85
		0.012	0.04	2.3	0.11	2.4	0.10
900	7.2	3.765	2.66	317.2	11.60	206.4	6.42
		0.016	0.04	3.0	0.15	2.9	0.13
975	12.1	3.643	2.40	293.5	12.77	228.8	7.49
		0.011	0.03	2.0	0.11	2.8	0.11
1025	12.6	3.610	2.04	287.5	14.69	270.1	9.14
		0.012	0.03	2.2	0.14	3.4	0.13
1075	19.0	3.610	1.75	287.4	17.03	315.0	10.67
		0.011	0.02	1.8	0.14	3.7	0.14
1115	13.0	3.618	1.43	288.9	20.63	384.2	13.07
		0.017	0.02	3.0	0.26	5.5	0.22
1175	9.0	3.679	1.37	300.3	23.08	401.5	14.82
		0.022	0.02	4.2	0.35	6.9	0.26
1300	4.0	3.711	0.88	306.5	38.56	624.3	24.93
		0.050	0.03	9.7	1.29	20.7	0.87
1600	0.9	3.590	0.54	283.8	66.71	1016.8	45.03
		0.277	0.10	50.4	13.66	181.1	9.35
Piplia Kalan (0.0421 g) J = 0.02641 ± 0.00010							
350	7.4	4.284	11.94	368.9	2.75	46.1	7.09
		0.019	0.18	4.1	0.07	0.7	0.18
450	9.5	3.880	9.68	287.3	2.12	56.8	1.43
		0.016	0.13	2.7	0.05	0.8	0.11
550	25.4	3.797	10.57	272.7	1.86	52.0	1.24
		0.010	0.12	1.3	0.03	0.6	0.05
610	38.2	3.654	9.79	249.0	2.18	56.2	1.48
		0.008	0.10	0.8	0.03	0.6	0.04
650	28.0	3.583	8.31	238.0	2.66	66.1	1.84
		0.009	0.09	1.1	0.03	0.7	0.05

Table 1A. *Continued.*

Temp (°C)	^{39}Ar cc/g $\times 10^{11}$	Age (Gyr)	K/Ca ratio $\times 1000$	40/39 $\pm \times 1$	38/39 $\pm \times 10$	37/39 $\pm \times 1$	36/39 $\pm \times 10$
700	39.3	3.541	6.76	231.7	3.34	81.3	2.23
		0.008	0.07	0.9	0.03	0.9	0.05
750	52.4	3.563	5.82	234.9	3.88	94.5	2.64
		0.008	0.06	0.7	0.03	1.0	0.04
800	44.4	3.598	5.45	240.4	4.14	100.9	2.81
		0.009	0.06	1.0	0.03	1.1	0.10
850	27.9	3.586	5.41	238.5	4.37	101.8	3.00
		0.011	0.06	1.3	0.04	1.2	0.06
900	17.5	3.603	4.44	241.1	5.77	124.0	3.97
		0.014	0.06	1.9	0.07	1.6	0.10
960	16.2	3.577	3.33	237.1	8.18	165.4	5.66
		0.015	0.04	2.0	0.09	2.2	0.12
1050	33.6	3.603	1.16	241.1	23.46	474.4	15.97
		0.015	0.02	2.1	0.22	6.2	0.22
1100	6.5	3.785	0.89	270.7	28.72	618.9	19.30
		0.037	0.02	6.3	0.77	15.6	0.60
1180	9.2	3.906	0.77	292.1	33.26	716.4	22.33
		0.027	0.01	4.8	0.62	13.9	0.51
1300	1.9	3.966	1.66	303.3	15.79	331.3	9.79
		0.101	0.11	19.0	1.23	21.0	1.01
1450	0.2	3.861	1.10	283.9	27.93	501.9	12.98
		0.634	0.44	113.1	11.81	200.1	5.73
1600	0.4	0.162	8.45	3.6	5.84	65.1	1.89
		0.080	4.37	1.8	3.37	33.7	1.13
Sioux County (0.0244 g) J = 0.02088 ± 0.00008							
350	19.0	2.189	81.27	113.3	5.37	6.8	4.91
		0.020	1.50	1.8	1.00	0.1	0.19
425	2.3	4.737	9.56	613.8	22.82	57.5	13.91
		0.034	0.21	12.2	0.59	1.3	0.43
485	15.2	4.384	9.26	496.3	10.73	59.4	8.64
		0.014	0.12	3.7	0.11	0.7	0.10
525	11.3	4.134	10.21	425.9	6.32	53.8	7.20
		0.040	0.27	10.5	0.22	1.4	0.26
575	23.0	3.977	9.50	386.3	5.45	57.9	5.20
		0.010	0.11	2.0	0.04	0.7	0.05
605	29.9	3.922	10.21	373.3	4.83	53.9	4.93
		0.009	0.11	1.6	0.04	0.6	0.04
625	22.8	3.865	10.24	360.3	4.60	53.7	4.67
		0.011	0.12	2.1	0.04	0.6	0.05
650	25.5	3.685	10.70	321.4	4.75	51.4	4.13
		0.011	0.12	1.9	0.04	0.6	0.05
675	25.0	3.704	9.38	325.4	4.46	58.6	4.08
		0.011	0.11	1.8	0.04	0.7	0.05
700	39.5	3.668	8.79	317.9	4.60	62.5	3.87
		0.008	0.09	1.2	0.03	0.7	0.03

Table 1A. *Continued.*

Temp (°C)	^{39}Ar cc/g ×10^{11}	Age (Gyr)	K/Ca ratio ×1000	40/39 ± ×1	38/39 ± ×10	37/39 ± ×1	36/39 ± ×10
725	46.8	3.619	8.13	308.2	4.77	67.7	3.68
		0.008	0.09	1.0	0.03	0.7	0.03
750	46.8	3.607	7.78	305.8	4.75	70.7	3.46
		0.008	0.08	1.1	0.03	0.8	0.03
770	31.6	3.599	7.65	304.2	4.71	71.9	3.40
		0.010	0.09	1.5	0.04	0.8	0.04
800	37.2	3.626	7.64	309.5	4.84	72.0	3.57
		0.009	0.08	1.3	0.03	0.8	0.04
825	30.2	3.652	7.82	314.7	4.87	70.3	3.59
		0.010	0.09	1.5	0.04	0.8	0.04
850	26.3	3.679	7.99	320.2	5.07	68.8	3.79
		0.010	0.09	1.7	0.04	0.8	0.04
875	20.8	3.714	7.66	327.4	5.99	71.8	4.38
		0.012	0.09	2.2	0.05	0.9	0.05
925	16.6	3.694	6.60	323.2	7.53	83.3	5.48
		0.014	0.09	2.7	0.09	1.1	0.08
975	14.7	3.661	5.26	316.5	9.58	104.6	6.53
		0.016	0.07	3.1	0.11	1.5	0.08
1000	11.6	3.635	4.17	311.4	11.91	131.9	7.90
		0.021	0.07	3.9	0.17	2.1	0.12
1050	14.3	3.635	3.07	311.3	15.54	179.1	10.30
		0.019	0.05	3.6	0.20	2.7	0.15
1125	21.9	3.800	0.86	345.6	49.74	638.5	32.92
		0.021	0.01	4.4	0.66	10.4	0.49
1200	3.3	3.939	0.64	377.2	61.38	857.5	39.99
		0.155	0.06	36.5	6.21	83.4	4.07
1300	9.9	4.204	1.77	444.4	23.58	310.1	15.86
		0.045	0.05	12.3	0.70	9.1	0.49
1400	7.8	4.513	1.84	536.6	27.73	298.8	19.19
		0.056	0.06	18.1	1.07	10.5	0.76
1600	0.0	4.212	1.76	446.8	–4.29	312.5	109.78
		0.955	1.03	261.8	–2.81	183.2	69.67
Asuka-87272,49 (0.0442 g) J = 0.02197 ± 0.00004							
350	38.6	0.342	240.38	9.5	15.85	2.3	0.13
		0.011	8.97	0.3	0.81	0.1	0.02
450	20.0	1.805	131.41	78.3	22.05	4.2	0.23
		0.016	2.24	1.1	0.40	0.1	0.03
500	10.2	2.523	141.09	138.8	9.58	3.9	0.23
		0.026	3.00	2.6	0.24	0.1	0.05
585	18.0	3.030	49.49	198.6	8.06	11.1	0.82
		0.017	0.75	2.3	0.13	0.2	0.05
650	8.7	2.952	36.04	188.2	5.85	15.3	1.05
		0.033	0.90	4.3	0.18	0.4	0.10
725	13.8	3.005	18.75	195.2	9.97	29.3	2.08
		0.021	0.33	2.8	0.18	0.5	0.08

Table 1A. *Continued.*

Temp (°C)	^{39}Ar cc/g ×10^{11}	Age (Gyr)	K/Ca ratio ×1000	40/39 ± ×1	38/39 ± ×10	37/39 ± ×1	36/39 ± ×10
775	12.2	2.967	11.17	190.2	8.63	49.2	3.53
		0.021	0.20	2.8	0.18	0.9	0.11
825	22.9	2.936	6.92	186.1	9.63	79.5	5.27
		0.013	0.09	1.7	0.11	1.1	0.08
875	23.7	2.880	6.12	179.1	9.78	89.9	5.88
		0.011	0.08	1.3	0.11	1.1	0.08
910	16.6	3.005	5.76	195.2	10.07	95.5	6.24
		0.015	0.08	2.0	0.13	1.4	0.11
950	2.9	2.657	5.91	153.0	10.31	93.0	6.10
		0.074	0.32	8.2	0.71	5.0	0.49
1075	211.7	3.400	3.52	254.1	16.51	156.4	10.38
		0.009	0.04	1.5	0.17	1.8	0.12
1125	13.7	3.548	4.42	279.7	12.50	124.3	8.04
		0.025	0.08	4.4	0.24	2.3	0.17
1160	14.5	3.454	4.73	263.2	12.16	116.4	7.64
		0.026	0.09	4.5	0.25	2.3	0.18
1200	9.6	3.605	4.54	290.2	12.08	121.2	7.65
		0.029	0.09	5.3	0.30	2.5	0.21
1260	15.0	3.652	4.57	299.0	11.85	120.3	7.48
		0.020	0.07	3.9	0.20	2.0	0.13
1325	2.9	3.644	4.31	297.6	13.23	127.5	8.28
		0.090	0.25	17.0	0.81	7.4	0.54
1450	0.4	3.610	4.82	291.1	15.64	114.1	9.41
		0.357	1.10	66.6	4.74	26.1	3.13
1600	0.1	1.990	blank	91.6	4.20	blank	0.86
		0.514		39.1	2.10		0.45
Macibini glass (0.0558 g) J = 0.03111 ± 0.00005							
400	31.8	2.906	42.42	128.8	6.41	13.0	27.97
		0.062	36.55	5.5	0.74	11.2	3.64
450	19.5	2.621	44.18	105.3	1.71	12.4	2.38
		0.021	12.53	1.6	0.06	3.5	0.11
550	68.5	3.040	33.05	141.2	1.92	16.6	1.70
		0.005	0.34	0.4	0.02	0.2	0.02
600	60.5	3.355	27.37	174.3	2.24	20.1	1.69
		0.005	0.28	0.5	0.02	0.2	0.02
650	140.4	3.687	22.73	216.0	2.71	24.2	2.05
		0.004	0.23	0.4	0.02	0.2	0.01
675	55.8	3.857	21.03	240.6	2.90	26.1	2.06
		0.005	0.22	0.7	0.02	0.3	0.02
700	41.3	3.960	19.77	256.6	3.10	27.8	2.19
		0.007	0.21	1.1	0.03	0.3	0.03
750	85.5	4.071	17.27	275.0	3.56	31.8	2.52
		0.007	0.19	1.1	0.03	0.3	0.03
785	70.3	4.161	15.68	290.5	3.92	35.1	2.83
		0.005	0.16	0.9	0.02	0.4	0.02

Table 1A. *Continued.*

Temp (°C)	^{39}Ar cc/g ×10^{11}	Age (Gyr)	K/Ca ratio ×1000	40/39 ± ×1	38/39 ± ×10	37/39 ± ×1	36/39 ± ×10
825	73.9	4.161	14.66	290.6	4.19	37.5	3.08
		0.005	0.15	0.8	0.02	0.4	0.02
850	64.9	4.097	14.11	279.4	4.40	39.0	3.30
		0.005	0.15	0.8	0.02	0.4	0.03
875	60.8	4.038	13.75	269.2	4.58	40.0	3.45
		0.006	0.15	0.9	0.03	0.4	0.03
910	84.6	3.954	13.44	255.5	4.81	40.9	3.75
		0.005	0.14	0.7	0.02	0.4	0.03
950	129.9	3.814	12.57	234.1	5.33	43.8	4.30
		0.004	0.13	0.5	0.02	0.4	0.02
985	128.9	3.740	11.54	223.4	5.95	47.7	4.89
		0.005	0.12	0.5	0.02	0.5	0.02
1025	212.0	3.704	8.63	218.4	8.28	63.8	6.68
		0.005	0.09	0.6	0.03	0.7	0.03
1050	82.0	3.787	5.87	230.1	12.05	93.7	8.85
		0.007	0.06	0.9	0.05	1.0	0.05
1075	19.8	3.834	4.44	237.1	15.95	123.9	11.31
		0.031	0.10	4.7	0.42	2.7	0.32
1125	93.9	3.787	4.66	230.2	15.68	117.9	11.13
		0.008	0.05	1.1	0.08	1.3	0.07
1150	6.9	4.186	5.16	295.2	13.43	106.5	9.54
		0.030	0.11	5.4	0.32	2.2	0.26
1250	21.9	4.216	5.15	300.5	13.40	106.7	9.55
		0.014	0.07	2.5	0.15	1.4	0.12
1350	13.9	4.316	5.86	319.6	11.24	93.8	7.49
		0.038	0.15	7.5	0.36	2.4	0.30
1575	0.1	5.788	2.99	763.0	26.98	184.1	11.48
		0.468	0.81	206.4	9.94	49.9	4.52
QUE 94200,13 (0.0464 g) J = 0.02919 ± 0.00005							
400	2.6	3.362	4.70	186.6	5.55	116.9	4.44
		0.064	0.20	7.9	0.29	5.1	0.31
500	8.1	3.169	5.39	164.1	5.60	102.1	4.04
		0.031	0.12	3.4	0.15	2.3	0.14
600	19.5	3.470	4.90	200.2	6.13	112.3	4.19
		0.014	0.07	1.8	0.07	1.5	0.07
650	20.0	3.367	5.82	187.2	5.20	94.5	3.61
		0.020	0.10	2.4	0.09	1.5	0.10
700	23.1	3.621	4.83	220.7	6.23	113.9	4.22
		0.017	0.07	2.4	0.09	1.7	0.08
750	34.4	3.644	4.44	223.9	6.68	124.0	4.51
		0.010	0.05	1.4	0.05	1.5	0.06
800	41.0	3.678	4.21	228.9	6.93	130.6	4.67
		0.011	0.05	1.5	0.06	1.6	0.06
850	44.3	3.704	4.10	232.7	7.20	134.3	4.82
		0.010	0.05	1.4	0.05	1.6	0.06

Table 1A. *Continued.*

Temp (°C)	^{39}Ar cc/g ×10^{11}	Age (Gyr)	K/Ca ratio ×1000	40/39 ± ×1	38/39 ± ×10	37/39 ± ×1	36/39 ± ×10
900	39.1	3.707	3.86	233.1	7.81	142.5	5.21
		0.011	0.05	1.5	0.06	1.7	0.06
950	19.3	3.651	3.24	224.9	9.72	169.8	6.57
		0.016	0.05	2.3	0.11	2.4	0.11
1025	12.2	3.438	1.40	196.1	24.68	393.1	17.08
		0.034	0.03	4.3	0.60	9.4	0.44
1150	15.2	3.548	0.42	210.6	85.22	1299.9	59.33
		0.081	0.02	11.0	4.51	69.1	3.17
1250	0.9	3.428	0.28	194.7	133.55	1960.3	91.35
		0.516	0.09	65.5	48.07	659.8	33.08
1400	0.4	3.232	0.20	171.2	180.89	2705.1	120.50
		1.211	0.16	137.9	153.12	2179.3	102.46
1575	0.1	3.724	0.13	235.6	290.99	4260.6	187.22
		2.618	0.21	391.6	496.13	7082.2	320.10
EET 87509,24 (0.0478 g) J = 0.04969 ± 0.00014							
400	3.0	7.496	6.04	1262.7	1059.10	91.1	41.84
		0.094	0.32	66.7	56.02	4.9	2.45
600	15.0	4.039	5.94	168.7	365.26	92.5	3.47
		0.023	0.10	2.3	5.19	1.6	0.20
750	28.4	4.054	5.92	170.3	224.18	92.9	2.50
		0.013	0.07	1.3	1.71	1.2	0.11
850	37.2	4.026	6.58	167.3	23.98	83.6	1.83
		0.021	0.11	2.2	0.33	1.4	0.09
925	51.4	4.050	7.64	169.8	8.41	72.0	1.62
		0.009	0.08	0.8	0.05	0.8	0.07
975	230.8	4.068	8.33	171.7	7.78	66.0	1.59
		0.006	0.08	0.3	0.03	0.7	0.03
1025	27.3	4.052	5.79	170.1	5.99	95.0	2.46
		0.022	1.09	2.2	6.22	17.8	2.98
1100	53.8	4.070	3.76	171.9	7.79	146.4	3.55
		0.010	0.04	0.9	0.06	1.7	0.08
1200	182.0	4.136	3.16	179.2	7.09	174.0	4.04
		0.006	0.03	0.4	0.04	1.8	0.07
1250	40.8	4.160	2.83	181.8	8.18	194.2	4.93
		0.012	0.03	1.2	0.09	2.3	0.11
1350	85.4	4.154	2.99	181.1	7.98	184.1	4.82
		0.007	0.03	0.7	0.05	2.0	0.08
1450	4.5	4.279	2.68	195.5	8.44	204.8	5.86
		0.061	0.10	7.3	0.60	7.9	0.62
EET 87509,71 (0.0276 g) J = 0.05264 ± 0.00021							
400	9.0	3.640	6.84	123.9	29.91	80.4	2.07
		0.055	0.25	4.4	1.17	2.9	0.45
550	48.4	3.558	6.85	117.5	10.98	80.3	1.04
		0.015	0.09	1.0	0.13	1.1	0.13

Table 1A. *Continued.*

Temp (°C)	^{39}Ar cc/g ×10^{11}	Age (Gyr)	K/Ca ratio ×1000	40/39 ± ×1	38/39 ± ×10	37/39 ± ×1	36/39 ± ×10
675	123.0	3.926	8.16	148.4	3.23	67.4	1.13
		0.009	0.09	0.6	0.03	0.7	0.07
725	101.3	4.308	9.34	187.9	3.43	58.9	2.39
		0.011	0.11	1.0	0.04	0.7	0.08
775	121.2	3.992	9.07	154.6	1.86	60.6	1.05
		0.009	0.10	0.6	0.03	0.6	0.07
850	194.7	3.999	8.84	155.4	1.74	62.2	1.00
		0.008	0.09	0.4	0.03	0.6	0.05
925	152.2	4.040	8.31	159.4	1.92	66.2	1.04
		0.008	0.09	0.5	0.03	0.7	0.06
1000	123.3	4.038	7.73	159.1	2.11	71.1	1.09
		0.010	0.09	0.8	0.03	0.8	0.07
1100	176.3	3.989	6.31	154.4	2.52	87.2	1.38
		0.007	0.06	0.4	0.03	0.9	0.06
1200	286.6	4.001	4.37	155.5	3.66	126.0	2.09
		0.008	0.05	0.4	0.03	1.3	0.06
1250	13.3	4.021	2.01	157.5	7.48	273.6	4.32
		0.041	0.05	4.0	0.29	7.4	0.50
1400	147.7	4.050	2.01	160.4	7.44	273.5	4.63
		0.012	0.02	1.0	0.06	3.2	0.12
1500	11.7	4.156	1.74	171.2	8.59	315.4	4.89
		0.049	0.05	5.1	0.43	9.9	0.59
1650	1.2	4.449	0.00	204.7	7.77	296.2	0.14
		0.264	0.00	32.7	2.04	47.4	0.32
EET 87509,74 (0.0351 g) J = 0.05264 ± 0.00021							
400	286.8	0.873	32.01	11.8	36.24	17.2	2.23
		0.012	26.57	0.2	3.80	14.3	0.27
500	46.5	3.268	12.45	97.2	111.83	44.2	0.78
		0.014	0.32	0.8	1.01	1.1	0.11
600	46.2	3.838	11.22	140.4	35.00	49.0	0.66
		0.017	0.16	1.4	0.38	0.7	0.11
700	137.1	3.915	13.21	147.4	9.77	41.6	0.75
		0.009	0.25	0.5	0.05	0.8	0.05
775	218.2	3.899	16.17	146.0	3.05	34.0	0.96
		0.007	1.26	0.3	0.02	2.6	0.03
825	233.9	3.894	17.17	145.4	1.45	32.0	0.51
		0.008	0.18	0.5	0.02	0.3	0.03
875	260.6	3.907	17.13	146.7	1.19	32.1	0.50
		0.007	0.18	0.4	0.02	0.3	0.03
925	260.5	3.931	16.82	148.8	1.24	32.7	0.51
		0.007	0.17	0.3	0.02	0.3	0.03
975	189.2	3.975	15.63	153.0	1.56	35.2	0.57
		0.007	0.16	0.3	0.03	0.4	0.04
1050	146.5	4.023	12.56	157.6	2.34	43.8	0.75
		0.008	0.13	0.5	0.03	0.5	0.05

Table 1A. *Continued.*

Temp (°C)	^{39}Ar cc/g ×10^{11}	Age (Gyr)	K/Ca ratio ×1000	40/39 ± ×1	38/39 ± ×10	37/39 ± ×1	36/39 ± ×10
1200	114.4	4.036	6.06	159.0	4.18	90.8	1.56
		0.010	0.07	0.8	0.04	1.0	0.08
1400	140.7	4.160	1.98	171.7	9.34	277.1	4.41
		0.011	0.02	0.9	0.07	3.1	0.12
1600	320.1	4.296	4.32	186.6	3.50	127.4	1.95
		0.008	0.04	0.5	0.03	1.3	0.05
1660	19.9	4.645	0.00	230.4	2.68	0.0	1.38
		0.036	0.00	4.8	0.18	0.0	0.24
EET 87531,21 (0.0473 g) J = 0.04969 ± 0.00014							
450	31.4	3.301	102.13	105.3	36.14	5.4	0.94
		0.014	1.35	0.9	0.34	0.1	0.10
600	131.6	3.755	10.08	141.2	14.50	54.6	1.06
		0.007	0.11	0.5	0.06	0.6	0.04
700	161.6	3.823	12.32	147.4	3.48	44.6	0.90
		0.006	0.13	0.3	0.02	0.5	0.03
750	162.6	3.808	12.10	146.0	2.21	45.5	0.90
		0.007	0.13	0.5	0.02	0.5	0.03
800	160.8	3.820	10.65	147.1	2.18	51.7	1.02
		0.005	0.11	0.3	0.02	0.5	0.03
850	143.1	3.840	9.50	149.0	2.46	57.9	1.13
		0.006	0.10	0.3	0.02	0.6	0.04
900	114.7	3.877	8.87	152.5	2.74	62.0	1.25
		0.007	0.09	0.5	0.03	0.7	0.05
975	80.4	3.898	7.58	154.5	4.09	72.5	1.53
		0.007	0.08	0.5	0.04	0.8	0.06
1050	52.5	3.894	4.40	154.1	6.79	125.0	2.78
		0.009	0.05	0.7	0.06	1.4	0.10
1150	57.6	3.939	1.77	158.5	13.53	310.0	6.74
		0.012	0.02	1.1	0.11	3.8	0.15
1225	52.5	4.120	1.03	177.4	19.51	534.9	11.77
		0.015	0.01	1.6	0.19	7.1	0.25
1300	19.7	4.176	2.00	183.6	10.15	274.6	5.91
		0.034	0.05	3.9	0.29	6.4	0.30
1450	34.9	3.944	15.60	159.0	4.80	35.3	3.16
		0.044	0.67	4.3	0.20	1.5	0.18
EET 87503,53 (0.0455 g) J = 0.03368 ± 0.00009							
400	15.4	5.209	8.58	503.1	21.69	64.1	14.30
		0.025	0.15	7.2	0.34	1.1	0.30
500	48.5	3.826	9.82	217.9	5.75	56.0	1.93
		0.007	0.10	0.8	0.05	0.6	0.06
575	57.1	3.788	10.08	212.8	4.15	54.6	1.70
		0.009	0.11	1.0	0.05	0.6	0.06
650	88.0	3.778	10.20	211.4	3.27	53.9	1.95
		0.006	0.10	0.5	0.03	0.6	0.04

Table 1A. *Continued.*

Temp (°C)	^{39}Ar cc/g $\times 10^{11}$	Age (Gyr)	K/Ca ratio $\times 1000$	40/39 $\pm \times 1$	38/39 $\pm \times 10$	37/39 $\pm \times 1$	36/39 $\pm \times 10$
700	92.1	3.677	9.37	198.2	3.13	58.7	1.87
		0.007	0.10	0.7	0.03	0.6	0.04
750	79.5	3.679	8.47	198.4	3.41	64.9	2.10
		0.007	0.09	0.7	0.03	0.7	0.05
825	78.7	3.691	7.84	200.0	3.86	70.1	2.40
		0.010	0.09	1.1	0.04	0.8	2.67
925	55.3	3.682	5.72	198.9	6.10	96.1	3.78
		0.008	0.06	0.8	0.05	1.0	0.07
1025	77.8	3.568	3.11	184.9	10.90	176.9	6.76
		0.007	0.03	0.6	0.05	1.9	0.08
1125	51.6	3.625	1.53	191.7	20.35	359.3	12.96
		0.012	0.02	1.4	0.17	4.5	0.18
1250	11.7	3.864	1.76	223.1	17.47	312.4	11.40
		0.025	0.03	3.4	0.33	5.8	0.36
1450	23.4	3.893	2.15	227.2	14.19	256.3	9.34
		0.017	0.03	2.3	0.18	3.6	0.20
EET 87503,23 (0.0490 g) J = 0.03368 ± 0.00009							
400	12.9	3.413	18.99	167.2	7.03	29.0	1.39
		0.017	1.36	1.8	0.13	2.1	0.12
500	26.8	3.297	21.56	155.0	2.31	25.5	1.05
		0.010	0.85	0.9	0.05	1.0	0.07
600	54.9	2.912	21.94	119.5	1.74	25.1	0.95
		0.005	0.65	0.3	0.03	0.7	0.04
675	83.1	2.490	21.35	88.3	1.69	25.8	0.93
		0.005	0.55	0.2	0.02	0.7	0.03
725	90.6	2.329	20.74	78.3	1.48	26.5	0.96
		0.005	0.61	0.2	0.02	0.8	0.03

Table 1A. *Continued.*

Temp (°C)	^{39}Ar cc/g $\times 10^{11}$	Age (Gyr)	K/Ca ratio $\times 1000$	40/39 $\pm \times 1$	38/39 $\pm \times 10$	37/39 $\pm \times 1$	36/39 $\pm \times 10$
775	119.1	2.294	18.72	76.2	1.60	29.4	1.03
		0.006	0.20	0.3	0.02	0.3	0.02
825	111.5	2.415	17.28	83.6	1.72	31.8	1.06
		0.005	0.18	0.2	0.02	0.3	0.03
875	130.5	2.688	15.08	102.0	2.02	36.5	1.29
		0.005	0.16	0.3	0.02	0.4	0.02
925	123.1	3.169	12.13	142.3	2.50	45.3	1.59
		0.005	0.12	0.3	0.02	0.5	0.03
975	106.4	3.560	9.84	184.0	3.05	55.9	1.94
		0.006	0.10	0.5	0.02	0.6	0.03
1025	202.9	3.993	6.82	241.8	4.36	80.7	2.81
		0.007	0.07	0.8	0.03	0.9	0.04
1075	187.9	4.407	5.88	311.8	4.91	93.6	3.26
		0.006	0.06	0.7	0.03	1.0	0.04
1125	145.9	4.422	6.54	314.8	4.34	84.1	2.90
		0.005	0.07	0.6	0.02	0.9	0.04
1200	116.0	4.390	8.52	308.7	3.30	64.5	2.22
		0.005	0.09	0.6	0.02	0.7	0.03
1275	44.0	4.412	13.13	312.9	2.10	41.9	1.52
		0.009	0.15	1.5	0.04	0.5	0.06
1400	67.0	4.404	11.52	311.3	2.49	47.7	1.76
		0.007	0.12	1.0	0.04	0.5	0.03
1600	1.2	5.324	7.06	538.3	9.06	77.9	10.47
		0.256	1.07	80.6	1.57	11.8	2.06